The Arabidopsis MTERF protein PAM48 is required for plastid gene expression and development

Dissertation
zur Erlangung des Doktorgrades der Fakultät für Biologie
der Ludwig-Maximilians-Universität München

Vorgelegt von
Arianna Morosetti
aus Mailand,
Italien

Diese Dissertation wurde angefertigt
unter der Leitung von Prof. Dr. Leister
am Institut für Botanik
and der Ludwig-Maximilians-Universität München

Erstgutachter: Prof. Dr. Dario Leister
Zweitgutachter: Prof. Dr. Wolfgang Frank

Tag der Abgabe: 24. Mai 2012

Tag der mündlichen Prüfung: 12. September 2012

"The world is but a school of inquiry."
Michel de Montaigne

Summary

As a consequence of endosymbiosis, plants possess three different genomes located in the nucleus, the mitochondrion and the chloroplast. Owing to the massive relocation of organellar genes to the nucleus and the loss of organellar genes during evolution, the organellar genomes are now highly impoverished and have lost most of their genetic autonomy. Thus, organellar gene expression relies on nuclear-encoded factors.

The MTERF (Mitochondrial Transcription tERmination Factor) proteins form a large family found in metazoans and plants. In metazoans, members of this family have been shown to interact with the mitochondrial chromosome and to be able to regulate transcription of ribosomal RNA genes, via mechanisms that involve termination of transcription, as well as its initiation. Structural studies of a human MTERF protein have demonstrated a unique binding mode to DNA.

In this work, the Arabidopsis T-DNA insertion mutant *pam48-1* (*photosynthesis altered mutant 48-1*), identified through a screening for alterations in the effective quantum yield of photosystem II, was characterized. The mutant is defective for a nuclear-encoded MTERF-related protein, PAM48, found to be dual-targeted to chloroplasts and mitochondria. Blue native gel electrophoresis and Western blot analysis of photosynthetic proteins revealed a malformation of thylakoid complexes assembly and a specific depletion in the translation of chloroplast-encoded photosynthetic subunits. Transcript levels of the genes of the corresponding subunits were not affected, indicating that the defect is restricted to translational activity. Because of the demonstrated DNA binding activity of metazoan MTERFs, a bacterial one-hybrid screening was set up, aimed to identify putative DNA binding sites of PAM48. Indeed, the screening in combination with electrophoretic mobility shift assays led to the identification of specific DNA binding sites located downstream of the chloroplast genes *rrn16* and *trnv.1* coding for 16S rRNA and $tRNA^{Val}$. Downregulation of PAM48 results in defects in ribosomal RNA maturation, which in turn accounts for improper protein translation in *pam48-1* chloroplasts. A stronger allele – *pam48-2* – leads to seedling lethality and improper plastid development, but mitochondrial biogenesis seems to be unaltered. In addition, a chloroplast targeted PAM48 fusion construct successfully complemented the *pam48-1* phenotype, while *pam48-1* plants were not complemented by a mitochondrial targeted PAM48 construct. These results indicate that PAM48 has an essential function in plastid gene expression and a distinct, but not yet characterized, role in mitochondria.

Zusammenfassung

Als Folge der Endosymbiose besitzen Pflanzen drei verschiedene Genome, die sich im Zellkern, in den Mitochondrien und in den Chloroplasten befinden. Aufgrund des massiven Gentransfers von den Organellen in den Zellkern und des Verlusts von Organellen-Genen im Laufe der Evolution, haben die Organellen ihre genetische Autonomie verloren. Daher ist die Genexpression in den Organellen von zellkernkodierten Faktoren abhängig.

Die MTERF (Mitochondrial Transcription tERmination Factor) Proteine bilden eine große Familie, welche in Metazoen und Pflanzen vorkommt. Metazoen-MTERF-Proteine interagieren mit dem mitochondrialen Chromosom und sind in der Lage, die Transkription der ribosomalen RNA-Gene auf der Ebene der Termination und Inititation der Transkription zu regulieren. Struktur-Studien an menschlichen MTERF-Proteinen haben eine einzigartige Bindung der DNA gezeigt.

In dieser Arbeit wurde die Arabidopsis T-DNA Insertionsmutante *pam48-1* (*photosynthesis altered mutant 48-1*) charakterisiert, die durch ein Screening auf Änderungen in der effektiven Quantenausbeute des Photosystems II identifiziert worden ist. Diese Mutante hat einen Defekt in einem zellkernkodierten MTERF-Protein, PAM48, welches im Laufe dieser Arbeit in Mitochondrien und Chloroplasten nachgewiesen wurde. Blue-Native Gelelektrophorese und Western-Blot-Analyse von Photosynthese-Proteinen zeigten eine Beeinträchtigung bei der Bildung der Thylakoidkomplexe und eine spezifische verminderte Translation der chloroplastenkodierten Photosynthese-Proteine. Die Transkriptmengen der Gene der entsprechenden Proteine waren unverändert, was darauf hinweist, dass der Defekt auf die Translation beschränkt ist. Aufgrund der nachgewiesenen DNA-Bindungsaktivität von MTERF-Proteinen bei Metazoen, sollten die möglichen DNA-Bindungsstellen von PAM48 mit einem "bacterial one-hybrid" Screening identifiziert werden. Tatsächlich hat das Screening in Kombination mit elektrophoretischen Mobilitäts-Shift-Assays zur Identifizierung der spezifischen DNA-Bindungsstellen geführt, welche sich „downstream" von den chloroplastidären Genen *rrn16* und *trnv.1*, die für 16S rRNA und $tRNA^{Val}$ kodieren, befinden. Die Deregulierung von PAM48 führt zu Defekten in der ribosomalen RNA-Maturation, die wiederum für den Translations-Defekt in *pam48-1* Chloroplasten verantwortlich ist. Ein stärkeres Allel – *pam48-2* - zeigt Keimlingsletalität und fehlerhafte Plastidentwicklung, jedoch scheint die Mitochondrienbiogenese nicht beeinträchtigt zu sein. Außerdem wurde der *pam48-1* Phänotyp durch spezifisches chloroplasten-lokalisiertes PAM48 komplementiert, jedoch nicht durch exklusiv mitochondrien-lokalisiertes PAM48. Diese Ergebnisse zeigen, dass PAM48 eine wesentliche Funktion in der plastidären Genexpression hat, sowie eine zusätzliche Funktion in den Mitochondrien.

Index

Abbreviations

ATP	adenosine triphosphate
B1H	bacterial one-hybrid
BN	blue native
bp	base pair
CaMV 35S	35S promoter of the Cauliflower Mosaic virus
BSA	bovine serum albumin
cDNA	complementary deoxyribonucleic acid
Col-0	Columbia 0
cTP	chloroplast targeting peptide
cyt	cytochrome
DNA	deoxyribonucleic acid
g	standard gravity
GFP	green fluorescent protein
IPTG	isopropyl β-D-1-thiogalactopyranoside
LHC	light-harvesting complex
mTP	mitochondrion targeting peptide
NPQ	non-photochemical quenching
OGE	organelle gene expression
PAGE	polyacrylamide gel electrophoresis
PAM	pulse amplitude modulation
PCR	polymerase chain reaction
PFD	photon flux density
PSI	photosystem I

PSII	photosystem II
qPCR	quantitative polymerase chain reaction
RNA	ribonucleic acid
ROS	reactive oxygen species
RT-PCR	reverse transcriptase-polymerase chain reaction
SD	standard deviation
T-DNA	transfer-DNA
WT	wild-type
β-DM	n-dodecyl β-D-maltoside
Φ_{II}	effective quantum yield of photosystem II

Units

°C	degree Celsius
g	gram
h	hour
kDa	kilodalton
m	meter
M	molarity
mA	milliampere
min	minute
mol	mol
s	second
V	volt
v/v	volume per volume
w/v	weight per volume
µE	microeinstein

1 INTRODUCTION

1.1 Origin of the plant cell

The endosymbiotic theory, which posits that mitochondria and chloroplasts originated from free-living prokaryotes, is nowadays widely accepted (Gould et al., 2008).

Analyses of mitochondrial genes and their genomic organization and distribution indicate that mitochondrial genomes are derived from an α-proteobacterium–like ancestor, probably due to a single ancient invasion of an Archea-type host that occurred more than 1.5 billion years ago (Dyall et al., 2004; Gray et al., 1999). This first endosymbiotic event represents the origin of all eukaryotic organisms, animal, fungi and plant; indeed, all of them today contain mitochondria, with the exception of some parasitic organisms that have modified anaerobic form of mitochondria, named mitosomes (Dyall et al., 2004). A second endosymbiotic event occurred – between 1.5 and 1.2 billion years ago - when a mitochondria-containing ancestor cell engulfed a cyanobacterium, leading to the formation of plastids and to the production of three major photoautotrophic lineages: the green algae and the descendant plants, the glaucophytes and the red algae (Yoon et al., 2004; Gould et al., 2008).

One of the consequences of the establishment of endosymbiotic relationships was a strong reduction of organellar genomes. Nowadays, mitochondrial genomes contain from 3 to 67 genes (Szklarczyk and Huynen, 2010), while plastidial genomes code for 15 to 209 proteins (Keeling and Palmer, 2008). On the other hand, cyanobacterial genomes code for at least 1500 proteins; the genes originally belonging to the pre-plastid were mostly lost or transferred to the nucleus and only a few retained in the plastidial genome (Raven and Allen, 2003). The Arabidopsis chloroplast is predicted to contain between 2500 and 3000 proteins, of which about one half is of cyanobacterial origin (Richly and Leister, 2004). In the same way, mitochondria synthesize only 2 to 5% of the different proteins necessary for their functioning, being the rest coded by the nucleus (Gray et. al, 1999).

1.2 Retrograde Signalling

As the nucleus retains most of the genetic information products that are required by the organelles, organellar multi-protein complexes are often composed by mosaics of nuclear-encoded and organellar-encoded subunits. Consequently, the plant cell has the unique need

of coordinating three genomic compartments; the efficient and prompt coordination of nucleus, chloroplast and mitochondria, under the stimulus of internal and external inputs, requires a tight network of information exchange, composed of a number of different signals (Kleine et al., 2009; Pfannschmidt, 2010).

The information network between nucleus and organelles has necessarily many directions; the nucleus communicates with both chloroplasts and mitochondria through a series of signals that are commonly categorised under the definition of "anterograde signalling", while organelles respond to the nucleus through signals that are referred to as the "retrograde signalling". The last direction – present only in plant cells - is the cross-talk between the chloroplast and mitochondrion (Woodson and Chory, 2008).

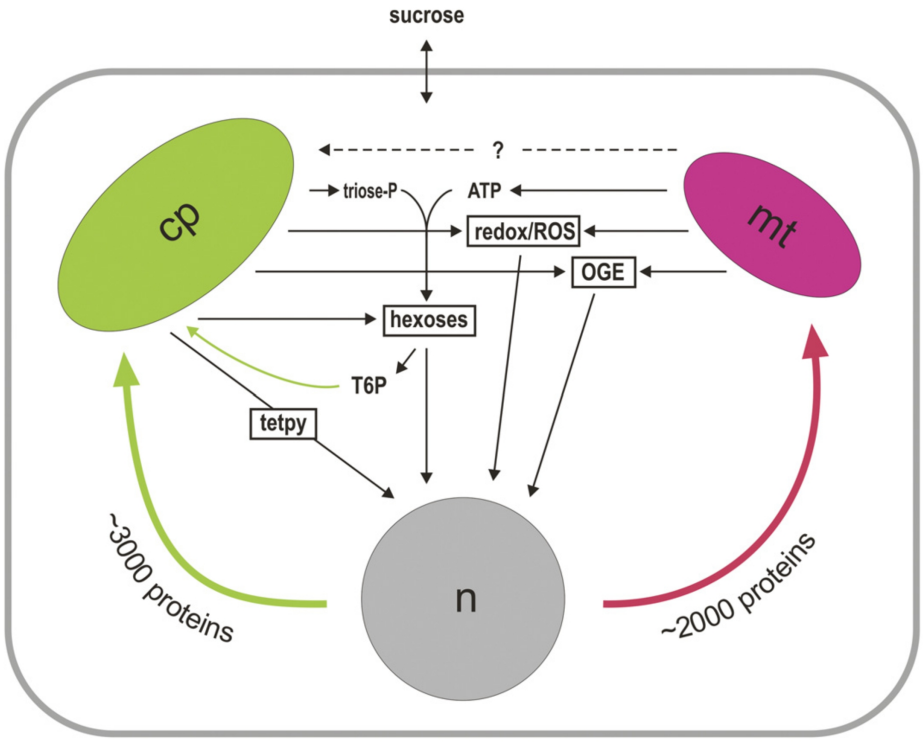

Figure 1.2.1 - An overview of genome co-ordination between the nucleus and organelles. The diagram depicts communication between the nucleus, chloroplast and mitochondrion. It is not clear where signals originating from chloroplasts and mitochondria merge. Moreover, the identity of signalling molecules, particular those that transit the cytosol, is largely unknown. cp, chloroplast; mt, mitochondrion; n, nucleus; tetpy, tetrapyrrole; OGE, organelle gene expression; ROS, reactive oxygen species; T6P, trehalose-6-phosphate (taken from Pesaresi et al., 2007).

Owing to its crucial role for the whole plant cell functioning, interorganellar signalling – and in particular retrograde signalling between chloroplast and nucleus - has been the subject of extensive studies for more than 30 years (Pfannschmidt, 2010). Despite extensive efforts, to date the identity of the actual components involved is still unclear, but the general categories of possible signal pathways under investigation are four: i) organellar gene expression (OGE) including transcription and translation, ii) pigment biosynthesis, such as intermediates of

carotenoids and tetrapyrrole biosynthesis; iii) reactive oxygen species (ROS) generation; iv) redox processes in photosynthesis (Pfannschmidt, 2010). A last hypothetical role in signalling was proposed for changes in the metabolite pool, but it represents a speculation still to be experimentally addressed (Kleine et al., 2009; Pfannschmidt, 2010). In particular, sugars such as glucose, sucrose and trehalose-6-phosphate, have been suggested to act as possible mediators in intracellular signalling (Pesaresi et al., 2007).

According to the picture described above (summarized in Figure 1.2.1, taken from Pesaresi et al., 2007), the difficulties in identifying the components in interorganellar signalling are clear; each of the above processes can affect the other or even all of them, as they are physiologically interconnected, making it hard to distinguish between cause and consequence in experimental approaches (Kleine et al., 2009).

1.3 Organellar gene expression as part of interorganellar signalling

Efforts in understanding retrograde signalling in plants led to the individuation of many candidate mechanisms that might represent the signal originated by the chloroplast and directed to the nucleus; one of them is the plastid gene expression (PGE), or in its wider sense organellar gene expression (OGE), as mitochondria seem to contribute to this signalling pathway (Pesaresi et al., 2006; Kleine et al., 2009; Pfannschmidt, 2010).

Originally, retrograde signalling elements were referred to as the "plastid factor". A first evidence that signals from chloroplasts regulate nuclear gene expression came from studies with *albostrians* mutants of barley, which contain undifferentiated plastids that lack ribosomes. Cells containing these albino plastids failed to accumulate nuclear-encoded photosynthetic mRNA transcripts (Woodson and Chory, 2008; Bradbeer et al., 1979; Taylor et al., 1989). Referring to more recent studies, the Arabidopsis *prors1* mutant, which is defective in a prolyl-tRNA synthetase found in both plastids and mitochondria and exhibits a decrease in protein synthesis in both organelles, shows at the same time specific down-regulation of nuclear photosynthesis genes (Pesaresi et al., 2006). The synergistic action of plastids and mitochondria gene expression seems to be necessary to activate the nuclear response; the specific down-regulation of photosynthesis genes does not occur in the *prpl11* or *mrpl11* mutants (in which plastid or mitochondrial ribosome function, respectively, is impaired), but only in the *prpl11 mrpl11* double mutant. This confirms that both chloroplast and mitochondrial translation rates contribute synergistically to regulation of nuclear gene expression (Pesaresi et al., 2006 and 2007).

One aspect that has been partially neglected is the contribution of the mitochondrion to retrograde signalling. Although there are recent studies dedicated to the signalling between mitochondria and nucleus within the plant cell (Noguchi et al., 2008; Raghavendra et al., 2003), the topic has been mostly investigated in animal or yeast cells. Nonetheless, the plant mitochondrion presents unique features when compared to its pendant in other heterotrophic organisms. Esamples of this uniqueness are the glycine decarboxylase complex involved in photorespiration and the cyanide-resistant alternative oxidase (AOX), an enzyme belonging to the nonphosphorylating pathways of the respiratory chain that dissipates excess reductants from chloroplast (Raghavendra et al., 2003; Noguchi et al., 2008, Pfannschmidt, 2010). Moreover, during seed and seedling development the exchange between chloroplast and mitochondrion is supposedly intense, as the plant passes from a heterotrophic stage - where mitochondria respirate cotyledonary nourishment stock - to an autotrophic phase, where chloroplasts commence photosynthesis in the first true leaves (Pfannschmidt, 2010). Therefore integration of mitochondria in experimental approaches is essential to the understanding of the whole organellar signalling pathway (Pfannschmidt, 2010).

1.4 Control of transcription and gene expression in plant mitochondria and chloroplasts

Among the estimated thousand and more proteins that constitute the functional plant mitochondrion (Millar et al., 2001), only 33 proteins - belonging either to respiration chain complexes or to ribosomes - are encoded by the *Arabidopsis thaliana* mitochondrial genome (Unseld et al., 1997; Giegé et al., 2005). Remarkably, in plant mitochondria transcription fully relies on nuclear-encoded proteins and consequently, RNA-polymerases, as well as transcription factors, are all imported from the cytoplasm (Marienfeld, 1999).

Transcription of mitochondrial genes is carried out by a single nucleus-encoded phage-type RNA polymerase (Hedtke et al., 1997). On the contrary, transcription of genes in the chloroplast of land plants relies on three enzymes: two nuclear-encoded RNA polymerases (NEP), RPOTp and RPOTmp, and the plastid-encoded RNA polymerase (PEP). The two NEPs are single-subunit phage-type enzymes, while PEP is a bacterial-type polymerase, encoded by three genes (*rpoA*, *rpoB* and *rpoC*) and homologous to the α, β, and β' subunits of the bacterial RNA polymerase (Lerbs-Mache, 2011). Interestingly, the σ -factors - essential components of the RNA polymerase holoenzyme in bacteria, involved in the recognition of promoter elements and transcription initiation - are coded by the nucleus and imported in plastids. Indeed, six different σ -factors (SIG1 to SIG6) are found in the nuclear genome of

land plants (Schweer et al., 2010). The presence of three different RNA polymerases and six different σ-factors points to the complexity of plastid transcription and hence this process is not yet fully understood (Lerbs-Mache, 2011). First of all, it is not yet clear why two different types of RNA polymerases are existing; it was proposed that NEP would serve for transcription of those genes involved in housekeeping functions (tRNAs, rRNAs, ribosomal proteins, and PEP itself), while PEP would be needed for the transcription of photosynthetic genes (Hajdukiewicz et al., 1997). Such division of labour between the two enzymes is thought too simplistic, as it is now clear that most chloroplast genes can be transcribed by both NEP and PEP (Liere and Börner, 2007). However, none of the enzymes alone is sufficient for the biogenesis of photosynthetically competent chloroplasts, indicating that some chloroplast genes specifically require one of the two polymerase for adequate expression (Barkan, 2011).

The complexity of transcription is confirmed by the fact that the six σ-factors are expressed at different developmental stages and have different functions and specialisation in plastidial gene expression, thus, they are thought to be modulator of transcription. For instance, SIG1 was shown to have a regulatory role in PSI expression (Shimizu et al., 2010); SIG2 seems to be involved in regulation of translation, chlorophyll biosynthesis and PSI stability, as well as determination of RNA polymerase switching from NEP to PEP during early plant development (Hanaoka et al., 2003; Nagashima et al., 2004). SIG3 is specific for transcription of *psbN* (Zghidi et al., 2007), SIG4 for *Ndhf* (Schweer et al., 2010) and SIG5 is responsible for the specific transcription of *psbD* from the blue light responsive promoter (Nagashima et al., 2004). Eventually, SIG6 seems to be the principal sigma factor during early development (Ishizaki et al., 2005; Loschelder et al., 2006).

Despite the variety of mechanisms required for transcription, the regulation of OGE was long thought to occur mainly at a post-transcriptional level. Mullet and Klein (1987) showed that transcript stability and translational efficiency are determinants of the overall synthesis of many proteins. The control of gene expression is a crucial difference between chloroplasts and their bacterial ancestors: whereas in bacteria transcription initiation is critical, in plastids the regulation of post-transcriptional steps is prominent (Eberhard et al., 2002). Moreover, the analysis of nonphotosynthetic mutants in plant model organisms (*Zea mays, Arabidopsis thaliana* and *Chlamydomonas reinhardtii*) has revealed numerous nucleus-encoded RNA-binding proteins that participate in the expression of chloroplast genes. For instance, the pentatricopeptide repeat family (PPR) is known to be one of the largest families in angiosperm species, as most genomes encode 400–600 members. As the number of PPR

genes in other eukaryotic organisms, including green algae, is generally only 10 to 20, the family has obviously greatly expanded during land plant evolution (Fujii and Small, 2011). PPRs are thought to be involved in RNA metabolism and to be able to influence RNA stability and translation, representing most likely an instrument of control of OGE from the nucleus (Schmitz-Linneweber and Small, 2008).

Even though the control of OGE seems to occur mostly at a post-transcriptional level, there are examples that demonstrate the importance of transcriptional control, such as redox regulation of transcription of genes for photosystem components. Pfannschmidt et al. (1999) showed that transcription of genes for PSII components increased when plants were transferred to light favouring PSI and *vice versa*. This was shown to depend on the redox state of the plastoquinone pool. Puthiyaveetil et al. (2008) identified a nuclear-encoded prokaryotic-type sensor kinase in chloroplasts that is required for this regulation (Barbrook, 2010).

Dissection of transcription mechanisms in organelles is still far to be complete and it is made more difficult by the complexity of the mechanisms involved. For example, the exact roles of each member of the transcriptionally active chromosome in plastids (pTAC, or the proteins associated to chloroplast DNA-protein complex) are not characterized yet. It was though demonstrated by knock-out mutant analysis that three members (pTAC2, -6 and -12) are important for plastid gene expression (Pfalz et al., 2006). Other pTACs are represented by Whirly family transcription factors, encoded by the nucleus and targeted to the chloroplast (Desveaux et al., 2004; Prikryl et al., 2008). Furthermore, termination of transcription in plant organelles, a mechanism important for transcription rate regulation in metazoan mitochondria, has received little attention until yet.

1.5 The Mitochondrial Transcription tERmination Factors (MTERF) protein family

The Mitochondrial Transcription tERmination Factor (MTERF) family is a large protein family, identified in metazoans and plants, but not in fungi. The evolutionary relations of MTERF proteins in metazoans, described by Linder et al., (2005), indicate the existence of four MTERF paralogue genes in vertebrates, defining four sub-families, namely MTERF1, 2, 3 and 4. According to targeting prediction analysis (Linder et al., 2005), in metazoans the majority of the MTERFs are targeted to the mitochondrion, and all the MTERFs characterized so far in animal models are experimentally confirmed mitochondrial proteins (Roberti et al., 2009).

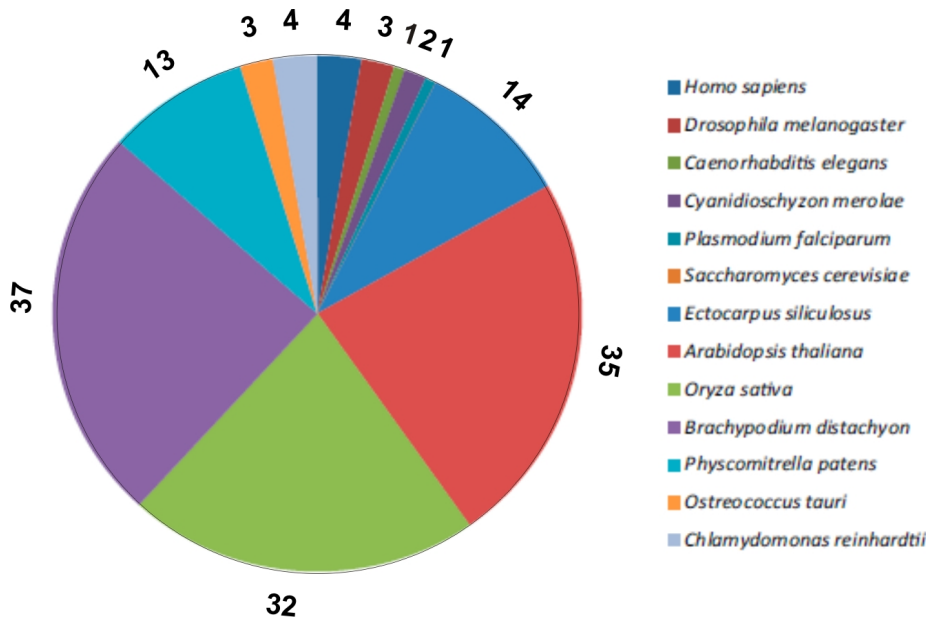

Figure 1.5.1 - Diagrams of MTERFs in different model species. Adapted from Babiychuk et al., 2011

Flowering plants have the highest number of MTERF genes among eukaryotes, as they have undergone a large number of duplications during evolution. For instance, *Arabidopsis thaliana* contains 35 MTERFs, while *Oryza sativa* contains 32 (http://smart.embl-heidelberg.de/smart/selective.domains=mterf&terms); a more detailed list of MTERFs in different model organisms is reported in Figure 1.5.1.

The products of these genes are predicted to be targeted either to the mitochondrion or the chloroplast (Linder et al., 2005). In 2011, Babiychuk et al. performed fluorescence microscopy of GFP fusions of all members of the Arabidopsis MTERFs family and confirmed the targeting to the chloroplast for 11 MTERF proteins and to the mitochondrion for 17 MTERFs, while only one member was equally distributed between nucleus and cytoplasm. Thus, the overall studies in metazoans and plants led to the conclusion that MTERFs are predominantly organellar proteins.

The protein structure of MTERFs has been an open question for many years. MTERF proteins have a modular architecture due to the repetition of a variable number of a common motif of 30 amino acids, named the MTERF motif. The distinctive feature of this motif is the conservation of a proline residue at position 8, and of a leucine or another hydrophobic amino acid at positions 11, 18 and 25 (Roberti et al., 2009).

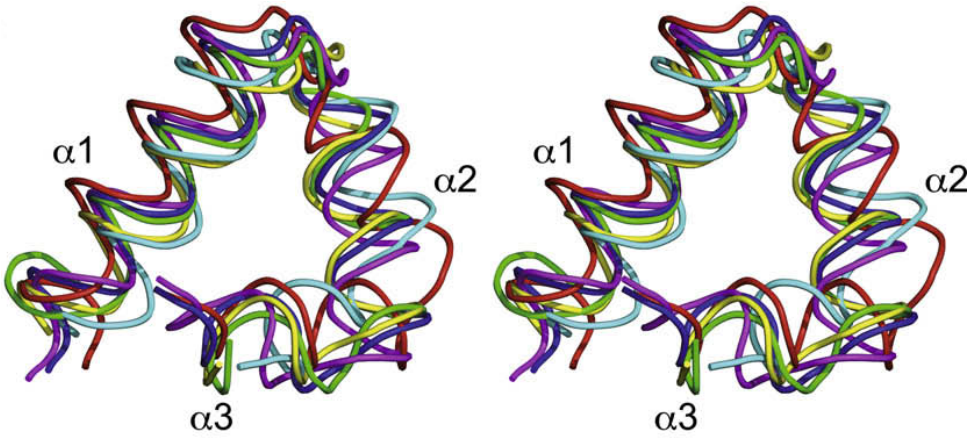

Figure 1.5.2 - Stereo-view of a structural alignment of MTERF-motif. α1, 2 and 3 represent three different MTERF-motifs. Taken from Spåhr et al., 2010.

The positively charged path stretching from one protein side to the other suggests that the MTERF-domains bind to double-stranded nucleic acids as a half clamp. The backbone of both DNA strands is bound along the positively charged grooves in the protein surface and each MTERF motif contributes to this binding (Yakubovskaya et al., 2010). Most of the interactions that are observed in the structure are electrostatic in nature and are established with the phosphate groups of the DNA strands (Yakubovskaya et al., 2010). As the inner diameter of the MTERF3 half-doughnut is about 2.5 nm, both double stranded DNA and double stranded RNA would fit across the concave side of the protein (Spåhr et al., 2010). Furthermore, given that the half-doughnut form is slightly twisted, the positive surface is perfectly organized to interact along one strand of a dsDNA or a dsRNA.

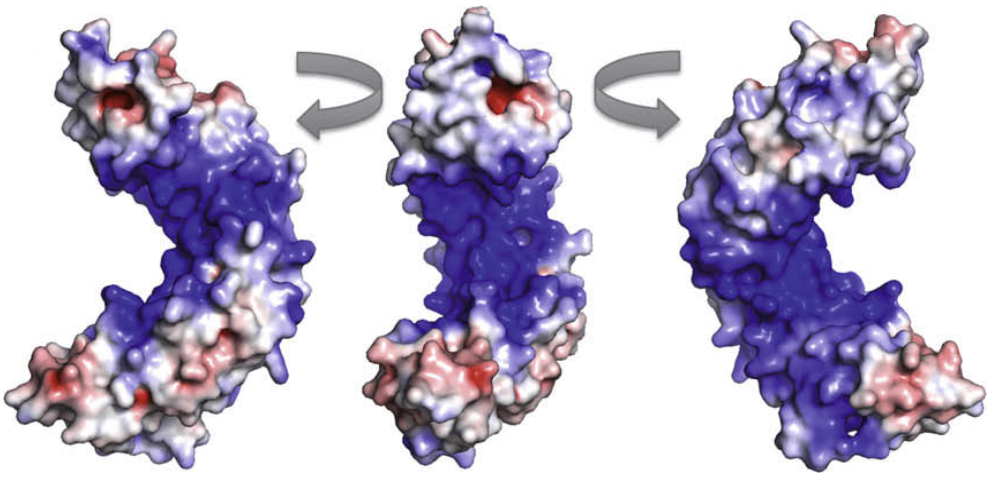

Figure 1.5.3 - Side and front views of the molecular surface of MTERF3, coloured by the local electrostatic potential (blue, positive charges; red, negative charges). Taken from Spåhr et al., 2010

Although the correct tertiary structure and the mechanism of DNA binding were elucidated only recently, the study of MTERFs started as early as 1989, when the first MTERF protein in

human – referred to as hMTERF1 – was identified, when the MELAS syndrome (mitochondrial myopathy, encephalopathy, lactic acidosis, and stroke-like episodes) caused by a pathogenic mutation in the mitochondrial *tRNA^{Leu}* gene was investigated (Kruse et al., 1989). The MELAS mutation occurs within the mtDNA binding site for the mTERF1, a 28 nucleotides sequence located immediately downstream of the 3' end of the *16S rRNA* gene within the *tRNA^{Leu}* gene (Chomyn et al., 1992). It has been shown that the binding of the protein to the DNA region arrests mitochondrial RNA polymerase progression *in vitro* (Fernandez-Silva et al., 1997).

Further studies demonstrated that mTERF1 binds simultaneously both to a region upstream of the *16S rRNA* gene (HSP1 initiation site) and to its termination region resulting in the looping out of intervening rDNA (Asin-Cayuela et al., 2004). This event is thought to promote the recruitment of the transcription complexes, which are comprised of mitochondrial RNA polymerase (POLRMT), Tfam - a stimulatory factor that unwinds DNA - and one of the two TFB isoforms (TFB1M or TFB2M) that function as dissociable specificity factors that contact both the polymerase and Tfam (Scarpulla, 2008 and Figure 1.5.4). These interactions are proposed to enhance reinitiation rate, resulting in a higher rate of rRNA synthesis; the efficiency of the proposed interaction can be considered fundamental, as generally rRNAs levels are 40 to 50 folds higher than mRNAs (Martin et al., 2005; Roberti et al., 2009).

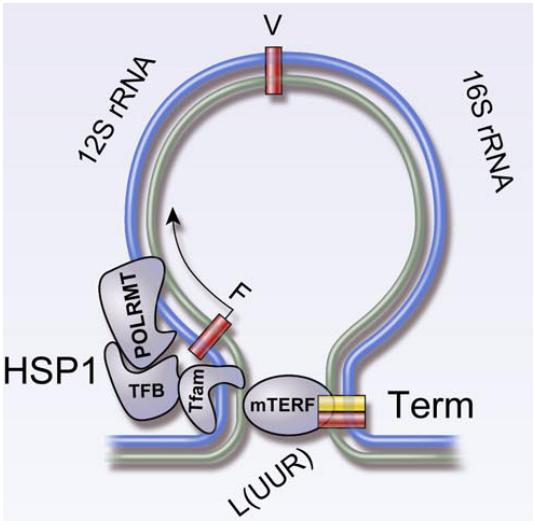

Figure 1.5.4 - Schematic representation of mtDNA transcription within the D-loop regulatory region in *Homo sapiens*. The transcription termination factor mTERF binds simultaneously both HSP1 and Term (yellow bar) resulting in the looping out of the intervening 12S and 16S rDNA. This is thought to promote efficient recycling of the transcription complexes (POLMRMT, TFB, Tfam) resulting in a high rate of rDNA transcription. The mechanism likely contributes to maintaining a high ratio of rRNA to mRNA required for operation of the mitochondrial translation machinery. Taken from Scarpulla, 2008.

It is known that regulation of rRNA synthesis and hence ribosome amounts is an important mechanism to internal and external stimuli response both in eukaryotes (Nomura, 1999) and prokaryotes (Condon et al., 1995), as ribosomes are responsible for translation, a crucial mechanism for the cell. The mechanisms involved in the control of rRNA and ribosome synthesis are still not completely understood, neither for prokaryotic and eukaryotic cytoplasmatic ribosomes, nor for organellar ribosomes.

1.5.1 MTERFs in plants

Despite the fact that flowering plants contain the highest number of MTERF proteins, only four plant MTERFs have been characterized to date. The first MTERF identified in a photosynthetic organism was MOC1 (mterf-like gene of *Chlamydomonas reinhardtii*) (Schönfeld et al., 2004). MOC1 is targeted to the mitochondrion, shows a light-sensitive regulation and its loss causes defects in the mitochondrial respiratory chain, but the exact molecular function has not been elucidated so far (Schönfeld et al., 2004). Another plant MTERF was identified among the components of the Transcriptionally Active Plastid Chromosome (pTAC) and named PTAC15, but its function has also not yet been elucidated (Pfalz et al., 2006).

In 2009, Meskauskiene et al. found that a mutation in the MTERF protein SOLDAT10 (singlet oxygen-linked death activator) is able to partially suppress the phenotype of the conditional *Arabidopsis thaliana flu* mutant, which generates singlet oxygen ($^1O_2$) in plastids during dark to light shifts. T-DNA insertion lines of *soldat10* single mutants are lethal and produce white embryos, while a single point mutation line shows a specific defect in 16S rRNA and 23S rRNA accumulation, which is indicated as the most likely origin of defects in plastid protein translation rates (Meskauskiene et al., 2009).

Babiychuk et al. (2011) characterized a MTERF protein targeted to chloroplasts, named BSM (BELAYA SMERT, or white death in Russian). In the Arabidopsis *bsm* mutant, immature seeds remained white, indicating a failure of the embryo to differentiate chloroplasts, and embryo development was arrested. *In vitro* cultured seeds developed slowly and led to poorly developed and malformed albino seedlings. An allelic mutant of BSM was isolated by Quesada et al. (2011), and named *rugosa2* (*rug2*). In the same study, it was demonstrated that BSM was dually targeted to chloroplasts and mitochondria. Thus, BSM is the first MTERF to be found both in mitochondria and chloroplasts. The *rug2* mutant showed a pleiotropic phenotype that included leaf variegation, reduced growth and perturbations in mitochondrial

and chloroplastic gene expression and development. Genes encoding the 16S, 23S and 4.5S rRNAs were downregulated both in *rug2* and *bsm* allelic mutants (Quesada et al., 2011; Babiychuk et al., 2011).

Taken together, the data available in the literature indicate that MTERFs represent crucial players in the ontogenesis of organelles. The study of this protein family in plants could therefore lead to a better understanding of mechanisms that regulate essential functions such as gene expression in chloroplasts and mitochondria.

1.6 Aim of the thesis

The present work is focused on the characterization of a novel plant MTERF in *Arabidopsis thaliana*, referred to as PHOTOSYNTHESIS AFFECTED MUTANT 48 (PAM48), in particular concerning its possible involvement in organellar gene expression.

The first aim of the thesis was to understand the physiological role of the protein in the plant, pursued trough a detailed characterization of different *pam48* allelic mutants, involving analyses of their phenotype, photosynthetic performance and transcriptional and translational rates. Secondly, the subcellular targeting of the protein was studied and the effects of the mutation in different cellular compartments were investigated.

The final aim of the work was to dissect the molecular function of the protein and confirm its putatively conserved DNA binding function as well as to find its nucleic acid targets within the organellar chromosomes. To this end, a bacterial one-hybrid screening was performed for the first time for a plant protein. The possible consequences of the binding of PAM48 to its DNA targets were investigated also *in vivo*, through the analysis of the maturation patterns of the target gene transcripts.

2 MATERIALS AND METHODS

2.1 Plant material and growth conditions

Previous screening of the Arabidopsis GABI-KAT T-DNA insertion collection (Rosso et al., 2003) for plants showing alterations in the effective quantum yield of PSII (Φ_{II}) resulted in the identification of a set of mutants with defects in photosynthesis (Varotto et al., 2000). Among this collection, the line GABI_152G06 was isolated as homozygous recessive mutant and renamed as *pam48-1* (*photosynthesis affected mutant 48-1*). The mutant carries a T-DNA insertion in the 5'UTR region of the AT4g38160 locus (AGI).

Two other T-DNA insertion lines for the At4g38160 locus were identified in the SIGnAL database (Alonso et al., 2003): *pam48-2* (SAIL_360_H09) and *pam48-3* (SAIL_143_B01). For all lines the insertion site has been determined using gene-specific and T-DNA specific primers, followed by sequencing of the PCR products (see paragraph 2.4).

Arabidopsis thaliana wild-type (ecotype Columbia 0) and mutant seeds were sown in Petri dishes on water soaked Whatman paper and incubated two days at 4°C in the dark to break dormancy and to synchronise germination. Plants were grown on soil under greenhouse controlled conditions (PFD: 70-90 µE m^{-2} s^{-1}, 16 h light: 8 h dark cycles) or under controlled environmental chamber (phytotrone) conditions at 22°C/18°C with a 8 h/16 h light/dark photoperiod.

For microarray analysis, after cold treatment (2 days, 4°C in the dark), seeds were sown in plastic pots with Stender Vermehrungssubstrat (A210) soil (Stender AG, 46514 Schermbeck). Col-0 and *pam48-1* leaves were harvested at 1.09 stage (leaf production stage with 9 rosette leaves >1 mm in length, according to Boyes et al., 2001), after 8 h of light. Plants were grown under controlled environmental chamber with short-day conditions: day period of 8 hours with 22°C, humidity 55%, light intensity 100 µ$Em^{-2}s^{-1}$ (Sylvania LUXLINE PLUS, T5, 39W, light colour 830); night period of 16 hours with 18°C, humidity 65%.

For *in vitro* growth conditions, after sterilization with 60% (v/v) sodium hypochlorite and cold treatment, seedlings were grown on Murashige and Skoog medium (MS medium; Murashige and Skoog, 1962; Sigma-Aldrich, Schnelldorf, Germany) containing 1.0 % (w/v) sucrose and 1 % (w/v) agar.

2.2 DNA isolation from plant material

Harvested leaves were homogenized in 400 µl extraction buffer containing 200 mM Tris-HCl (pH 7.5), 25 mM NaCl, 25 mM EDTA and 0.5 % (w/v) SDS. After centrifugation for 15 min at 16,100 x *g*, 300 µl of isopropyl alcohol were added to the supernatant to precipitate DNA.
After 15 min of centrifugation at 16,100 x *g*, the resulting pellet was washed with 70 % (v/v) ethanol, centrifuged again (5 minutes at 16,100 x *g*) and dried. DNA was then resuspended in distilled water.

2.3 Total RNA isolation from plant material

Harvested leaves were frozen and homogenized in liquid nitrogen. 1 ml of TRIZOL (Invitrogen) was added to approximately 100 mg of frozen material. Samples were incubated for 5 min at room temperature and 500 µl of chloroform were added; after vortexing and 5 further minutes of incubation at room temperature, samples were spun for 20 min at 16,100 x *g* to allow phase separation. The upper aqueous phase was carefully taken and precipitated with 400 µl of isopropyl alcohol; the RNA was then collected by centrifugation for 30 minutes at 16,100 x *g,* 4 °C. The resulting pellet was washed with 70 % (v/v) ethanol and centrifuged for 5 min at 16,100 x *g*, 4°C and let dry at room temperature. The resulting RNA pellet was eventually resuspended in RNases-free water and stored at -80 °C until further use.
Alternatively, total RNA from 100 mg of leaf tissue was extracted with the RNeasy Mini kit (Qiagen) and treated with the on column DNase Set (Qiagen), according to the manufacturer's instructions.
Isolated RNA was quantified with NanoDrop (Thermoscientific) and analyzed via electrophoresis on a 2 % (w/v) agar-gel containing ethidium bromide.

2.4 Screening for T-DNA insertion lines

Arabidopsis DNA was isolated from leaf tissue as described in paragraph 2.2. Insertion junction sites were isolated by PCR reaction using a combination of gene and T-DNA insertion specific primers. PCR runs were performed with Taq polymerase (Qiagen) and the following cycling conditions: 3 min at 94 °C initial denaturation, followed by 32 cycles of 20 s denaturation at 94 °C, 30 seconds annealing at 55 °C and 1 min 45 s elongation at 72 °C. After a final elongation step of 10 min at 72 °C, the PCR products were separated by a 1 % agarose gel. The primer combination used for the *pam48-1* T-DNA insertion derived from the pAC161 vector was the insertion-specific primer LBgk1

(5'-CCCATTTGGACGTGAATGTAGACAC-3') and the gene-specific primer PAM48-360s (5´-GTGGATAAGCTTCTCACTTTCAG-3´). Primer specific for the *pam48-2* and *pam48-3* T-DNA insertions derived from the pCSA110 vector were the insertion-specific primer LB3 (5´-TAGCATCTGAATTTCATAACCAATCTCGA TACAC-3´) and the gene-specific primer PAM48-as (5´-CTAGAAGCTTGCAGTTACCTCC-3'). PCR products were isolated, purified and sequenced in order to confirm the insertion positions within the *At4g38160* gene.

2.5 cDNA synthesis and real-time PCR

cDNA was prepared from 1 µg of total RNA using the iScript cDNA Synthesis Kit (Bio-Rad) according to the manufacturer's instructions. Prior to cDNA synthesis, RNA samples were treated with DNase I (New England BioLabs), according to manufacturer's instruction, to remove any possible genomic DNA contamination. To quantify and to check the quality of the synthesized cDNA, the reverse transcriptase (RT)-PCR was performed using an exon-exon boundary primer combination for the housekeeping gene *UBIQUITIN* (see Table 2.5.1, RT primers). Thermal cycling consisted of an initial step at 95 °C for 3 min, followed by 30 cycles of 10 s at 95 °C, 30 s at 55 °C and 10 s at 72 °C. 2 µl of 1:10 cDNA dilution was used in 20 µl of reaction for both RT- PCR and for real-time PCR.

For real-time PCR analysis, the cDNA and specific primers were added to a solution containing iQ™ SYBR® Green Supermix (Bio-Rad), and the thermal cycling consisted of an initial step at 95°C for 3 min, followed by 40 cycles of 10 s at 95 °C, 30 s at 55 °C and 10 s at 72 °C, after which a melting curve was performed. The genes investigated, and the corresponding primers, are listed in Table 2.5.1. Whenever possible, primers were designed to flank intron sites to make it possible to discriminate amplification of genomic DNA. RT-PCR was monitored by using the iQ5™ Multi Color Real-Time PCR Detection System (Bio-Rad). The adjustment of baseline and threshold was done according to the manufacturer's instructions. Relative transcript abundances were normalized with respect to the level of the constitutively expressed mRNA for an ubiquitin-protein ligase-like protein (At4g36800). The data were analyzed by using LinRegPCR (Ramakers et al., 2003) and according to Pfaffl (2001).

Table 2.5.1 – List of primer pairs used in RT-PCR analysis

Gene	Locus identifier	Forward primer sequence (5'-3')	Reverse Primer sequence (5'-3')
PAM48.1	*AT4G38160.1*	GTGGATAAGCTTCTCACTTTCAG	TCGGCATCCAGAAGCTTGCAGTTACCTC
PAM48.2	*AT4G38160.2*	GTGGATAAGCTTCTCACTTTCAG	TCATCGGCATCCACGCAGCACACTTC
PAM48.3	*AT4G38160.3*	GTGGATAAGCTTCTCACTTTCAG	TCAAATGTGACCTTTGACTAGGG
UBIQUITIN	*At4g36800*	GGAAAAAGGTCTGACCGACA	CTGTTCACGGAACCCAATTC

2.6 Northern blot analysis

Northern blotting and hybridisation of probes were performed using standard procedures (Sambrook and Russel, 2001). 2 to 10 µg of total RNA were denatured for 5 minutes at 95 °C in loading dye (40% (w/v) MOPS, 3,1% (v/v) formamide, 20% (v/v) glycerol, 1,2 M formaldehyde; 0,05 M EDTA) and separated on a denaturing 1.2 % (w/v) agarose gel containing 2% (v/v) 12.5 M formaldehyde, blotted on nylon membrane (Roche, Grenzach-Wyhlen, Germany) and hybridised for 16 h at 65 °C (hybridisation buffer: 1.8 % (w/v) NaH_2PO_4 x H_2O; 6.6 % (w/v) Na_2HPO_4 x 2 H_2O; 7 % (w/v) SDS; 1 % (w/v) BSA; 1 mM EDTA) with cDNA probes labelled with ^{32}P-dCTP using random hexamer primer and Klenow Fragment (New England Biolabs) reaction. After washing three times (20 min at 65 °C; washing buffer: 1 % (v/v) SDS; 0.4 % (v/v) 0.5 M EDTA; 8 % (v/v) Na-P [74.4 % (v/v) 0.5 M Na_2HPO_4 x 2 H_2O and 25.6 % (v/v) 0.5 M NaH_2PO_4 x H_2O]), filters were exposed to a phosphorimager screen and analysed by a Typhoon Variable Mode Imager (GE Healthcare) using ImageQuant version 5.2 (GE Healthcare).

Primer pairs used to generate specific cDNA probes are listed in Table 2.6.1.

Table 2.6.1 - List of primes used in Northern blot hybridization analysis

Gene	**Locus identifier**	**Forward primer sequence (5'-3')**	**Reverse primer sequence (5'-3')**
psaB	*ATCG00340*	TCCGGTGCCATTATTCCTAC	CTTCTTCTTGCCCGAATCTG
CP43	*ATCG00280*	TCCAGCAACAACAAAAGCTG	TCCAGCAACAACAAAAGCTG
CP47	*ATCG00680*	CGGGTCTTTGGAGTTACGAA	TCCAGCAACAACAAAAGCTG
PSBP	*AT1G06680*	CTCCTGAACAGTTCCTCTCT	ACACTGAAGGACGTAGCAGC
LHCA1	*AT3G54890*	GTCAAGCCACTTACTTGGGA	GGGATAACAATATCGCCAATG
LHCA2	*AT3G61470*	GAGTTCCTAACGAAGATCGG	AAGATTGTGGCGTGACCAGG
LHCB1.2	*AT1G29910*	GACTTTCAGCTGATCCCGAG	CGGTCCCTTACCAGTGACAA
LHCB2.2	*AT2G05070*	GAGACATTCGCTAAGAACCG	CCAGTAACAATGGCTTGGAC
ACT1	*At2g37620*	TGCGACAATGGAACTGGAATG	GGATAGCATGTGGAAGTGCATACC
rrn16	*ATCg00920*	AGTCATCATGCCCCTTATGC	CAGTCACTAGCCCTGCCTTC
rrn23	*AtC00950*	GTTCGAGTACCAGGCGCTAC	CGGAGACCTGTGTTTTTGGT
rrn5	*ATCG00970*	TATTCTGGTGTCCTAGGCGTAG	ATCCTGGCGTCGAGCTATTTTTCC
rrn18	*AtMg01390*	AGTTTTTGACCCAGGTGACG	CCAACTTCATGTTCCCGAGT
rrn26	*AtMg00020*	AAGCAGCCATCCTTTGAAGA	AAGCAGCCATCCTTTGAAGA
rrn5	*AtMg01380*	GGCACTACGGTGAGACGTG	GACCATGTCTCCCGAACAAT

2.7 Bacterial one-hybrid assay (B1H)

B1H assay was performed according to the protocol described in Meng and Wolfe (2006). PAM48 splice form 1 (*At4g38160.1*) was amplified by PCR with the primer pair 5'-GAGGTACCATGGAGGTGACAAATACG-3' and 5'-GATCTAGACTAGAAGCTTGCAG TTAC-3'. The PCR product was cloned in the pB1H2w2-Prd vector (obtained from Prof. Wolfe's laboratory, University of Massachusetts), using KpnI and XbaI restriction enzymes (New England Biolabs). The vector was then introduced into the *E. coli* strain USO hisB-pyrF-rpoZ (Prof. Wolfe's laboratory, University of Massachusetts). The 18 nucleotide random library was generated by cloning the 5'-ACTGCGGCCGCTATCAGNNNNNNNNNNNNNNNN NNGAATTCATACTACTA-3' sequence into the pH3U3-mcs vector (Prof. Wolfe's laboratory, University of Massachusetts). Self-activating sequences were eliminated by negative 5-FOA selection. The rescued vector library was then introduced in the *E. coli* USO hisB$^-$ pyrF$^-$ rpoZ$^-$ strain containing the pB1H2w2-PAM48.1 vector and the selection screen was performed on selective medium w/o histidine, containing appropriate antibiotics (ampicillin 100 µg/ml, kanamycin 50 µg/ml and tetracycline 10 µg/ml), 10 µM IPTG, and increasing concentrations of 3-AT (0, 1, 2, 4 mM). Surviving colonies were screened via colony PCR using the primers 5'-CAAATATGTATCCGCTCATGAC-3' and 5'-GGGCTTTCTGCTCTGTCATAG-3' flanking the random region in the pH3U3-mcs vector, and the PCR products were sequenced. The resulting sequences were analyzed with MEME software (http://meme.sdsc.edu/meme/cgi-bin/meme.cgi) to obtain a consensus motif binding sequence and then analyzed with the MAST software (http://meme.sdsc.edu/meme/cgi-bin/mast.cgi) to find the putative binding motif within the chloroplast and mitochondrion genome sequences of *A. thaliana,* retrieved from the National Center for Biotechnology Information (NCBI, http://www.ncbi.nlm.nih.gov/).

2.8 Cloning of mTP-PAM48-GFP and cTP-PAM48-GFP constructs

The chloroplast targeting peptide (cTP) sequence of *RBCS* (*At1g67090*) and the mitochondrial targeting peptide sequence of *FUM1* (*At2g47510*) were amplified by PCR from WT cDNA using the primer pairs 5'-ATGGCTTCCTCTATGCTCTCTTCCG-3', 5'-CTCGAGGT TAACTCTTCCGCCGTTGCTTG-3' and 5'-ATGTCGATTTACGTCGCGTCGC-3', 5'-CTCGAG ATAAGATCTCAGAGAGGTGGCATAACGC-3' respectively, with the addition of XhoI cleavage site (5'-CTCGAG-3') at 3' end. The PCR products were cloned into pGEM T-easy vector (Promega), according to manufacturer's instructions.

PAM48.1 was amplified by PCR with the primers 5'-CTCGAGGTGACAAATACGAGCAGCAT CATG-3' and 5'-CTCGAGGAAGCTTGCAGTTACCTCCGAAAAG-3' with the addition of a

XhoI cleavage site (5'-CTCGAG-3') at 3' end. The PCR product was digested with XhoI restriction enzyme (New England Biolabs) to generate sticky ends. The digested product was cloned into cTP-RBCS and mTP-FUM1 vectors. The ligated constructs were used for GATEWAY subcloning in the pB7FWG2 vector, generating a fusion product with enhanced GFP (eGFP, Clonetech laboratories) under the control of the cauliflower mosaic virus 35S promoter.

2.9 Affymetrix ATH1 array hybridization and transcriptome data analysis

1 µg of total RNA from three biological replicates of different pools (10 plants each pool) at the 1.09 stage (leaf production stage with 9 rosette leaves >1 mm in length, according to Boyes et al., 2001) of wild type and *pam48-1* plants was processed and hybridized to a GeneChip Arabidopsis ATH1 Genome Array using the One-Cycle Target Labelling and Control Reagents according to the manufacturer's instructions (Affymetrix). Reverse transcription was employed to generate first-strand cDNA. After second-strand synthesis, double-stranded cDNA was used in an *in vitro* transcription reaction to generate biotinylated cRNA. The fragmented, biotinylated cRNA was used for hybridization. Hybridization, washing, staining, and scanning procedures were performed as described in the Affymetrix technical manual. A Hybridization Oven 640, a Fluidics Station, and a GeneChip Scanner 3000 were used. Transcriptome Data Analysis CEL files were imported into FlexArray (http://genomequebec.mcgill.ca/FlexArray) for further analysis. Raw intensity data were normalized using the robust multiarray average algorithm (RMA) (Irizarry et al., 2003). The data were log transformed, and a list of differentially expressed genes was generated. The significance of differential gene expression was estimated by comparing the observed and expected d values. A threshold of 2 for Δ (observed d value - expected d value) and a threshold of 0.05 for unadjusted P values (rawp < 0.05), together with the twofold change filter, were applied to identify differentially expressed genes. cRNA and hybridisation were carried out by NASC array service (http://affymetrix.arabidopsis.info/).

2.10 Total protein extraction from leaf material

Leaves from 4-week-old plants were harvested and homogenized in 2x SDS protein buffer (62.5 mM Tris-HCl (pH 6.8); 20 % (w/v) glycerine; 4 % (w/v) SDS; 100 mM DTT; 0.05 % (w/v) bromophenol blue). The homogenate was heated at 72 °C for 10 min and centrifuged 10 min at 16,100 x *g* for at room temperature to remove cellular debris.

The amount of proteins in the supernatant was quantified by amidoblack staining (Schaffner and Weissman, 1973). For that purpose 2.5 µl and 5 µl of each protein extract were used. After addition of 195 µl water and 800 µl staining solution (10 % (v/v) acetic acid (v/v), 90 (v/v) % methanol and small amount of amidoblack) solved material was centrifuged for 12 min at 16,100 x *g*. The obtained pellet was washed in 1 ml washing solution (10 % (v/v) acetic acid and 90 (v/v) % methanol), mixed and centrifuged again for 12 min at 16,100 x *g*. Air dried pellet was resolved in 1 ml 0.2 M NaOH. Extinction was measured at 615 nm and data were calibrated using a BSA calibration curve.

2.11 Thylakoids isolation

Thylakoids were isolated from 4 weeks old plants, according to the protocol of Bassi et al. (1985), with minor modifications. Leaves from 4 weeks old plants were harvested and homogenized in chilled T1 buffer (0.4 M sorbitol, 0.1 M Tricine-KOH pH 7.8, 0.5 % (w/v) milk powder). The homogenized plant material was filtered through two layers of Miracloth (Calbiochem) to remove cellular debris and the filtrate was centrifuged 5 min, 4 °C, 6000 rpm in a Beckmann centrifuge, rotor JA 25.50. After discarding the supernatant, the resulting thylakoid pellet was gently resuspended in 50 ml of chilled T2 buffer (25 mM HEPES/KOH pH 7.5, 10 mM EDTA) and centrifuged again 10 min, 4° C 10000 rpm in a Beckmann centrifuge, rotor Ja 25.50. The resulting pellet was resuspended in TMK buffer (10 mM Tris-HCl pH6.8, 10 mM $MgCl_2$, 20 mM KCl). Chlorophyll concentration was determined measuring the absorbance at different wavelengths (A_{750}, $A_{663.6}$ and $A_{646.6}$) after acetone precipitation as described in Porra (2002).

2.12 Intact chloroplasts isolation

Leaves of 4- to 5-week-old plants were homogenized in homogenization buffer (330 mM sorbitol, 20 mM Tricine (pH 7.6), 5 mM EGTA, 5 mM EDTA, 10 mM $NaHCO_3$, 0.1% BSA and 330 mg/L ascorbate) and the homogenate was filtered through two layers of Miracloth (Calbiochem). Chloroplasts were collected by centrifugation at 2,000 x *g* for 5 min at 4°C. The pellet was carefully resuspended in washing buffer (330 mM sorbitol, 20 mM HEPES/KOH (pH 7.6), 5 mM $MgCl_2$ and 2.5 mM EDTA). Chloroplasts were loaded on a two-step Percoll gradient as described in Aronsson and Jarvis (2002). Intact chloroplasts at the interface between the two Percoll phases were lysed by incubation for 30 min on ice in four volumes lysis buffer (20 mM HEPES/KOH (pH 7.5), 10 mM EDTA) and used for subsequent

experiments. To separate thylakoids and stroma phases, ruptured chloroplasts were centrifuged at 42,000 x *g*, 30 min at 4 °C.

2.13 Protein electrophoresis

2.13.1 SDS-PAGE

Protein preparations were separated via 12% polyacrylamide SDS gels, with SDS running buffer (25 mM Tris-HCl, 200 mM glycine, 0.1% (w/v) SDS), according to standard protocols (Sambrook et al., 1989)

2.13.2 Blue Native PAGE

Leaves from 4-week-old plants were harvested and thylakoids were prepared as described in paragraph 2.11. For the first dimension of Blue Native PAGE analysis, protein amounts equivalent to 100 µg of chlorophyll for each genotype were washed with 10 mM Tris-HCl (pH 6.8), 10 mM $MgCl_2$ and 20 mM KCl, and subsequently solubilised in 750 mM ε-aminocaproic acid, 50 mM Bis-Tris (pH 7.0), 5 mM EDTA (pH 7.0), 50 mM NaCl and 1.6 % (w/v) digitonin. Solubilised samples were then incubated for 1 h on ice and afterwards centrifuged for 1 h at 16,100 x *g* at 4° C. Supernatants were supplemented with 5 % (w/v) Coomassie-blue in 750 mM ε-aminocaproic acid, and directly loaded onto BN gels (4-12% acrylamide gels, containing 0.5 M ε-aminocaproic acid, 50 mM Bis-Tris (pH 7.0) and 10% (v/v) glycerol). One dimensional BN-PAGE was carried out at 750 V and 12 mA with cathode buffer (50 mM Tricine, 15 mM Bis-Tris (pH 7.0) and 0.02% Coomassie G) and anode buffer (50 mM Bis-Tris (pH 7.0)) as described by Schägger and von Jagow (1991). The gel slices corresponding to the first dimension were treated in denaturing buffer (0.125 M Tris-HCl (pH 6.8), 4 % (w/v) SDS and 1 % (v/v) β-mercaptoethanol) for 30 min at room temperature before the second dimension run. Separation of complexes through a 12 % polyacrylamide SDS-PAGE second dimension was performed as described in paragraph 2.13.1

2.14 Western blotting

After SDS-PAGE electrophoresis, proteins were transferred to PVDF (polyvinylidene fluoride) membranes (Millipore) by means of semi-dry blotting apparatus (Biorad) according to Towbin et al. (1979). The transfer was performed by applying a current corresponding to 0.8 mA cm^{-2} in transfer buffer (96 mM glycine, 10 mM Tris, 10 % (v/v) methanol).

After transfer, proteins were detected with Ponceau staining (2 % (w/v) Ponceau S in 30 % (w/v) TCA, 30 % (w/v) sulfosalicylic acid).

2.15 Immunodecoration

After western blotting, PVDF membranes were blocked in TBS-T buffer containing 0.5 % (w/v) milk powder for 1 h. Filters were probed with primary antibodies and subsequently with appropriate secondary antibodies, according to standard protocols (Sambrook et al., 1989). Antibodies for mitochondrial proteins detection were kindly provided by Dr. Iris Finkemeier (LMU University).

2.16 Heterologous protein expression and purification of inclusion bodies

The *At4g38160.1* full length coding sequence was amplified from wild type cDNA with the primer pair 5'-CACCATGGAGGTGACAAATACGAGC-'3 and 5'-CTAGAAGCTTGCAGTTACC TCC-3' and cloned into vector pET151/D-TOPO (Invitrogen). Protein over-expression was carried out in the BL21 (DE3) lysS *E. coli* strain, transformed with the mentioned construct. Liquid cell cultures were incubated at 37 °C, 180rpm shaking, in LB-medium supplemented with ampicillin for selection (Sambrook et al., 1989). Cells were grown to the mid-log phase (OD_{550} = 0.5 - 0.8), subsequently the protein expression was induced by adding 1 mM IPTG and carried out overnight at 37 °C.

E. coli cells overexpressing PAM48 were harvested by centrifugation at 7500 x *g* for 10 min, resuspended in RB buffer (50 mM Hepes, 50 mM NaCl, pH 7.5) and lysed by passage through a French pressure cell. The suspension was centrifuged at 30000 x *g* for 30 min and the resulting pellet was resuspended in DB1 buffer (20 mM Tris-HCl pH 7.5, 1 mM DTT, 0.5 % Triton X-100, 200 mM NaCl) and centrifuged 10 min at 7500 x *g*, 4 °C. The resulting pellet was resuspended in DB2 buffer (20 mM Tris-HCl pH 7.5, 1mM DTT, 0.5 % Triton X-100) and centrifuged 10 min at 7500 x *g* 4 °C. Finally, the pellet was washed twice in TB buffer (50 mM Tris-HCl pH 8.0, 1 mM DTT) by centrifuging at 7500 x *g*, 10 min, 4 °C.

2.17 Renaturation of PAM48 from inclusion bodies

500 µg of purified inclusion bodies obtained from *E. coli* BL21 (DE3) lysS strain expressing PAM48 protein (as described in paragraph 2.16) were resuspended in 500 µl of 1 % lithium dodecyl sulfate (LDS), 12.5 % (w/v) sucrose, 5 mM ε-aminocaproic acid, 1 mM benzamidine and 50 mM HEPES KOH, pH 7.8. Dithiothreitol (DTT) was added to a final concentration of 75 mM was added to prevent formation of disulphide bridges and the solution was subjected to three freezing-thawing cycles (20 min at -20 °C, 20 min at -80 °C, 20 min at -20 °C, thawing in a ice-water bath and 5 min at 25 °C). After completion of the three freezing-

thawing cycles, octyl-glucopyranoside (OGP) to a final concentration of 1 % (w/v) was added and kept on ice for 15 min. Afterwards, KCl to a final concentration of 75 mM was added to precipitate the LDS detergent. After centrifugation at 16000 x *g* at 4°C for 10 min to remove debris and aggregated proteins, the supernatant containing the refolded protein was collected and used for subsequent experiments or snap frozen in 10 % (v/v) glycerol with liquid nitrogen and stored at -80 °C, to avoid protein aggregation and precipitation.

2.18 Electrophoretic mobility shift assays

Electrophoretic mobility shift assay was performed according to the protocol of Hellman and Fried (2006), with some modifications.

2 µg of heterologously expressed and renaturated (according to protocols in paragraph 2.16 and 2.17) PAM48 were incubated for 30 min at 25 °C in 1 x binding buffer (10 mM Tris-HCl pH 7.5, 1 mM EDTA, 0.1 M KCl, 0.1 mM DTT, 5 % (v/v) glycerol, 0.01 mg ml^{-1} BSA) with 100 ng of ^{32}P-dCTP-labelled DNA probes (for sequences see Table 2.5.1; labelling of the probes was performed according to the protocol described in paragraph 2.6) and increasing concentration (0 ng, 100 ng, 250 ng, 500 ng, 1000 ng) of corresponding unlabelled DNA probe (competition assay).

Samples were resolved via vertical electrophoresis on a native 8 % polyacrylamide gel in TBE buffer (89 mM Tris-borate, 89 mM boric acid, 2 mM EDTA). After the run, dried gel were exposed to a phosphorimager screen and analysed with the Typhoon Variable Mode Imager (GE Healthcare).

Table 2.5.1 - List of DNA oligomers used as probes in EMSA analysis

Probe	**Locus identifier**	**Sequence (5'-3')**
TRNV	*ATCG00450*	NNNNNNNNNNNNNNCATTAAAATCAAAATNNNNNNNNN NNGAAAGGATGGGTGCGACGCG
16S rRNA	*ATCG00920*	NNNNNNNNNNNNNNATTGCGTCGTTCTGCNNNNNNNNN NNGAAAGGATGGGTGCGACGCG
RPS15	*ATCG01120*	NNNNNNNNNNNNNNGAATTGAGTCGTATNNNNNNNNN NGAAAGGATGGGTGCGACGCG
TRNV-s.n.w.	*ATCG00450*	NNNNNNNNNNNNNNCATNNNNNTCAAAATNNNNNNNNN NNGAAAGGATGGGTGCGACGCG
16S rRNA-s.n.w.	*ATCG00920*	NNNNNNNNNNNNNNNNNNCGTCGTTGTGCNNNNNNNN NNNGAAAGGATGGGTGCGACGCG
RPS12	*ATCG00065*	NNNNNNNNNNNNNNCAGTAAAAGCAAGACNNNNNNNNN NNGAAAGGATGGGTGCGACGCG
TRNT.1-first binding	*ATCG00260*	NNNNNNNNNNNNNNATATTGCGTTCCTGCNNNNNNNNN NNGAAAGGATGGGTGCGACGCG
TRNT.1-second binding	*ATCG00260*	NNNNNNNNNNNNNNATCATGACTATATCCNNNNNNNNN NNGAAAGGATGGGTGCGACGCG
TRNL	*ATCG00400*	NNNNNNNNNNNNNNATGGTATTCGTGAACNNNNNNNNN NNGAAAGGATGGGTGCGACGCG

2.19 *In vitro* transcription and translation

At4g38160.1 was cloned into the pGEM-T-Easy vector (Promega) under the control of the T7 promoter. 3 µg of the SpeI linearised vector were used in a in vitro transcription reaction, using the SP6/T7 transcription kit (Roche) following manufacturer's instructions.

The transcription product was directly used for *in vitro* translation using either the Rabbit Reticulocyte Lysate System or the Wheat Germ Extract from Promega following the manufacturers' protocol in presence of ^{35}S-methionine for radioactive labelling.

2.20 *In vitro* import into pea chloroplasts

Aliquots of PAM48 in vitro translation reaction (see paragraph 2.19) were centrifuged at 50,000 *x g* for 1 h at 4 °C prior to import experiments. The experiment was carried out according to the protocol described in Bölter and Soll (2007). Intact chloroplasts were isolated from 10-day-old pea leaves (*Pisum sativum*, var. Golf) and purified by Percoll-gradient centrifugation. Import assays were performed in 100 µl of import buffer (330mM sorbitol, 50mM HEPES/KOH pH7.6, 3mM MgSO4 10mM methionine, 10mM cysteine, 20mM K-gluconate, 10mM NaHCO3, 2% BSA (w/v)) with chloroplasts equivalent to 15 µg of chlorophyll. The import reaction was carried out at 25 °C for 20 min, followed by a repurification step of the chloroplasts using a 40 % Percoll cushion. For thermolysin treatment, chloroplasts were washed with 330 mM sorbitol, 50 mM HEPES pH 7.6, 0.5 mM $CaCl_2$ and subsequently incubated with 20 µg/ml thermolysin (Calbiochem, Darmstadt, Germany) for 20 min on ice. The reaction was stopped by adding EDTA to a final concentration of 10 mM.

Chloroplast were reisolated via centrifugation for 1 min at 800 x *g* and washed in washing buffer (330 mM sorbitol, 50mM HEPES/KOH, pH7.6, 5 mM EDTA). After centrifugation for 1 min at 800 x *g*, the chloroplasts were resuspended in Laemmli buffer (50 mM Tris-HCl pH 6.8, 100 mM β-mercaptoethanol, 2% (w/v) sodium dodecyl sulfate (SDS), 0.1% (w/v) bromophenol blue, 10% (v/v) glycerol. and used for SDS-PAGE analysis without further treatment. Labelled proteins were separated using SDS-PAGE and detected by phosphor-imaging (Typhoon; Amersham Biosciences).

2.21 MICROSCOPY

2.21.1 Subcellular localisation of PAM48-eGFP fusions in Arabidopsis protoplasts

The enhanced Green Fluorescent Protein (eGFP) was used as a reporter to determine the subcellular localisation of PAM48, using protoplasts of plants stably expressing the PAM48-GFP construct. Cotyledons of transformed two-week-old Arabidopsis plants were cut and incubated overnight at 23 °C in the dark in an appropriate cell wall lysis solution (10 mM MES, 20 mM $CaCl_2$, 0.5 M mannitol pH 5.8, 0.1 g/ml macerozyme (Duchefa), 0.1 g/ml cellulase (Duchefa)). Protoplasts were collected by centrifugation at 50 g for 10 min after filtration through a nylon mesh (Ø 75 µm), followed by resuspension in 8 ml of MSC solution (10 mM MES, 20 mM $CaCl_2$, 0.5 M mannitol, 120 g/l sucrose, pH 5.8). Subsequently, 2 ml of MMM solution (10 mM MES, 10 mM $CaCl_2$, 10 mM $MgSO_4$, 0.5 M mannitol, pH 5.8) were added on top of the protoplasts and intact protoplasts were recovered at the interface

between the two solutions after centrifugation at 70 g for 10 min as described in Dovzhenko et al. (2003). Microscopic analyses were carried out after overnight incubation at 23 °C in the dark using an Axio Imager fluorescence microscope with integrated ApoTome (Zeiss). Fluorescence was excited via an X-Cite Series 120 fluorescence lamp (EXFO) and detected at wavelength ranges of 460 - 500 nm (eGFP fluorescence) and 670 - 750 nm (chlorophyll autofluorescence).

2.21.2 Transmission electron microscopy

Embryos of wild-type and *pam48-2* plants were isolated from their seeds and fixed immediately with 2.5% (v/v) glutardialdehyde in fixative buffer (75 mM sodium cacodylate, 2 mM $MgCl_2$ pH 7.0) for 1 h at room temperature, rinsed several times in fixative buffer and post-fixed for 2 h with 1 % (w/v) osmium tetroxide in fixative buffer at room temperature. After two washing steps in distilled water, the cells were stained *en bloc* with 1 % uranyl acetate in 20 % acetone for 30 min. Dehydration was performed with a graded acetone series. Samples were infiltrated and embedded in Spurr's low-viscosity resin (Spurr, 1969). After polymerisation, ultra thin sections with a thickness between 50 and 70 nm were cut with a diamond knife and mounted on uncoated copper grids. The sections were post-stained with aqueous lead citrate (100 mM, pH 13.0). All micrographs were taken with an EM 912 electron microscope (Zeiss) equipped with an integrated OMEGA energy filter operated in the zero loss mode. TEM analysis was performed in collaboration with Prof. Dr. G. Wanner (LMU University) and his group.

3 RESULTS

3.1 Identification of mutants for the *PAM48* locus

In order to better investigate the effect of a misregulation of the *At4g38160* gene, three T-DNA insertion lines were chosen. The first line was isolated from a previous screening of the Arabidopsis GABI-KAT T-DNA insertion collection (Rosso et al., 2003) for plants showing alterations in the effective quantum yield of PSII (Φ_{II}) named *pam48-1* (*photosynthesis affected mutant 48-1*). This line was previously identified as a knock-down homozygous mutant in which the T-DNA was found to be inserted in the 5' untranslated region (UTR), at position -115 relative to the start codon. Other two lines were identified in the SIGnAL database (Alonso and Stepanova., 2003). *pam48-2* was found to be a homozygous mutant line, in which the T-DNA was inserted in an exonic region, at position +706 relative to the start codon. *pam48-3*, has been studied as a heterozygous line and carried a T-DNA insertion at +1178 bp from the start codon, corresponding to a intronic region for the splice variants *At4g38160.2* and *At4g38160.3*, and to the 3'UTR region for the splice variant *At4g38160.1* (for a scheme of the insertion, see Figure 3.1.1).

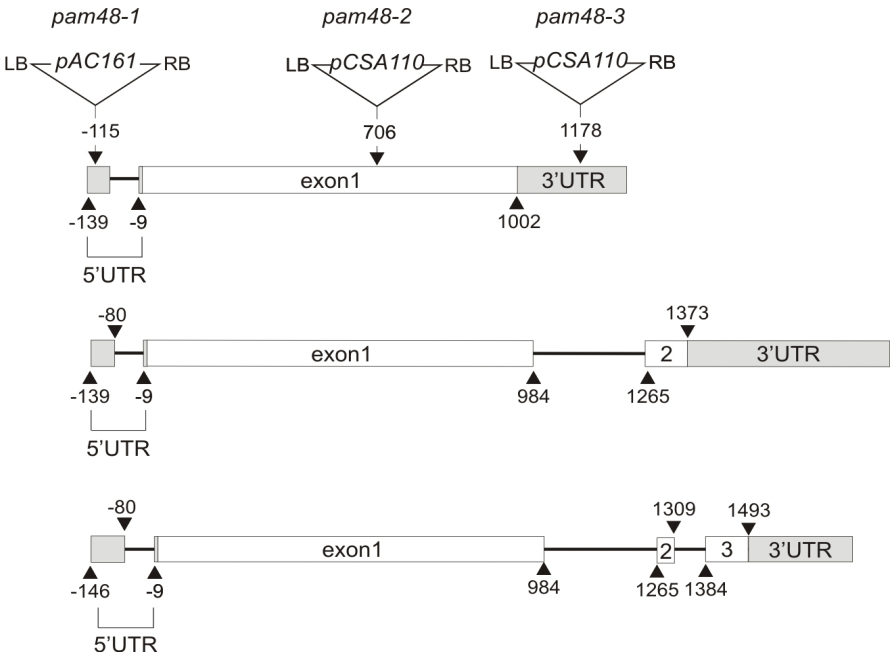

Figure 3.1.1 - Gene structure and *At4g38160* splice variants including T-DNA insertion sites. White boxes indicate exons, grey boxes 5'-UTR and 3'-UTR regions. Introns are depicted as thin lines.

T-DNA insertion and plant zygosis were confirmed via PCR on genomic DNA for all the lines, using primer pairs specific for the T-DNA insertion and for the *At4g38160* gene sequence, as illustrated in Figure 3.1.2.

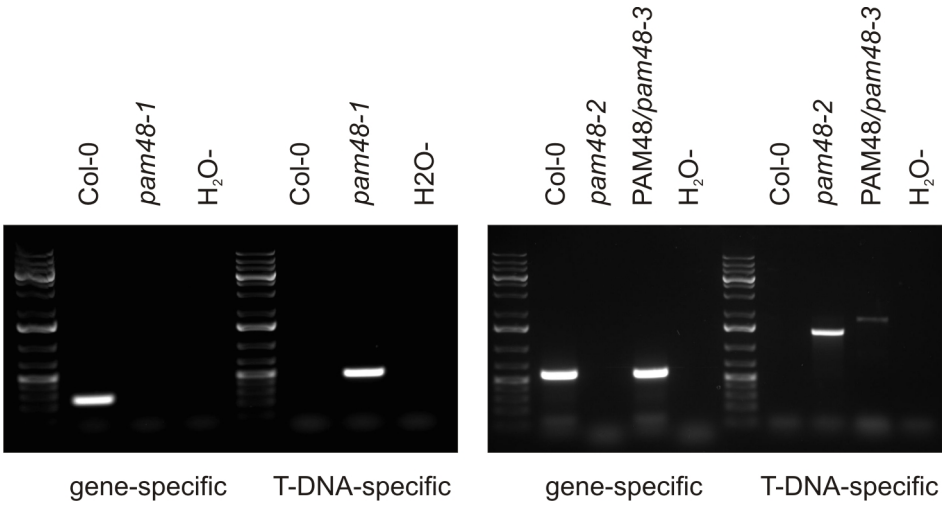

Figure 3.1.2 - T-DNA insertion and zygosis of *pam48-1*, *pam48-2* and *pam48-3*. PCR was performed using gene-specific and T-DNA insertion-specific primer pairs (for details see material and methods, paragraph 2.2.3)

3.2 Different allelic mutations of *PAM48* and their effects

The *pam48-1* knock down mutant is characterized by a photosynthetic phenotype with pale, chlorotic and small leaves in comparison to wild-type (Figure 3.2.1). Mutant plants are able to complete the growth cycle, although with a general delay in development, and produce viable seeds.

When grown on soil, one fourth of the seeds from heterozygous *pam48-2* and *pam48-3* plants were not able to germinate, suggesting a defect in the early stages of seed development. When grown on MS plates supplemented with sugar, *pam48-2* homozygous plants were able to germinate, producing seedlings with white cotyledons that developed into albino plants (Figure 3.2.2, A). These plants died normally after the 4th leaf stage, though in a few cases *pam48-2* mutants survived until the floral shoot stage. In these rare cases plants showed malformations and a general alteration in their morphogenetic pattern, generating curly white leaves and abnormal, shapeless floral shoot. Siliques of heterozygous *pam48-2* plants observed under the stereomicroscope revealed the presence of one fourth white seeds (Figure 3.2.2, B).

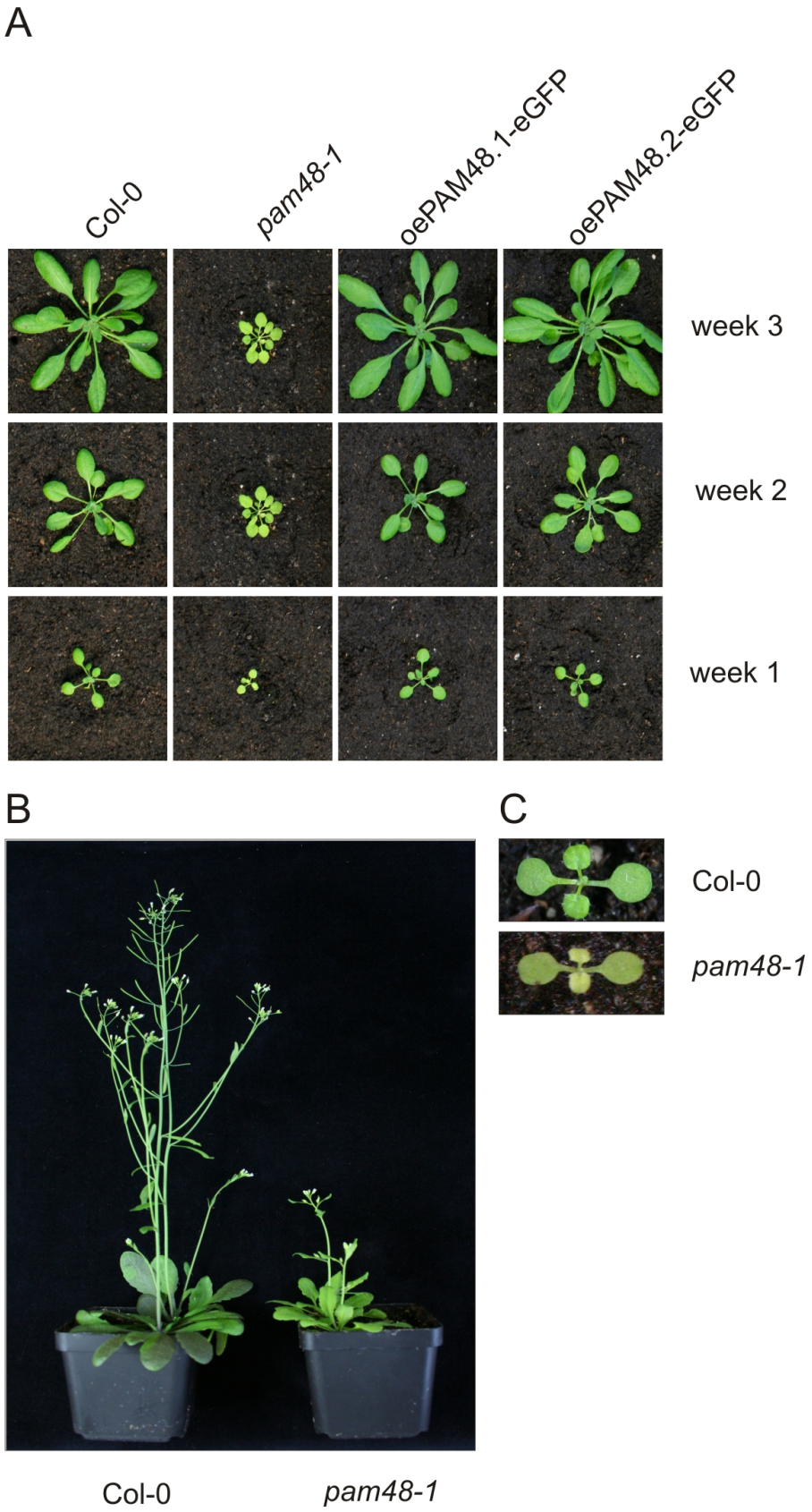

Figure 3.2.1 - Phenotype of the *pam48-1* mutant and complemented plants. A) Phenotypes of Col-0, *pam48-1* and *pam48-1* plants complemented with 35S:PAM48.1-eGFP (oePAM48.1-eGFP) and 35S:PAM48.2-eGFP (oePAM48.2-eGFP) after 1, 2 and 3 weeks of growth. B) Generative stage of Col-0 and *pam48-1*, after >5weeks growth. C) Seedlings with emerging first true leaves of Col-0 and *pam48-1*; while cotyledons appear similar in growth and colour, the first true leaves are much paler in the mutant.

Growth of the *pam48-3* heterozygous seeds on sugar did not lead to the isolation of a homozygous plant, suggesting a more severe phenotype for this line, which showed aborted seeds in the siliques (Figure 3.2.2, C).

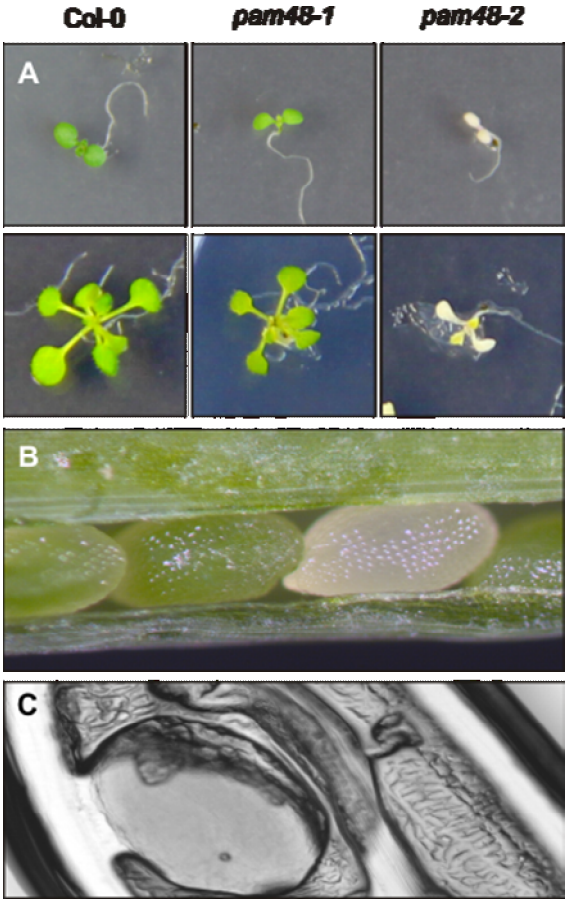

Figure 3.2.2 - Phenotypes of *pam48-2* and *pam48-3*. A) Seedlings (10 days) and plants (about 3 weeks) of Col-0, *pam48-1* and *pam48-2* grown on MS medium supplemented with sugar. B) PAM48/*pam48-2* heterozygous siliques containing immature seeds. The white seeds correspond to homozygous *pam48-2* seeds. C) PAM48/*pam48-3* heterozygous siliques. On the left a mature normally developed seed, on the right an early stage aborted seed, corresponding to homozygous *pam48-3*.

3.3 Complementation of the *pam48-1* mutant

In order to establish the linkage between the depletion of *At4g38160* transcription level and the *pam48-1* phenotype, complementation of the *pam48-1* mutant was performed. The full length coding sequence of the splice forms *At4g38160.1* and *At4g38160.2* were fused to the eGFP gene and cloned under the control of the 35SCaMV promoter. Subsequently, *pam48-1* plants were transformed by floral dip (Clough et al. 1998). After selection with appropriate media, the insertion was confirmed via PCR with specific primers. As shown in Figure 3.2.1, both splice variants are able to successfully complement the mutant phenotype.

3.4 Knock –down of PAM48 leads to defects in photosynthesis

To confirm the photosynthetic phenotype observed in *pam48-1* mutant plants, fluorimetric analysis was performed using a Pulse Amplitude Modulated chlorophyll fluorometer (PAM), comparing wild-type, *pam48-1,* and the complemented oePAM48.1 and oePAM48.*2* lines. In the *pam48-1* mutant, the maximum quantum efficiency of PSII photochemistry (F_V/F_M) showed a significant decrease, that was successfully complemented in the oePAM48.1 and oePAM48.2 lines, both showing values comparable to WT (Table 3.4.1).

The *pam48-1* mutant showed a drop in photosystem II efficiency, which was successfully rescued in the complemented lines. Also the effective quantum yield of PSII (Φ_{II}) was reduced in the *pam48-1* mutant. The fraction of the primary electron receptor of PSII (Q_A) present in the reduced state, estimated by the parameter 1-qP, was increased in *pam48-1* mutant plants and again comparable to WT values in the complemented lines. The overall picture deducible from the fluorimetric analysis suggests therefore a defect in the electron flow through PSII that influences also the downstream steps of photosynthetic electron transfer.

Table 3.4.1 – Spectroscopic data for WT, *pam48-1* and complemented plants, mean values (± SD).

line	Fv/Fm	Φ_{II}	NPQ	1-qp
WT	0.81 (+/- 0.01)	0.70 (+/-0.03)	0.14 (+/- 0.03)	0.11 (+/-0.03)
pam48-1	0.54 (+/-0.03)	0.43 (+/- 0.02)	0.11 (+/- 0.04)	0.57 (+/- 0.04)
oePAM48.1	0.82 (+/- 0.01)	0.69 (+/- 0.04)	0.16 (+/- 0.02)	0.14 (+/-0.03)
oePAM48.2	0.82 (+/- 0.02)	0.69 (+/- 0.03)	0.12 (+/- 0.04)	0.14 (+/-0.03)

3.5 Effects of T-DNA insertion on AT4g38160 transcription level

In order to determine the effects of T-DNA insertions on gene transcription, total RNA was isolated from leaves of wild-type, *pam48-1*, *pam48-2* and complemented plants (oePAM48.1). Equal amounts of RNA were reverse-transcribed and on the resulting complementary DNA (cDNA), gene-specific primers were used to quantify transcription levels.

According to quantitative real-time PCR (qRT-PCR) and semi-quantitative RT-PCR (Figure 3.5.1, A and B) the T-DNA insertion in *pam48-1* led to a strong decrease of *At4g38160*

transcript levels, while the insertion in *pam48-2* causes the complete loss of transcripts for the gene.

For *pam48-3* it was not possible to isolate a homozygous line, therefore the effect of the T-DNA insertion on transcript levels is not described.

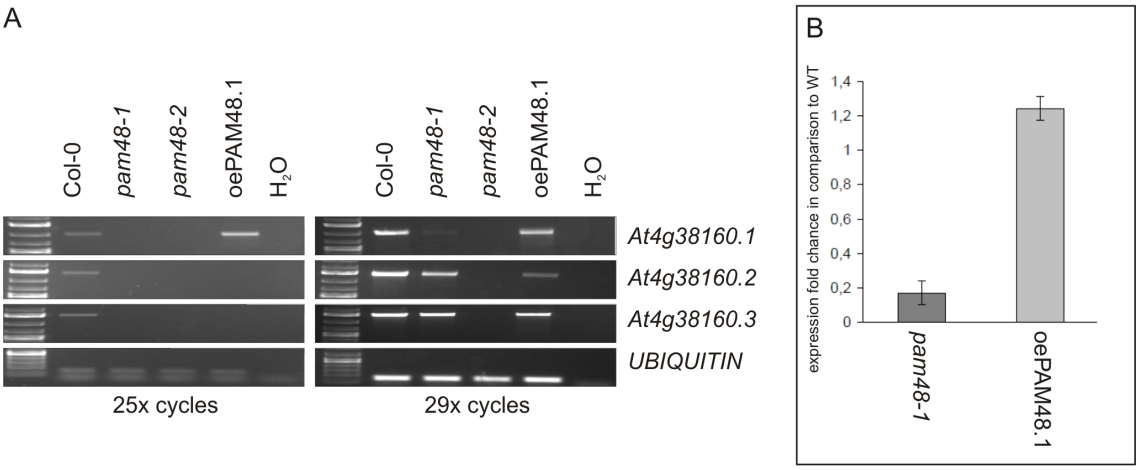

Figure 3.5.1 - A) Semi-quantitative reverse transcriptase RT-PCR analysis to verify the presence of the three splice variants in Arabidopsis WT leaves. Ubiquitin was amplified as a control for equal loading. Aliquots (10 µl) of representative semi-quantitative RT-PCR reactions (25 cycles and 29 cycles) were separated by electrophoresis on a 1 % (w/v) agar gel. B) real time RT-PCR. *At4g38160.1* transcript levels of *pam48-1* mutant and a representative complemented line, oePAM48.1. Expression levels are shown as fold change in respect to WT expression (=1), normalized to the expression levels of *UBIQUITIN,* used as a reference.

3.6 Expression of *At4g38160* in different tissues and developmental stages

By analyzing public microarray data collections (https://www.genevestigator.com/gv/plant.jsp), it emerged that *PAM48* is expressed in every developmental stage and every tissue. According to Genevestigator analysis (Figure 3.6.1), *PAM48* mRNA accumulation was found to be high in imbibed seeds and seedlings, especially in cotyledons, and shoot apical mersitem. In the rosette stage, the highest transcript accumulation was found in the leaf primordia and in general the expression of the gene appeared to be at its highest level in green tissues in a phase of differentiation. On the contrary, the expression in root tissues was low to medium.

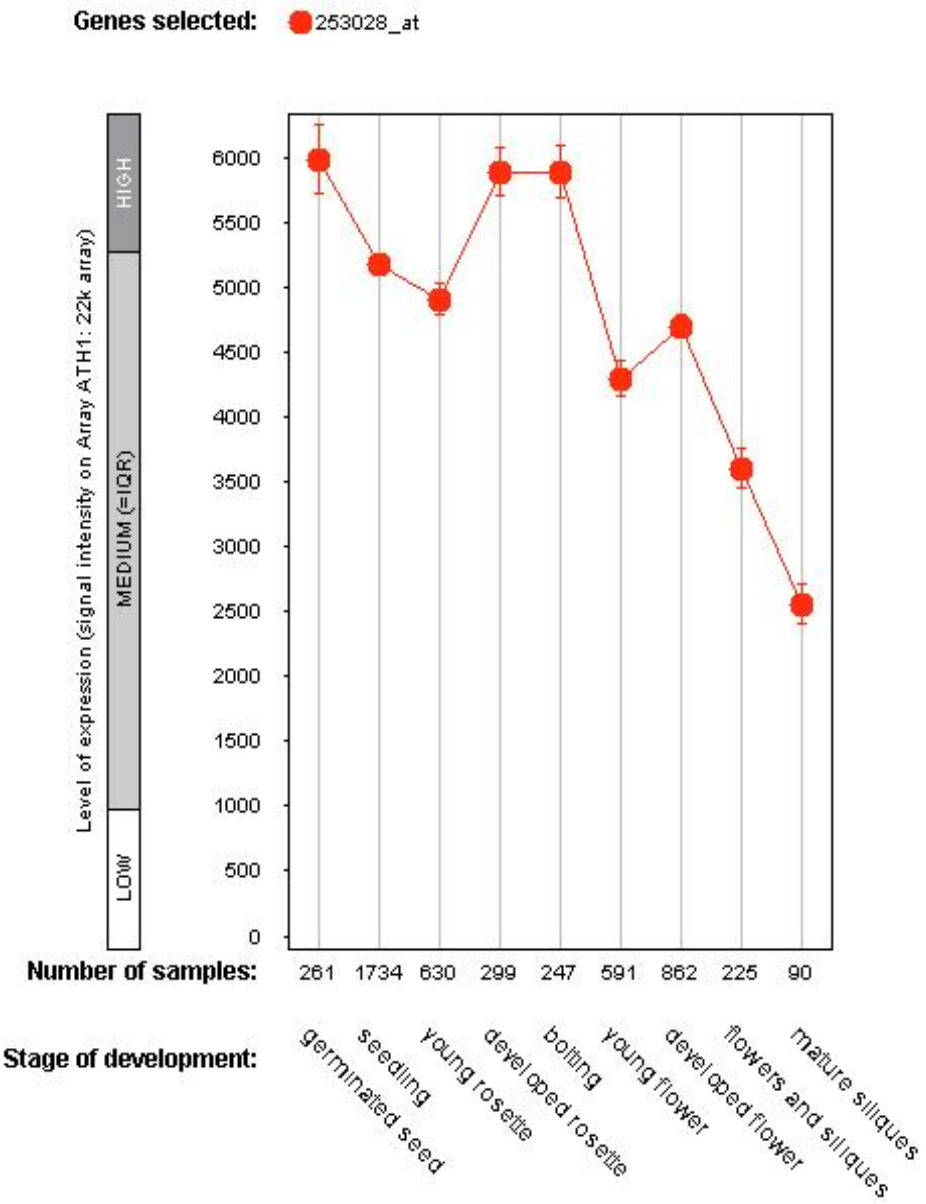

Figure 3.6.1 - Expression level of *At4g38160* in different stages of development, according to Genevestigator (https://www.genevestigator.com/gv/plant.jsp)

During different developmental stages, *AT4g38160* transcripts appeared to accumulate in germinated seeds, in the developed rosette and in the floral meristem bolting phase. In subsequent stages transcript amounts resulted to decrease constantly with a last peak corresponding to the developed flower (Figure 3.6.2).

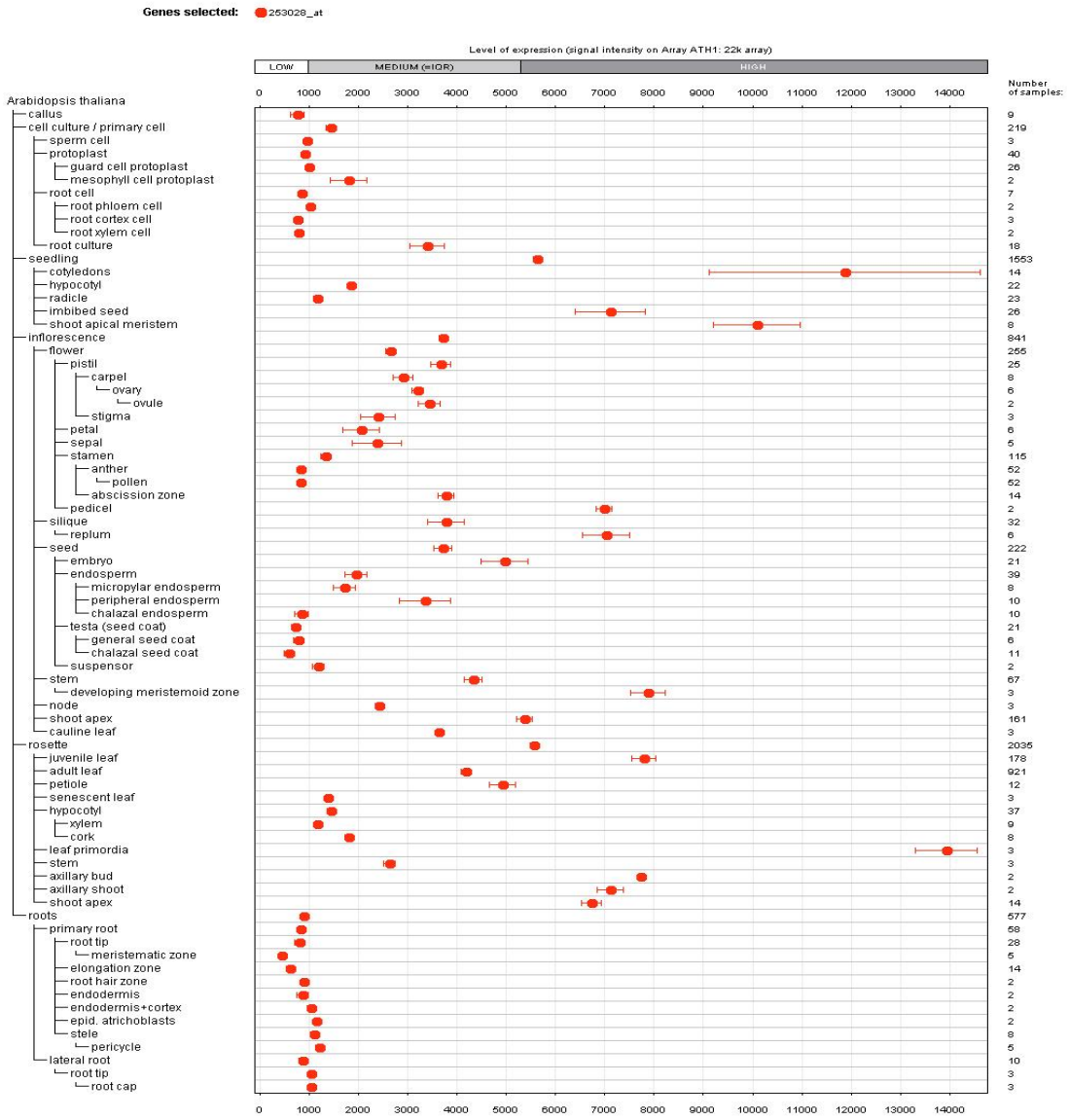

Figure 3.6.2 - Expression level of *At4g38160* in different tissue, according to Genevestigator (https://www.genevestigator.com/gv/plant.jsp)

3.7 *At4g38160* locus encodes a MTERF protein

The predicted protein secondary structure of PAM48 shows seven MTERF motifs (Figure 3.7.1); hence, the protein is included in the MTERF DNA binding proteins family.

The amino acid sequence of PAM48 was blasted against the Uniprot Database (http://www.uniprot.org/) and the resulting highest score sequences in plant model species were aligned with ClustalW (http://www.ebi.ac.uk/clustalw). The alignment result is reported in Figure 3.7.1; PAM48 is 99 % similar to the PDE191 of *Zea mays*, while the maximum similarity with a MTERF protein in *C. reinhardtii* reaches only 25 %.

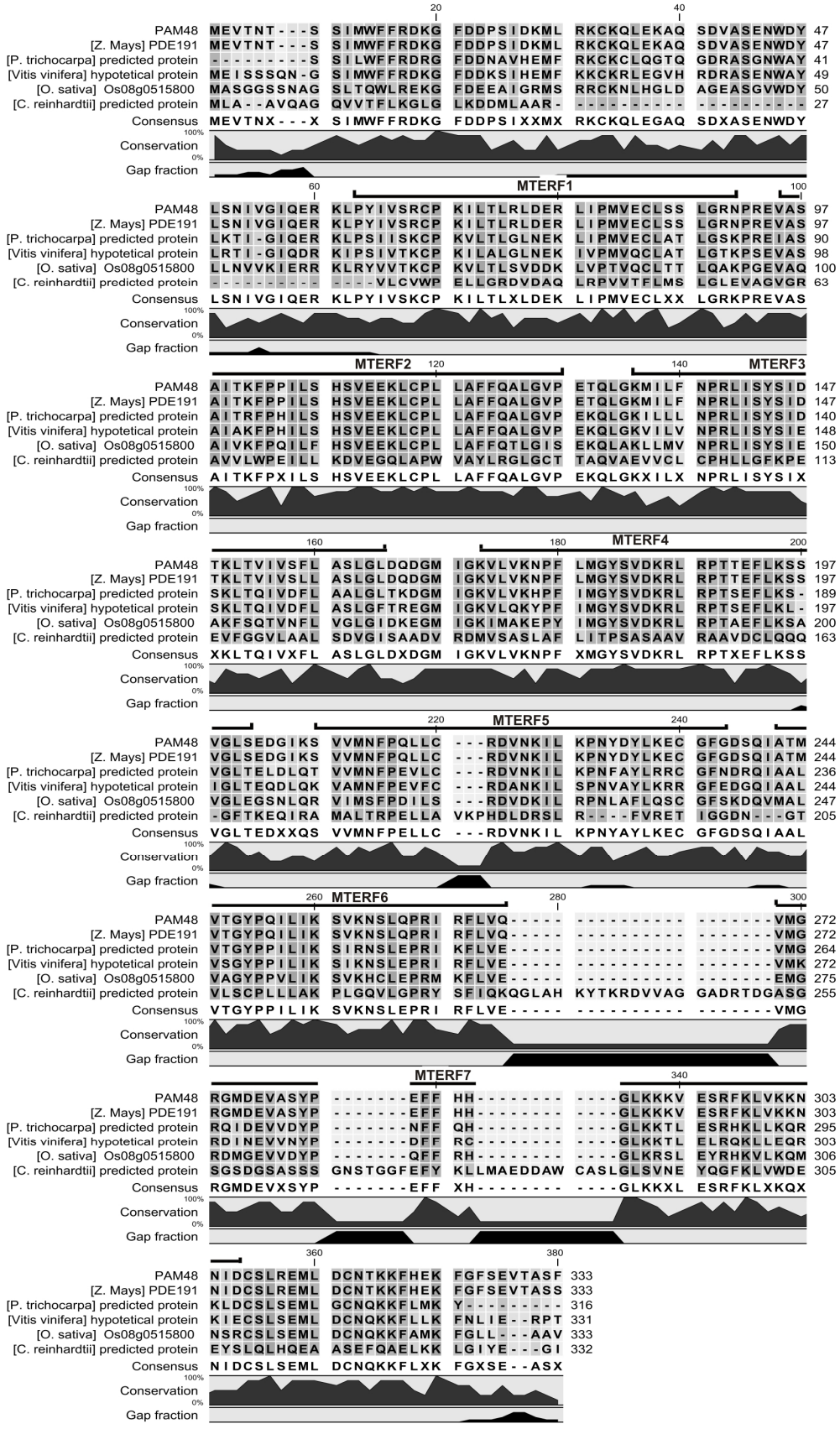

Figure 3.7.1 - Sequence alignment of the PAM48 protein in *A. thaliana* and other plant and algal species. The alignment has been created with the program ClustalW (http://www.ebi.ac.uk/clustalw/). Sequences have been obtained from the genome sequences available at http://genome.jgi-psf.org/ and http://www.ncbi.nlm.nih.gov/. The seven MTERF motifs are depicted as thin lines above the amino acid sequence.

In order to gather information about the MTERF family across all species, the PFAM protein database (http://www.sanger.ac.uk/resources/databases/pfam.html) was investigated. In eukaryotes, 737 MTERFs in a total of 103 species are listed. In Metazoa, 146 MTERF sequences are counted across 50 species, while in Viridiplantae, with 552 MTERF sequences in only 34 species, the number is sensibly increasing. Among Viridiplantae, and referring to the most studied species, *Zea mays* contains 38 MTERFs, *Oryza sativa subsp. Japonica* has 32 MTERFs, *Vitis vinifera* has 48 MTERFs sequences. *Chlamydomonas reinhardtii* contains 6 MTERFs. In the model plant studied in the present work, *A. thaliana*, 35 members are found, as shown in Figure 3.8.1, depicting the MTERFs phylogenetic tree in Arabidopsis. These numbers suggest how in plants MTERF genes have undergone a large number of duplication events.

3.8 Intracellular localization of PAM48

As represented in the phylogenetic tree in Figure 3.8.1, the targeting prediction (performed with the TargetP software, Emanuelsson et al., (2000); http://www.cbs.dtu.dk/services/TargetP/) for the 35 MTERFs in *A. thaliana* resulted to be either to the mitochondrion or to the chloroplast, except for 7 proteins with uncertain prediction. The *in silico* data of targeting prediction were confirmed experimentally by Babiychuk et al. (2011), by fluorescence microscopy of GFP fusions of all Arabidopsis MTERF members, expressed transiently in protoplast or stably in transgenic Arabidopsis plants.

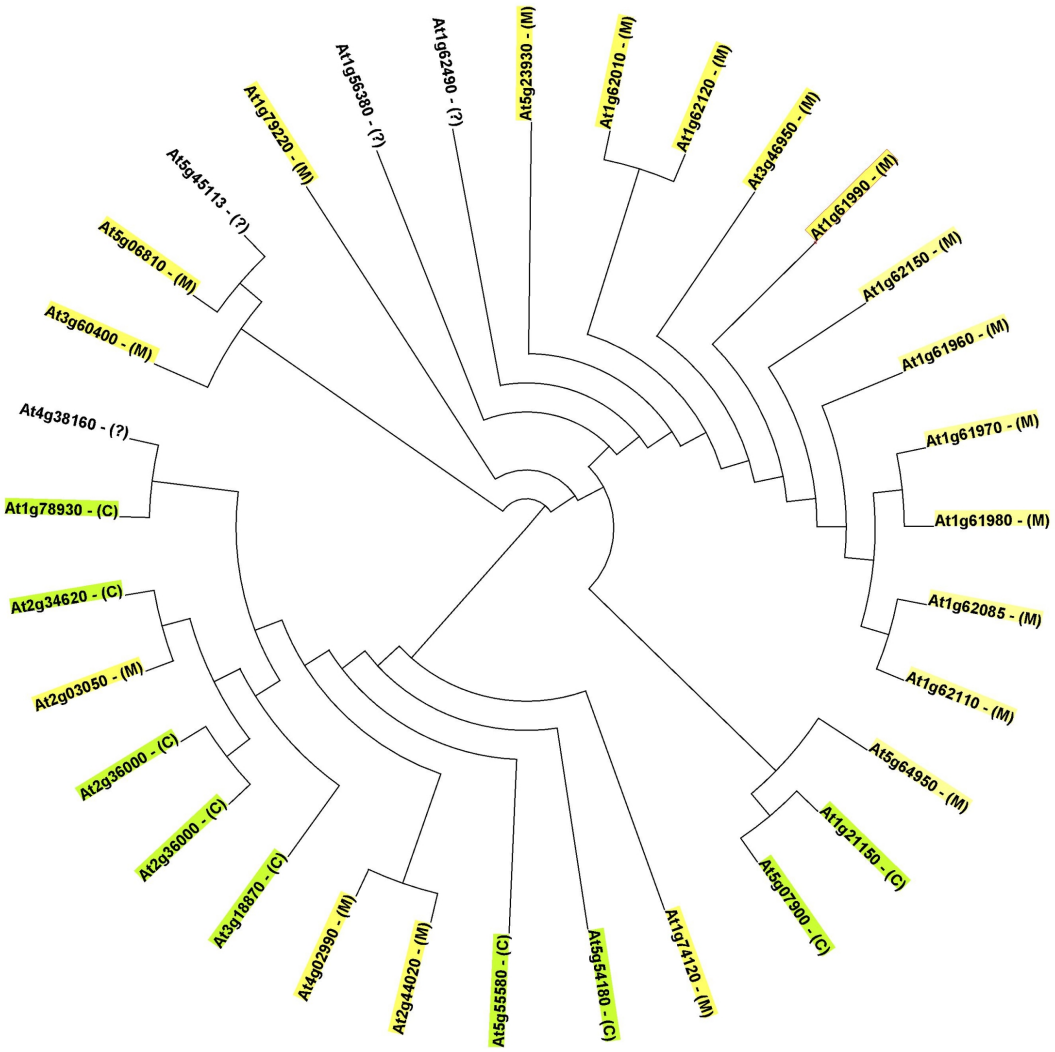

Figure 3.8.1 – Phylogenetic tree representing Arabidopsis MTERFs and their predicted subcellular localisation. Yellow labels represent mitochondrial targeted proteins (M), green labels chloroplast targeted proteins (C), while white labels represent proteins with unpredictable targeting (?).

In silico analysis with different subcellular localization prediction programs led to no unequivocal result (Table 3.8.1). According to the outcomes, PAM48 resulted to be most likely targeted to the mitochondrion (2 out of 9 predictors), although the majority of predictors (4 out of 9) were not able to give a clear outcome and some produced unexpected results, such as a peroxisomal or nuclear targeting. WOLFPSORT predicted PAM48 to be located in the plastid. In all cases, it was impossible to obtain a prediction of the target peptide cleavage site. To conclude, the algorithms were not sufficient for a preliminary prediction of the subcellular targeting of PAM48.

Table 3.8.1 - Subcellular localisation prediction for PAM48 with different prediction softwares

predictor	**targeting prediction**
iPSORT	no prediction
LOCtree	mitochondrion
MitoPRed	mitochondrion
Mitoprot 2	no prediction
PeroxP	peroxisome
Predotar	no prediction
SubLoc	nucleus
TargetP	no prediction
WOLFPSORT	plastid

In vitro import experiments were not suitable to clarify the subcellular of PAM48. As shown in Figure 3.8.2, when PAM48 was artificially imported into isolated pea chloroplasts, its translation product did not show any maturated form. On the contrary, the control protein Vipp was correctly maturated and protected from thermolysin digestion. Interestingly, a low amount of translation product was still present in the sample corresponding to PAM48 treated with thermolysin. Although the result could be artefactual, for the control the thermolysin treatment was sufficient to completely degrade the immature form. This might suggest a potential interaction of PAM48 with pea chloroplasts *in vitro* and could indicate that the failure in the import might be due to a false negative result.

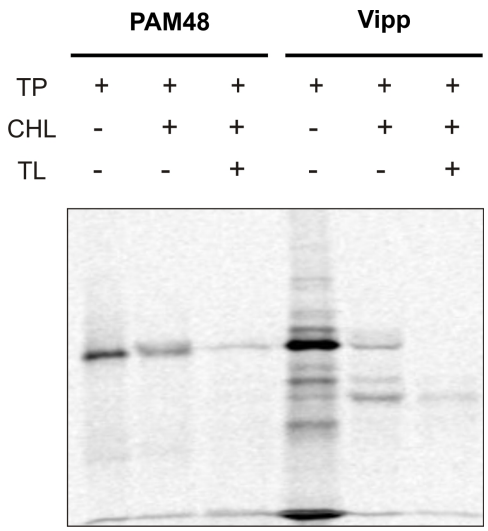

Figure 3.8.2 - *In vitro* import of PAM48. ^{35}S-labelled PAM48 and Vipp, translated *in vitro* (first lane in each import experiment, 1:10 translation product), were incubated with isolated chloroplasts for 30 min at 25°C and chloroplasts were recovered by centrifugation through 40% Percoll. Chloroplasts were incubated with 20 µg/ml thermolysin, subjected to SDS-PAGE, and proteins were visualized by autoradiography. Vipp served as positive controls. TP: translation product; CHL: pea chloroplast; TL: thermolysin.

In the previously mentioned study, Babiychuk et al. (2011) have reported At4g38160 to be localized to mitochondria in protoplasts and in stomata of transgenic Arabidopsis plants. As illustrated in Figure 3.8.3, the mitochondrial localization was confirmed via complementation of the *pam48-1* phenotype with a full length PAM48-GFP fusion protein. Beside the confirmation of mitochondrion localisation, the GFP signal was detected in the chloroplasts of stably transformed lines.

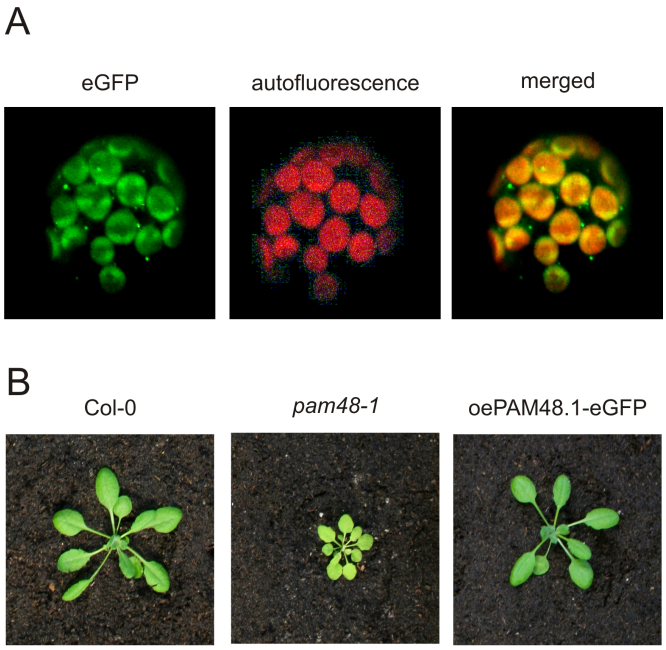

Figure 3.8.3 – A)Subcellular localisation of PAM48-GFP. Full-length PAM48-GFP was stably expressed in *pam48-1* plants. Protoplast were isolated and the signal visualised by fluorescence microscopy. eGFP: fusion protein; autofluorescence: chlorophyll autofluorescence; merged: overlay of the two signals. B) 2-weeks-old phenotype of Col-0, *pam48-1* and complemented plants.

Immunodetection with anti-GFP antibodies against chloroplast fractions isolated from complemented *pam48-1*/PAM48-GFP plants revealed the presence of PAM48 in the stromal fraction, as seen in Figure 3.8.4. The 70kDa band matches with the molecular weight of the PAM48-GFP fusion product (GFP has a molecular weight of approximately 28 kDa and PAM48 has a molecular weight of approximately 38 kDa). The secondary band at around 30 kDa represents most likely a spliced byproduct of GFP. According to the results obtained from GFP fluorescence and immunodetection analysis, PAM48 is a dual-targeted protein, imported into mitochondria and chloroplasts.

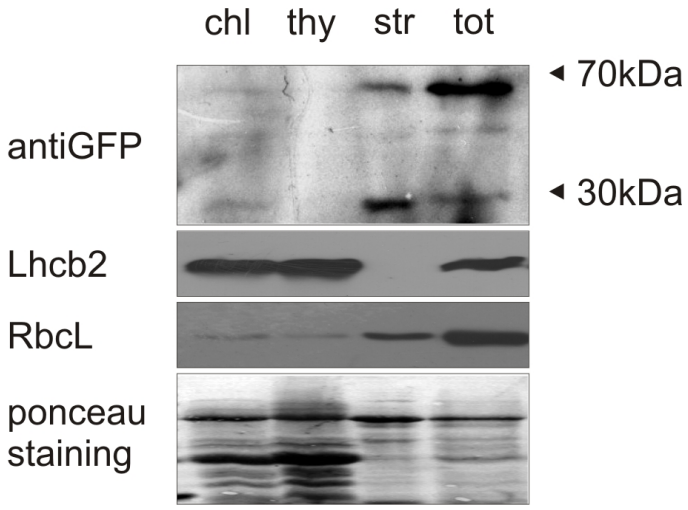

Figure 3.8.4 - Chloroplast fractionation and detection of PAM48-GFP complemented *pam48-1* plants. Chloroplasts were isolated from 4-week-old plants, fractionated into thylakoids and stroma and then immunoblotted. Total protein extract from the same plants was used as positive control. chl: intact chloroplasts; str: stroma; tot: total protein extraction.

3.9 PAM48 functions mainly in chloroplasts

As shown previously (Figure 3.8.3 and Figure 3.8.4), PAM48 is targeted to both mitochondria and chloroplasts. In order to better understand the role of PAM48 in the two compartments, the protein was targeted specifically to each compartment according to the strategy described below.

Two different constructs were designed; in the first, the mitochondrion targeting peptide sequence (mTP) of the *FUMARASE 1* gene (*FUM1, AT2G47510*) was fused to PAM48.1. FUM1 is a nuclear-encoded protein imported into the mitochondrial matrix and it catalyzes the reversible hydration of fumarate to malate in the tricarboxylic acid cycle. In the second construct, the chloroplast targeting peptide sequence (cTP) of Ribulose-1,5-bisphosphate carboxylase/oxygenase small subunit (*RBCS, AT1G67090*) was fused to PAM48.1. RBCS is

encoded by the nuclear genome and imported into the chloroplast stroma where it takes part to the Calvin cycle. These targeting peptides were chosen because they represent the most characterized targeting sequences and especially because they allow the import into the compartments where the organellar DNA is found, i.e. the matrix for the mitochondrion and the stroma for the chloroplast. The mTP-PAM48 and cTP-PAM48 fusions were then fused to the eGFP gene, and cloned under the control of the 35SCaMV promoter (for a scheme, see Figure 3.9.1). *pam48-1* plants were transformed via Agrobacterium-mediated transformation and the T1 generation was selected on BASTA and screened with primer pairs designed either on the mTP or cTP sequence and on the eGFP gene.

By phenotypical screening, it was already obvious that the cTP-PAM48-eGFP construct was able to fully complement the knock-down phenotype, while the mTP-PAM48-eGFP construct seemed to have no rescuing effect on the *pam48-1* phenotype (Figure 3.9.1). The cTP-PAM48-eGFP transformation produced more than 50 independent lines, while for the mTP-PAM48-eGFP construct only three independent lines were isolated.

To test the successful targeting of the two constructs, the lines isolated from the screening were then subjected to fluorescence microscope analysis for eGFP signal detection. Unfortunately, for the cTP-PAM48-eGFP lines it was not possible to detect a sufficiently strong eGFP signal to state unequivocally the targeting to the chloroplast, but on the other hand no signal to the mitochondrion was detectable.

The mTP-PAM48-eGFP construct produced a strong signal in the mitochondrion. It is remarkable that the targeting of the construct only to mitochondrion was not sufficient for the complementation of the *pam48-1* phenotype, on the contrary of the cTP-PAM48-eGFP fusion, indicating that the protein is essential for chloroplast function.

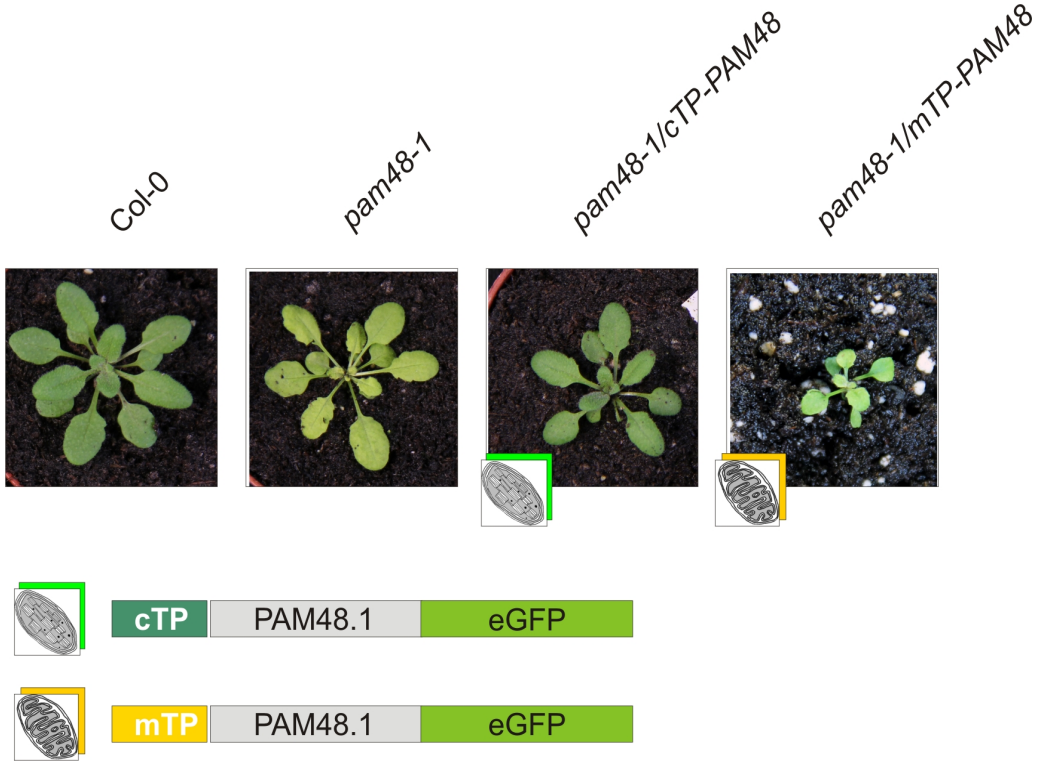

Figure 3.9.1 - Artificial targeting complementation. pam48-1 plants were transformed either with a cTP-PAM48-GFP or a mTP-PAM48-GFP construct (depicted in the scheme) in order to singularly target the protein either to mitochondria or chloroplasts. The pictures show phenotypes of 4 weeks old plants belonging to the T1 generation.

3.10 Blue Native PAGE analysis of *pam48-1* thylakoid

In order to investigate a possible effect on the thylakoid protein composition and assembly, Blue Native PAGE (BN PAGE) was performed on thylakoids isolated from wild-type and *pam48-1* leaves. After several attempts, it seemed that digitonin was the best detergent to resolve protein complexes in the mutant thylakoids, probably due to its milder effect with respect to other similar detergents, such as β-dodecyl-maltoside (β-DM). The first dimension gel showed that complex assembly occurs with no difference with respect to wild-type, as the typical separation pattern was respected in the mutant. However, depletion in PSI monomers and PSII dimers was observed, as well as in cytb6/f PSII-dimers (Figure 3.10.1, band II and III, respectively). The apparent lower molecular weight of bands corresponding to LHCBs in *pam48-1* might be due to a defect in the binding of pigments, resulting in lower molecular weight complexes (Figure 3.10.1, band VI).

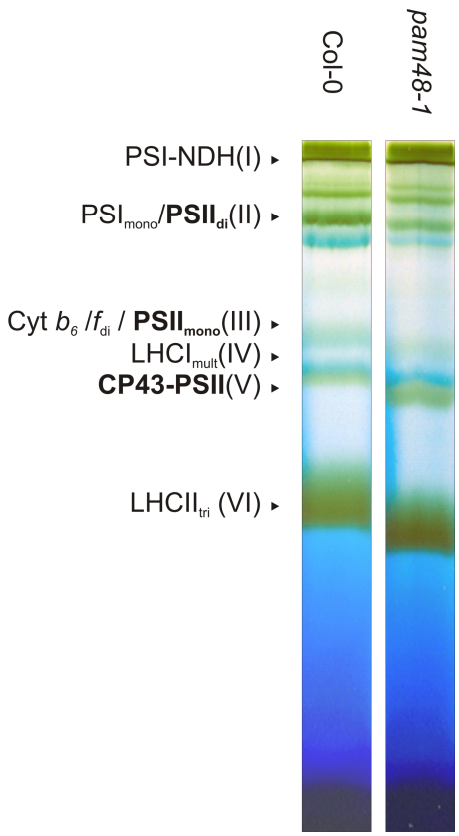

Figure 3.10.1 - First dimension Blue Native PAGE of Col-0 and *pam48-1* thylakoids. Identical amounts of thylakoid protein from WT and mutant were solubilised with digitonin (1.3%) and loaded on a native gel.

3.11 Transmission Electron Microscopy and autofluorescence microscopy of *pam48-2* embryos

Transmission Electron Microscopy (TEM) was performed in collaboration with Prof. Dr. Wanner's group (LMU, Munich). Seeds from wild-type siliques and white homozygous seeds from heterozygous *pam48-2* siliques were collected at different days after pollination (DAP), before development of seed teguments.

In order to better detect possible differences in development between wild-type and *pam48-2* embryos, two embryonic developmental stages were chosen*:* an early and a late torpedo stage.

Microscope analysis revealed a strong deficiency in the biogenesis of plastids in *pam48-2*; small and shapeless plastids were observed in both stages (Figure 3.11.1). In *pam48-2* embryos, the normal thylakoid structure failed to constitute, and lower amounts of lipids and starch were accumulated. These results are in accordance with the albino phenotype of *pam48-2* and give an indirect confirmation of a function within the plastid for PAM48. Mitochondria did not seem to be affected in *pam48-2* embryos: both shape and dimension were comparable, despite the demonstrated targeting of PAM48 to mitochondria.

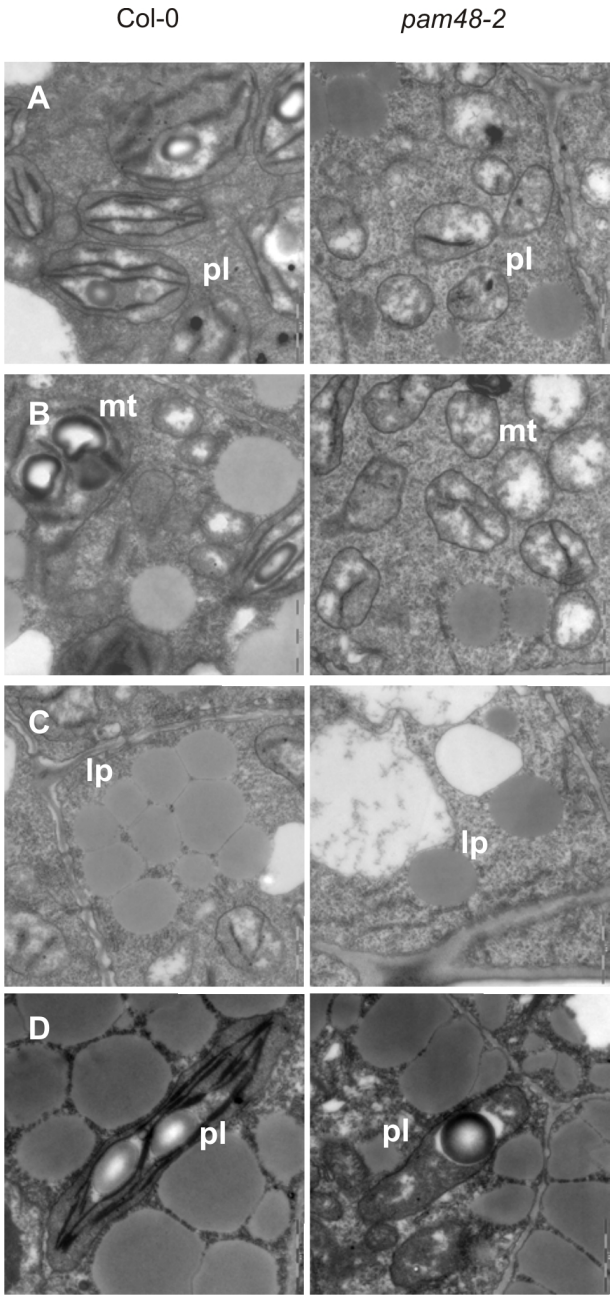

Figure 3.11.1 – Transmission electron microscopy of *pam48-2* embryos. Early torpedo stage embryos were isolated from WT seeds and albino seeds of heterozygous PAM48/*pam48-2* siliques and sections were analyzed with TEM. Pl: plastids; mt: mitochondria; lp: lipid drops.

Chlorophyll accumulation in WT, *pam48-1* and *pam48-2* was assessed via autofluorescence detection under the stereomicroscope. While *pam48-1* showed chlorophyll levels comparable to those of WT leaves, in *pam48-2* the chlorophyll amount dropped dramatically (Figure 3.11.2). The production of chlorophyll in the albino mutant, although in very low levels, indicates a residual functionality of plastids.

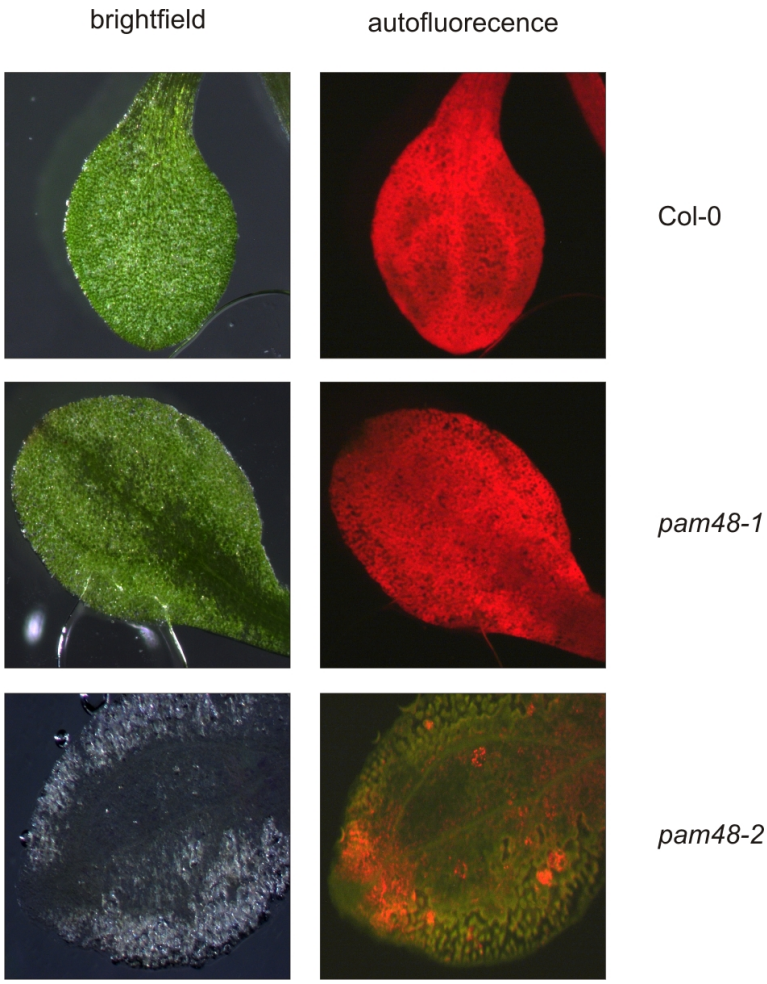

Figure 3.11.2 - Chlorophyll autofluorescence microscopy of three-week-old Col-0, *pam48-1* and *pam48-2* leaves. Plants were grown on MS medium supplemented with sugar. The autofluorescence of chlorophyll (right panels) show how in *pam48-2* knock out lines chlorophyll is accumulating in very low amounts.

3.12 Expression levels of subunits of photosynthetic complexes and mitochondrial proteins in *pam48-1*

As already shown in Figure 3.10.1, BN-PAGE of *pam48-1* thylakoids showed lower amounts of PSI and PSII complexes. In order to understand whether this is a general shared by all photosystem components or whether the lack of PAM48 is affecting the translation of specific subunits, an immunodetection analysis, dedicated to some of the most important photosynthesis-related proteins, was performed. At least one subunit was chosen for every complex.

As observable in Figure 3.12.1, while all nucleus-encoded proteins (PsbP, PsbS and the subunits of the light harvesting complexes) showed comparable protein levels in *pam48-1* and WT, chloroplast-encoded proteins (D1, CP43, CP47, PsaA, PsaB) showed deregulation in each case explored.

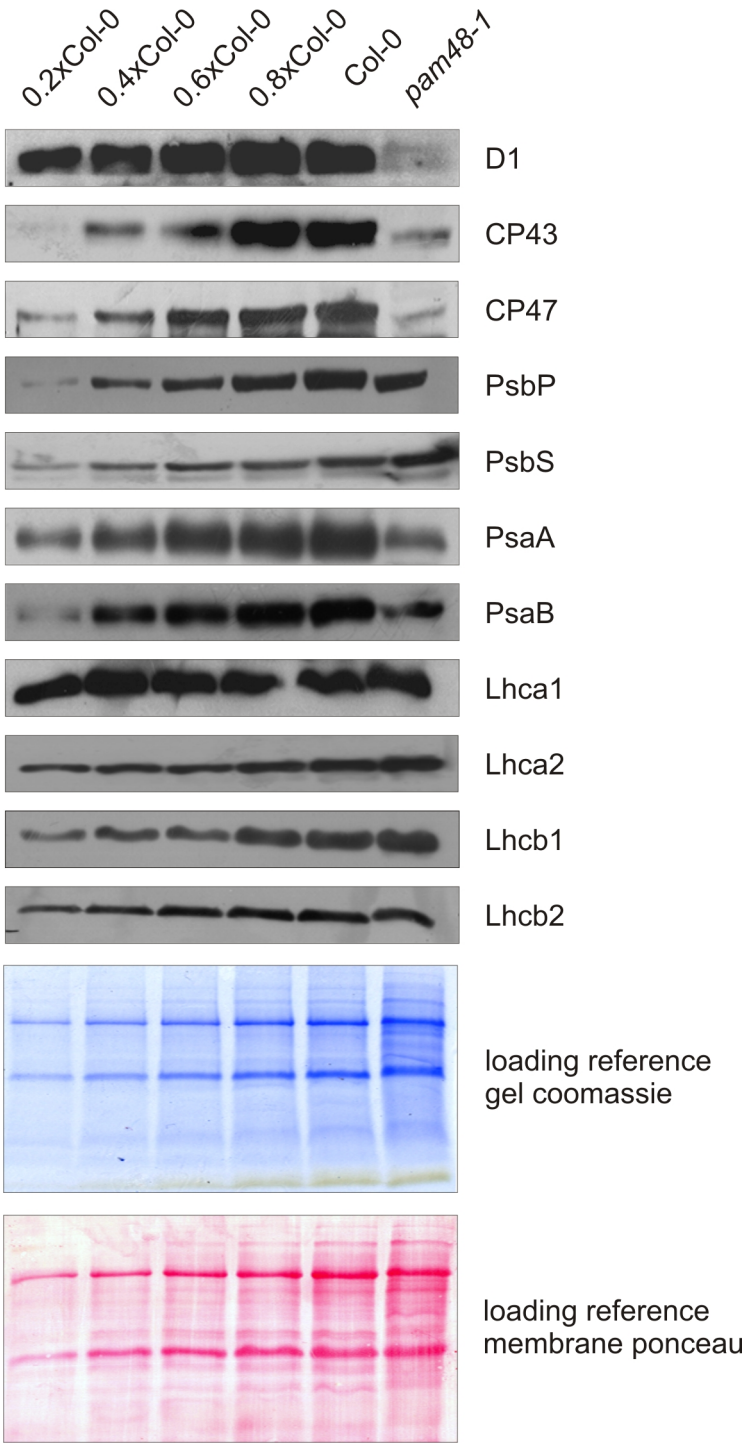

Figure 3.12.1 **–** Western blot analysis of photosynthetic subunit levels in *pam48-1*. Increasing amount of WT total protein extract (0.2, 0.4, 0.6, 0.8 and 1x) and 1x *pam48-1* were loaded. After blot transfer, different antibodies (listed on the side) were used to quantify protein contents. A replica gel stained with Coomassie Blue and Ponceau staining of membranes were used as loading controls (bottom panel).

To asses whether levels of mitochondrial proteins were also affected by the down-regulation of PAM48 activity in the leaky mutant, immunodetection of marker protein levels - such as F-ATPase, citrate synthase, AOX and aconitase - was performed.

In none of the investigated cases a change in translational levels could be observed, neither for nuclear-encoded proteins (CYS4, AOX, ACO), nor for the mitochondrial-encoded one

(ATP6) (Figure 3.12.2). It was already shown that in *pam48-2* embryos mitochondria biogenesis did not seem to be affected, as illustrated by TEM analysis in Figure 3.11.1. These results confirm again the importance of PAM48 activity in the chloroplast, while the protein seems to be not essential in the other compartment to which it is targeted, and according to this analysis, its deregulation does not perturb mitochondrial functions.

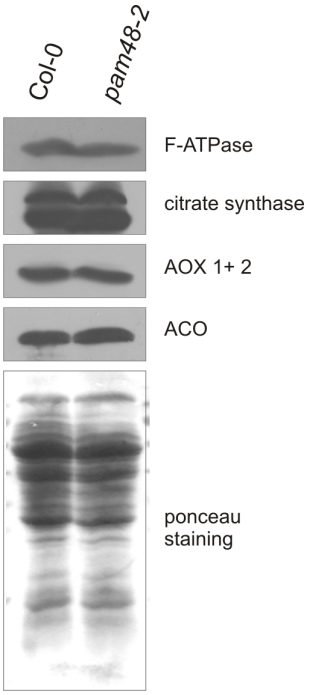

Figure 3.12.2 **–** Western blot analysis of mitochondrial subunit levels in WT and *pam48-1* plants. Mitochondria were isolated from both lines and identical amounts were loaded on a 12% SDS denaturing gel. After transfer blot, membranes were incubated with different antibodies (listed on the side), to detect differences in protein amounts. In the bottom panel, Ponceau staining of membranes was used as loading control.

3.13 Analysis of transcript levels of photosynthetic genes in *pam48-1* plants

As demonstrated by BN-PAGE (Figure 3.10.1) and immunodetection analysis (Figure 3.12.1), *pam48-1* has lower levels of photosynthetic subunits encoded by the chloroplast genome. Accordingly, two scenarios could explain this defect. In the first case, the defect could be the result of a direct impairment of translational or post-translational processes (e.g. protein stability or processing) in the chloroplast. The second possibility would be that the transcription of the genes for the plastidial subunits is affected. To explore a possible role of PAM48 in transcription, Northern blot analysis of transcript levels of wild-type and *pam48-1* plants was performed, investigating photosynthetic subunits from all complexes. The Northern blot analysis showed no changes in transcript levels for all of the genes investigated (Figure 3.13.1), with the exception of psaB that appears to be downregulated. These data were

though not confirmed by microarray analysis, while immunoblot analysis showed that levels of chloroplast-encoded proteins are specifically depleted in *pam48-1* mutants (Figure 3.10.1). Altogether, the information gathered from Northern blot and Western blot analysis indicates that *pam48-1* has impairment in translational activity of plastid-encoded photosynthetic subunits, while transcription of corresponding genes is fully functional.

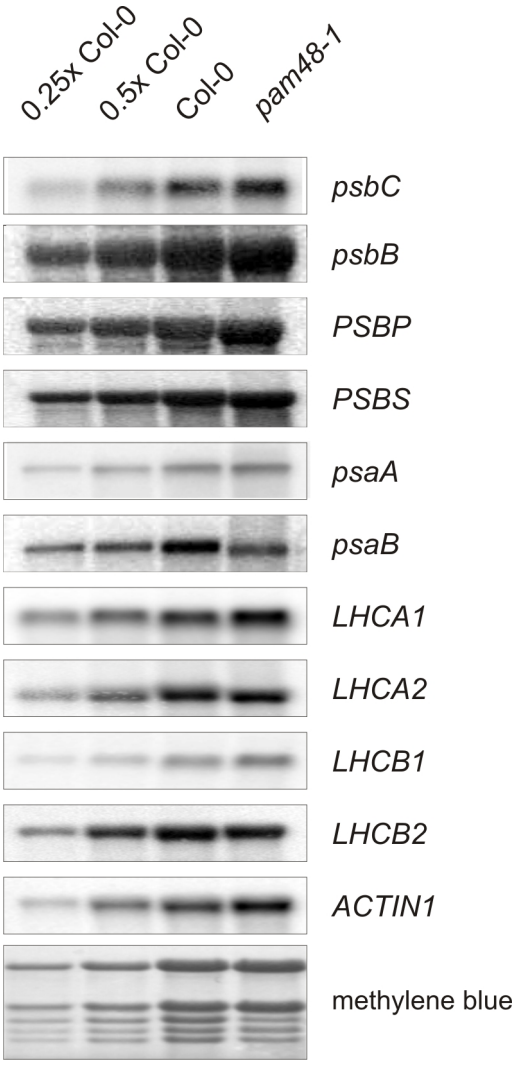

Figure 3.13.1 **-** Northern blot analysis of photosynthetic subunits in Col-0 and *pam48-1*. Increasing amounts (0.25, 0.5x and 1x) of total RNA extracted from Col-0 and *pam48-1* (1x) were loaded on denaturing formaldehyde gels. After blot transfer, the resulting membranes were hybridized with different ^{32}P-labelled DNA probes (listed on the side) and transcripts visualized by autoradiography. *ACTIN1* and Methylene blue staining of membranes (bottom panel) served a loading control.

3.14 Whole transcriptome analysis revealed a specific up-regulation of plastidial ribosome subunits

In order to investigate on a broader level the effects of the deregulation of PAM48 activity on gene expression, total RNA from *pam48-1* and WT was isolated and submitted to microarray

analysis, using the AFFYMETRIX ATH1 chip, which represents nearly the whole *A. thaliana* transcriptome.

In accordance with Northern blot analysis (Figure 3.13.1), no significant fold changes of transcript levels of photosynthesis-related genes was observed.

The most significant outcome was the up-regulation of some ribosomal proteins belonging to the plastidial translational machinery (see Figure 3.14.1). This effect occurred only within the chloroplast, while transcript levels of mitochondrial and nuclear ribosomal proteins were unaffected in the *pam48-1* mutant (Figure 3.14.1).

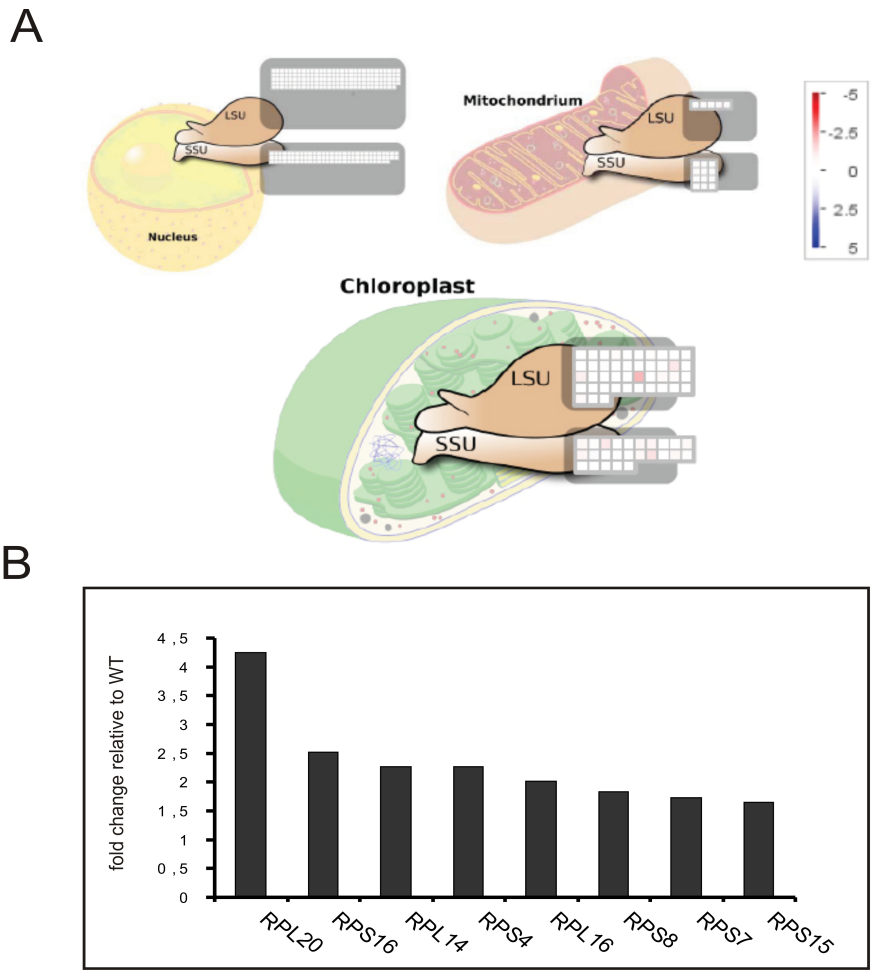

Figure 3.14.1 – A) Map of changes in transcript levels of ribosomal proteins in nucleus, mitochondrion and chloroplast. Microarray data were analyzed with the Robin software (http://mapman.gabipd.org/web/guest/robin). Fold changes of each ribosomal subunit are illustrated as a colour code (blue: decreased fold change, red: increased fold change). B) Graph showing the transcript fold change of *pam48-1* plastidial ribosomal subunits relative to WT.

Once again, the effects of the *pam48-1* mutation resulted to be narrowed to the chloroplast compartment. Moreover, it was possible to observe a specific perturbation in the expression of plastidial ribosomal subunits , indicating a potential disturbance of translational capacity in chloroplasts.

3.15 Tertiary structure prediction and identification of putative DNA interactors of PAM48

The tertiary structure of PAM48 was predicted by analyzing its primary structure with the I-TASSER algorithm (http://zhanglab.ccmb.med.umich.edu/I-TASSER). I-TASSER is a program for protein structure and function predictions. 3D models are built based on multiple-threading alignments by LOMETS and iterative TASSER assembly simulations; function insights are then derived by matching the predicted models with protein function databases (Zhang, 2008).

The protein structures database search resulted in a best score match between PAM48 and human MTERF1. The structure of the human MTERF 1 has been resolved by Yakubovskaya et al. (2010) and it is available at NCBI 3D structure database (http://www.ncbi.nlm.nih.gov) under the ID "3MVA_D". The crystal structure has been resolved together with a DNA fragment (5'-ATTACCGGGCTCTGCCATCTTA-3') corresponding to the termination sequence bound by the hMTERF1 in the human mitochondrion. As seen in Figure 3.15.1, the hMTERF1 folds in the typical half-doughnut structure; the protein wraps the DNA helix thanks to the stabilising effect of the positively charged residues exposed on the inner bow formed by the protein.

The predicted 3D structure of PAM48 matches and perfectly overlaps the structure of hMTERF1, suggesting that also PAM48 binds DNA.

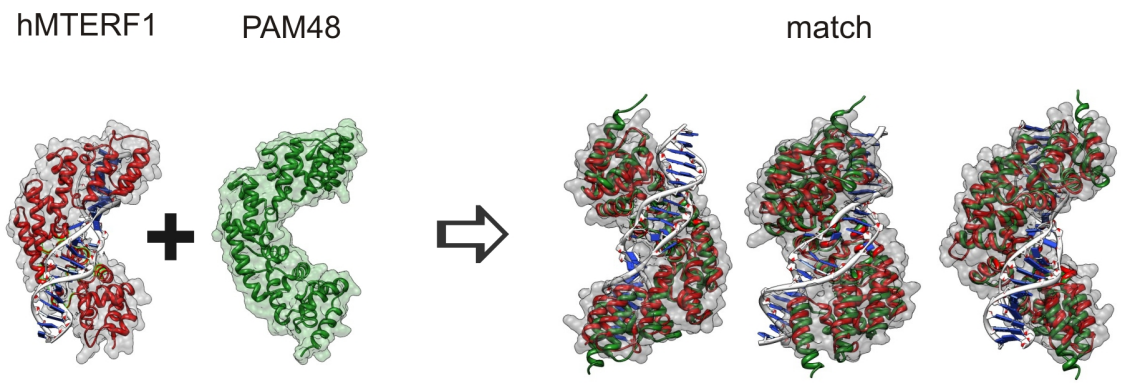

Figure 3.15.1 **-** The tertiary structure of human MTERF1 was downloaded from the NCBI structure database (http://www.ncbi.nlm.nih.gov) and matched to the predicted structure of PAM48. The 3D structure of PAM48 was calculated by the I-TASSER software (*http://zhanglab.ccmb.med.umich.edu/I-TASSER*) and the molecular graphics images were produced using the UCSF Chimera package from the Resource for Biocomputing, Visualization, and Informatics at the University of California, San Francisco (supported by NIH P41 RR001081).

It is known from studies conducted on animal models that MTERFs are able to bind DNA and regulate transcription of mitochondrial genes, in particular organellar rRNA operons (Roberti et al., 2009). To date, all the data supporting the DNA interaction function were produced by

in vitro analysis. In this study, a heterologous *in vivo* system to investigate putative DNA binding for PAM48 was used: the bacterial one-hybrid (B1H) screening (Meng and Wolfe, 2006).

The B1H system is conceptually similar to the yeast one-hybrid systems, which can detect and isolate protein-DNA interactions (Deplancke et al., 2004). The advantage of using a system constructed in bacteria is the greater complexity of binding-site library (up to ~10^9 unique clones, versus the ~10^8 unique clones of yeast based libraries) that can be reached in virtue of the higher transformation efficiency of bacteria (Joung et al., 2000).

The system consists of an interaction trap system, based on a powerful positive (Imidazoleglycerol-phosphate dehydratase, HIS3) and negative (orotidine 5-phosphate decarboxylase, URA3) selection, that allows to search within a large combinatorial library of random 18-bp-nucleotide stretches (also referred to as the "prey") for members that interact with a desired target (or the "bait"), i.e. the PAM48 protein (for a scheme see Figure 3.15.).

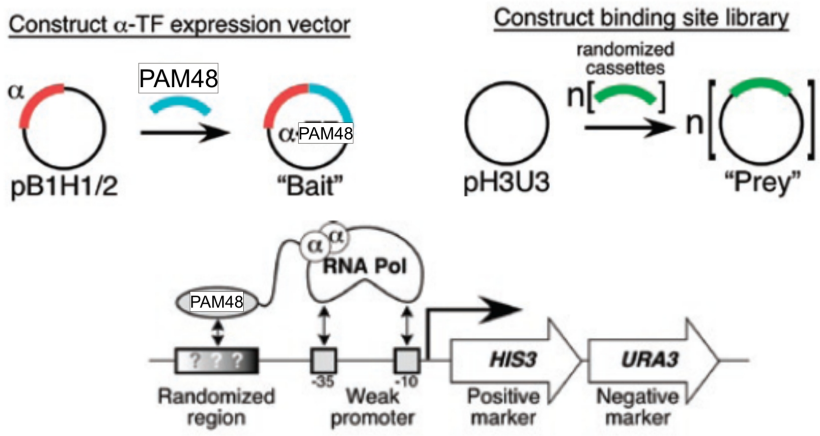

Figure 3.15.2 - Scheme of B1H selection - adapted from Meng and Wolfe 2006 – Above, two components must be constructed to carry out a selection: construction of the 'bait' vector (pB1H1 or pB1H2, left), which expresses the TF – in this case PAM48 - as a fusion product with the α subunit of bacterial RNA polymerase, and construction of the randomized binding-site library in the pH3U3 reporter, which provides the 'prey' for the selection system (left). Below, schematic illustration of the *HIS3-URA3* cistron in the pH3U3 reporter vector. If the TF binds to a sequence in the randomized region upstream of the promoter, it will recruit RNA polymerase through its direct fusion to the α-subunit, which will activate transcription of the reporter genes.

The selection procedure for PAM48 was successful and the colonies carrying the bait and prey vectors showed to be sensitive to increasing concentrations of 3-AT, giving a first indication of a specific DNA binding activity. More than 300 colonies surviving the selection were isolated and screened for prey vector sequences, via PCR with primers flanking the random region. The resulting 168 positive PCR products were sequenced, to generate a collection of interacting sequences. The resulting sequences were then selected to eliminate false positives (e.g. empty vector sequences) and tandem repeated insertions as described in

Meng and Wolfe (2006). The resulting pool of random 18mer nucleotides was submitted to MEME algorithm analysis (http://meme.sdsc.edu/meme/cgi-bin/meme.cgi) in order to find a consensus motif, with setting that allows zero or one motif present in each sequence.

By submitting 53 out of 168 sequences, it was possible to obtain a consensus motif of 15 bp, displayed as a Sequence Logo in Figure 3.15.3 with an expectation value (E-value) of $3.6°e^{-29}$. The E-value represents the probability of finding a similar number of motifs of the same width having the same log likelihood ratio in a similar population of random sequences. As reported in the protocol set out by Meng and Wolfe (2006), an E-value < e^{-20} is considered statistically significant for a putative binding motif.

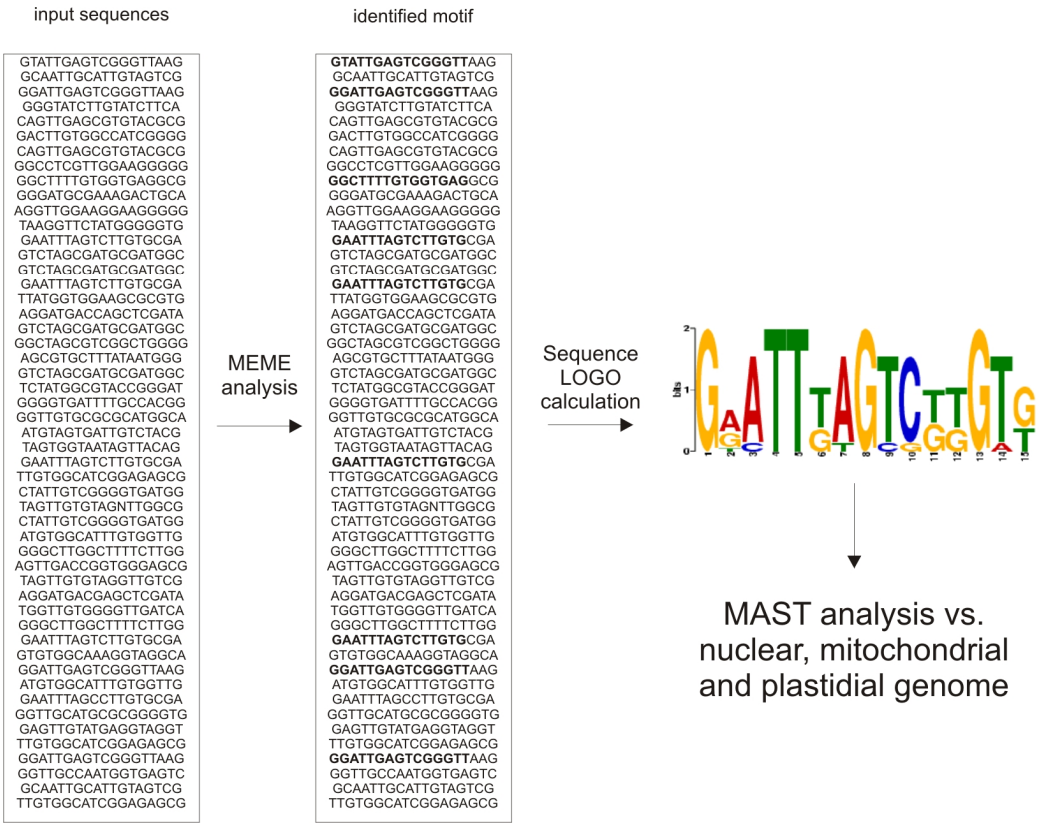

Figure 3.15.3 - Scheme of MEME analysis. The B1H selection system using PAM48 as "prey" resulted in 53 sequences. These sequences were analyzed by the MEME algorithm using the default settings, except that zero or one motif occurrence per dataset sequence was allowed (ZOOPS). MEME (http://meme.sdsc.edu/meme/intro.html) identified an 15-bp overrepresented motif (E-value = 3.6 e^{-29}). The 15-bp segments from each sequence were used to calculate a sequence logo (http://weblogo.berkeley.edu/logo.cgi) that shows the level of conservation at each position as a function of its information content and base frequency.

The 15-bp motif was analyzed with the MAST algorithm. MAST (http://meme.sdsc.edu/meme/cgi-bin/mast.cgi) is a tool for searching biological sequence databases for sequences that contain one or more of a group of known motifs. The algorithm

calculates the match scores between the input sequence and the sequences in the database, converting the scores in various types of p-values (position, sequence and combined p-value) that are used to determine the overall matches of the sequence to the group of motifs and the probable order and spacing of occurrences of the motifs in the sequence.

The on-line MAST database for *A. thaliana* is composed only of genomic regions belonging to the nuclear genome, while the targeting of PAM48 is limited to the two organelles. Therefore, it was necessary to use the algorithm against either the mitochondrial genome or the chloroplast genome sequences, obtained from the NCBI Organelle Genome Resource (http://www.hsls.pitt.edu/obrc/index.php?page=URL1152125326).

Through the MAST analysis a number of putative matching sequences were found both in the mitochondrial and plastidial genome. The corresponding region match, found downstream the indicated genes, within a distance of +500 bp from the stop codon, are reported in Table 3.15.1 and Table 3.15.2.

Table 3.15.1 **-** List of putative PAM48 binding targets within the plastidial genome. 15-bp sequences resulting from MEME analysis were analyzed with the MAST algorithm (http://meme.sdsc.edu/meme/cgi-bin/mast.cgi), matching the complete chloroplast chromosome sequence (downloaded from NCBI Organelle Genome Resource http://www.hsls.pitt.edu/obrc/index.php?page=URL1152125326).

locus	**name**	**function**
ATCG00450	*trnv.1*	triplet codon amino acid adaptor
ATCG00030	*trnk*	triplet codon amino acid adaptor
ATCG00905	*rps12*	ribosomal protein
ATCG00920	*rrn16*	chloroplast-encoded 16s ribosomal rna
ATCG01120	*rps15*	ribosomal protein
ATCG00260	*trnt*	triplet codon amino acid adaptor

Table 3.15.2 **-** List of putative PAM48 binding targets within the mitochondrial genome. 15-bp sequences resulting from MEME analysis were analyzed with the MAST algorithm (http://meme.sdsc.edu/meme/cgi-bin/mast.cgi), matching the complete mitochondrial chromosome sequence (downloaded from NCBI Organelle Genome Resource http://www.hsls.pitt.edu/obrc/index.php?page=URL1152125326)

locus	**name**	**function**
ATMG00650	*nadl4*	complex I - respiration
ATMG00510	*nad7*	complex I - respiration
ATMG00660	*putative protein*	unknown
ATMG00640	*orf25*	ATP synthase subunit
ATMG01190	*atp1*	ATP synthase subunit

It is remarkable that among the sequence matches within the plastome, many are falling in regions close to genes coding for ribosomal proteins or genes that are coding for elements involved in ribosomal functioning (tRNAs, rRNAs).

Especially the match with the downstream region of *rrn16* (coding for 16S rRNA) in the chloroplast genome is of striking interest; as reported in the literature, many metazoans MTERFs were found to bind DNA targets neighbouring the ribosomal operon and were demonstrated to regulate transcription of mitochondrial rRNA *in vitro* (Roberti et al., 2009).

3.16 PAM48 specifically binds to downstream sequences of chloroplast genes

The bacterial one-hybrid screening gave a first indication of DNA binding activity and a number of putative binding sequences were found in the chloroplast and mitochondrial genome (Table 3.15.1 and Table 3.15.2).

In order to confirm the DNA binding property of PAM48 and to establish which of the putative targets were actually bound by the protein, an independent *in vitro* experiment, the electrophoretic mobility shift assay (EMSA) was performed.

Probes were designed as 60 bp oligomers, carrying the original sequence derived from the corresponding genome match surrounded by random stretches and a 3' common sequence to allow the double-stranding. The probes were labelled as dsDNA with dCTP ^{32}P isotope, using the Klenow fragment. PAM48 was recombinantly overexpressed in *E.coli*, isolated and shock folded to its native form.

The putative binding sequences were chosen for EMSA testing on the basis of their e-value score and biological relevance. As the mitochondrial candidate targets were mostly corresponding to genes with unknown function, the subsequent analyses presented in this work were preliminarily applied to the most significant chloroplast target sequences.

As shown in Figure 3.16.1, probes designed on downstream regions of *rps12* (encoding S12 ribosomal protein), *trnk* and *trnt.1* (encoding $tRNA^{Lys}$ and $tRNA^{Thr}$) probes did not interact with the purified PAM48 protein.

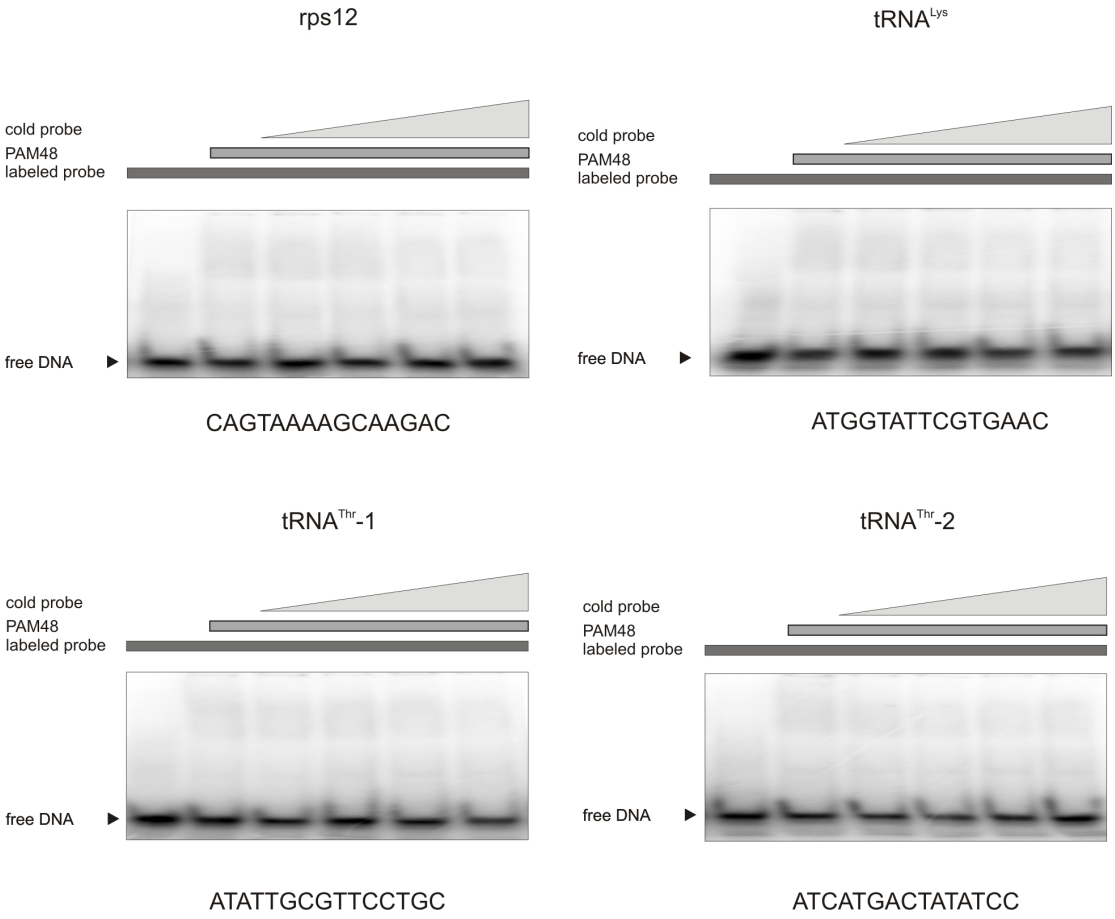

Figure 3.16.1 - EMSA for rps12, $tRNA^{Lys}$, $tRNA^{Thr}$ motif 1 and 2 downstream sequence probes. In all panels, in the first lane labelled probes were loaded as negative and size control. In the other lanes, identical amounts of purified and refolded PAM48 (1µg) and ^{32}P-labelled probe (100ng) was incubated with increasing amounts (0 ng, 100 ng, 250 ng, 500 ng, 1000 ng) of corresponding unlabelled (cold) probe.

A mobility shift was observed only when performing the EMSA assay with the probes designed on the downstream region of *rrn16* and *trnv.1* (encoding 16S rRNA and $tRNA^{Val}$; for a scheme, see Figure 3.17.1). PAM48 interacted with the two DNA probes, as a retarded band was observed when both protein and DNA fragment were present in the sample. Moreover, competition with increasing concentrations of an unlabelled probe decreased

proportionally the intensity of the retarded band, indicating the specific affinity of PAM48 for the examined DNA probes (Figure 3.16.2).

To assess the specificity of the interaction, the core sequences of the two DNA probes, corresponding to the original binding-site, were mutated by substitution with a stretch of four (*rrn16*) and five (*trnv.1*) random nucleotides (for the sequences, see Table 2.5.1 in Material and Methods). When testing the interaction between PAM48 and the mutated probes, no retarded bands could be observed in the gels (Figure 3.16.2). According to the results gathered from the EMSA assays, PAM48 binds DNA in a sequence-specific manner to target sequences found within the chloroplast genome. The target sequences correspond to regions flanking genes of biological relevance, with pertinence to the function found previously in metazoan models.

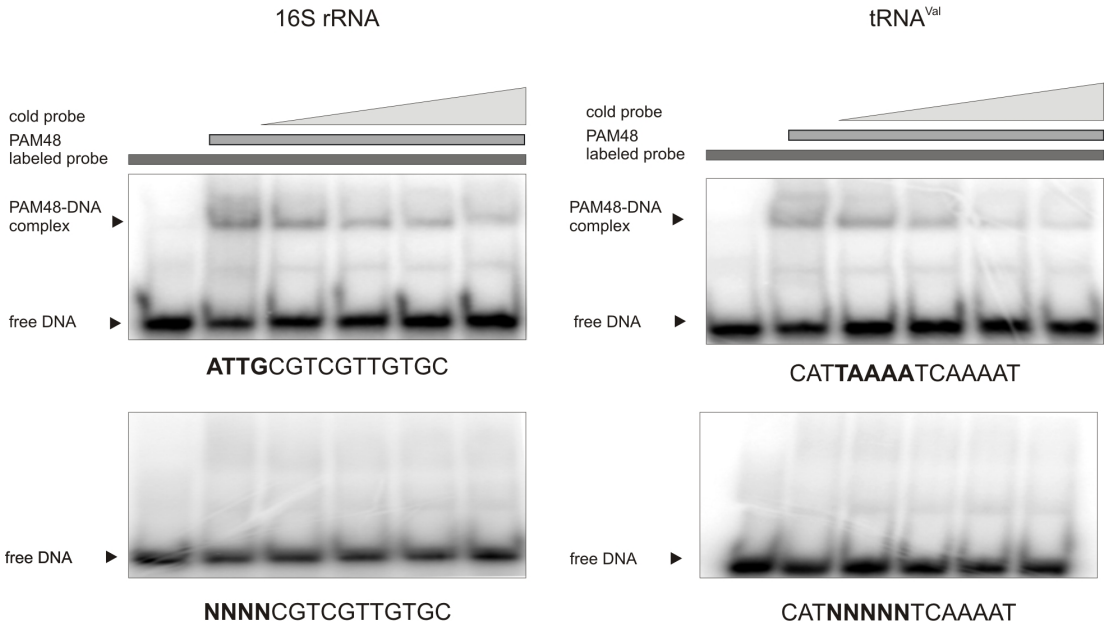

Figure 3.16.2 - EMSA for PAM48 with 16S rRNA and tRNA^{Val} downstream sequence probes and the corresponding mutated sequences. In all panels, in the first lane labelled probes were loaded as negative and size control. In the other lanes, identical amounts of purified and refolded PAM48 (1µg) and ^{32}P-labelled probe (100 ng) was incubated with increasing amounts (0 ng, 100 ng, 250 ng, 500 ng, 1000 ng) of unlabelled (cold) probe. In the above panels, purified re-folded PAM48 was incubated with ^{32}P-labelled 16S rRNA (left) or tRNA^{Val} (right) downstream sequence 15bp probes (indicated below the panels). In the bottom panels, the experiment was repeated with the corresponding sequences carrying a random stretch of nucleotide, to prove the specificity of binding between the protein and the target sequences.

3.17 *pam48-1* and *pam48-2* accumulate a 16S rRNA precursor

The outcomes of the B1H and EMSA experiments led to the conclusion that PAM48 is able to bind a specific 15-bp sequence downstream the *rrn16* gene sequence, found within the chloroplast rRNA operon (Figure 3.17.1). The consequent questions to address were if the

binding is taking place also *in planta*, and what could be the possible effects of a misregulation in PAM48 DNA binding activity.

Early studies on rRNA maturation in plants showed that in higher-plant chloroplasts a precursor rRNA transcript containing the 16S, 23S, 4.5S and 5S rRNA is produced from the rRNA operon (Figure 3.17.1; Bellaoui et al., 2003). This primary transcript is then processed into the 23S - 4.5S rRNA precursor, plus the mature 16S and 5S rRNA. The 23S-4.5S rRNA precursor is subsequently cleaved into the 23S and 4.5S rRNAs (Strittmatter and Kössel, 1984).

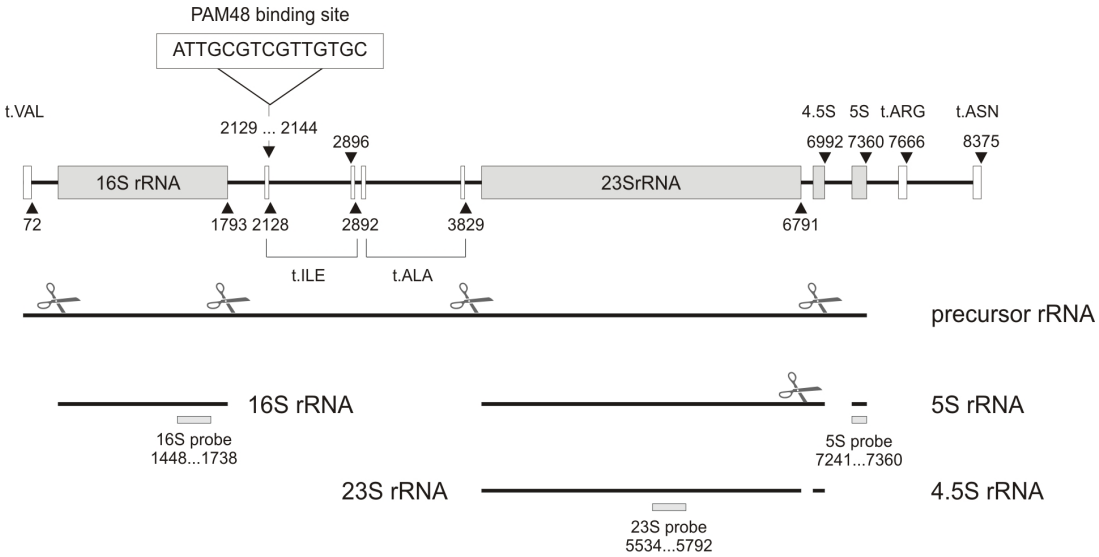

Figure 3.17.1 - Scheme representing the binding site of PAM48 downstream the *16S rRNA* gene and the splicing of plastidial rRNA (adapted from Bellaoui et al., 2003). In the white box, the sequence and exact binding position on plastidial DNA of PAM48 is indicated. rRNA genes are depicted as grey boxes, genes for tRNA as white boxes. Introns are depicted as solid lines. Below, the rRNA operon is transcribed as a single transcript (solid line) and then maturated through sequential splicing events (represented as scissors). Northern blot analysis probes used in the present work are depicted as grey lines and the corresponding hybridisation positions indicated on the mature rRNAs.

A Northern blot analysis was conducted to detect possible alterations in the transcription of the rRNA operon. Probes were designed to follow the maturation of 16S, 23S and 5S rRNA; the relative hybridization position within the chloroplast rRNA operon is illustrated Figure 3.17.1. While for the detection of 23S rRNA transcripts no evident changes in maturation was visible, for 16S rRNA a higher molecular weight band was visible above the mature transcript in *pam48-1* (Figure 3.17.2). Interestingly, also the 5S rRNA was showing alterations in the normal band maturation pattern.

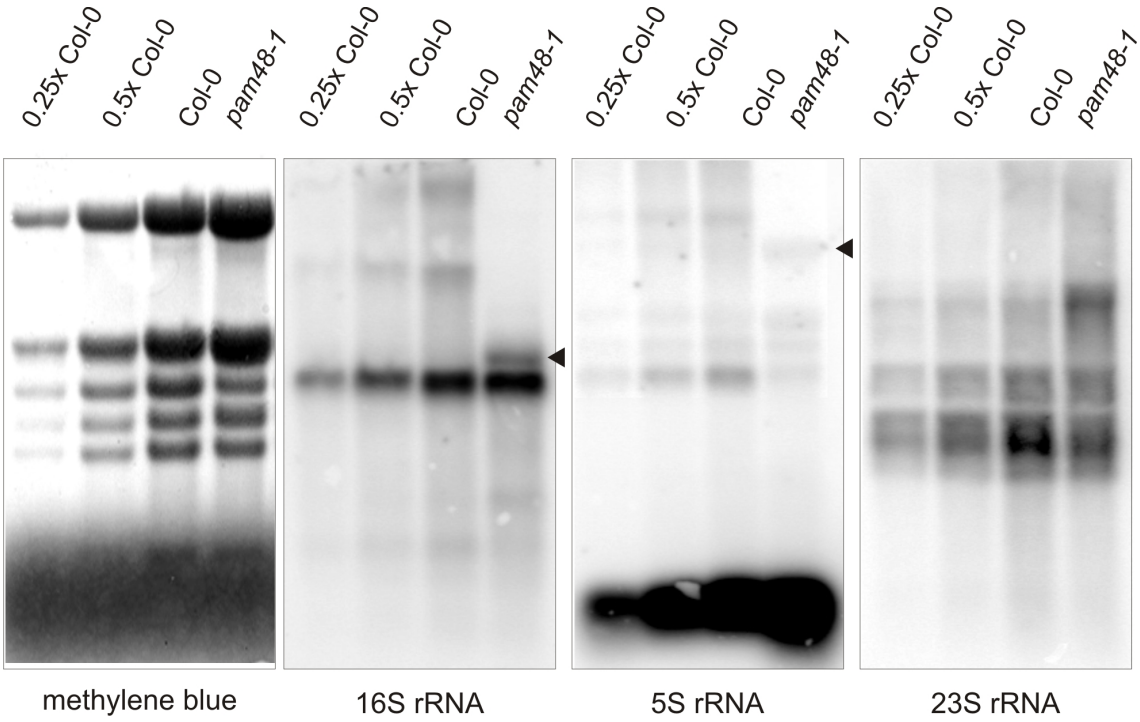

Figure 3.17.2 **-** Northern blot analysis of plastidial rRNA transcription and maturation in Col-0 and *pam48-1*. Increasing amounts (0.25, 0.5x and 1x) of total RNA extracted from WT and *pam48-1* (1x) were loaded on denaturing formaldehyde gels. After blot transfer, the resulting membranes were hybridized with different ^{32}P-labelled DNA probes (indicated above the panels) and transcripts visualized by autoradiography. Methylene blue staining of membranes (first panel) served a loading reference. Arrows indicate the additional bands in the mutant.

An additional band of identical molecular weight is present as well in the *pam48-2* mutant (Figure 3.17.3), which indicates a specific affection of 16S rRNA maturation linked to the *pam48* mutation. Moreover, the Methylene blue staining reveals a deficiency in the accumulation of plastidial ribosomal rRNAs in both mutants, with a gradient of severity that increases from the knock-down to the knock-out line.

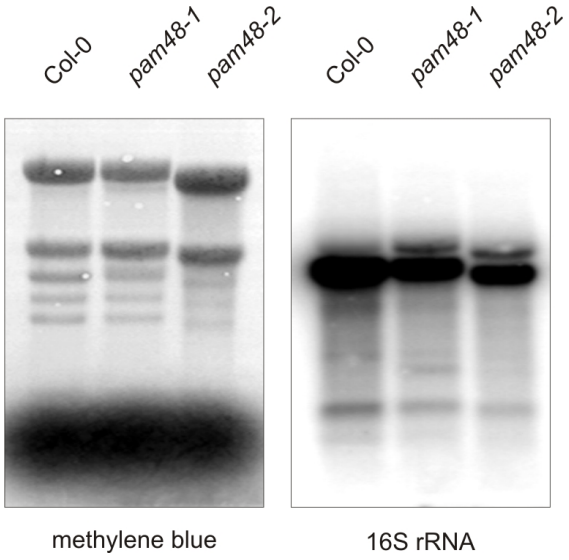

Figure 3.17.3 **-** Northern blot analysis of plastidial rRNA transcription and maturation in Col-0, *pam48-1* and *pam48-2*. Identical amounts (10 µg) of total RNA were loaded on denaturing formaldehyde gels. After blot

transfer, the resulting membranes were hybridized with a 16S rRNA ^{32}P-labelled DNA probe and transcripts visualized by autoradiography. Methylene blue staining of membranes (left panel) served a loading reference.

Since PAM48 was shown to be targeted also to mitochondria, the maturation of the mitochondrial rRNA operon was investigated in *pam48-1* mutant by Northern blot analysis. Total RNA isolated from WT and *pam48-1* leaves was blotted and hybridized with ^{32}P-labelled DNA probes designed on *18S rRNA* and *26S rRNA* genes (Figure 3.17.4). The maturation of the operon has identical pattern in the wild-type and mutant.

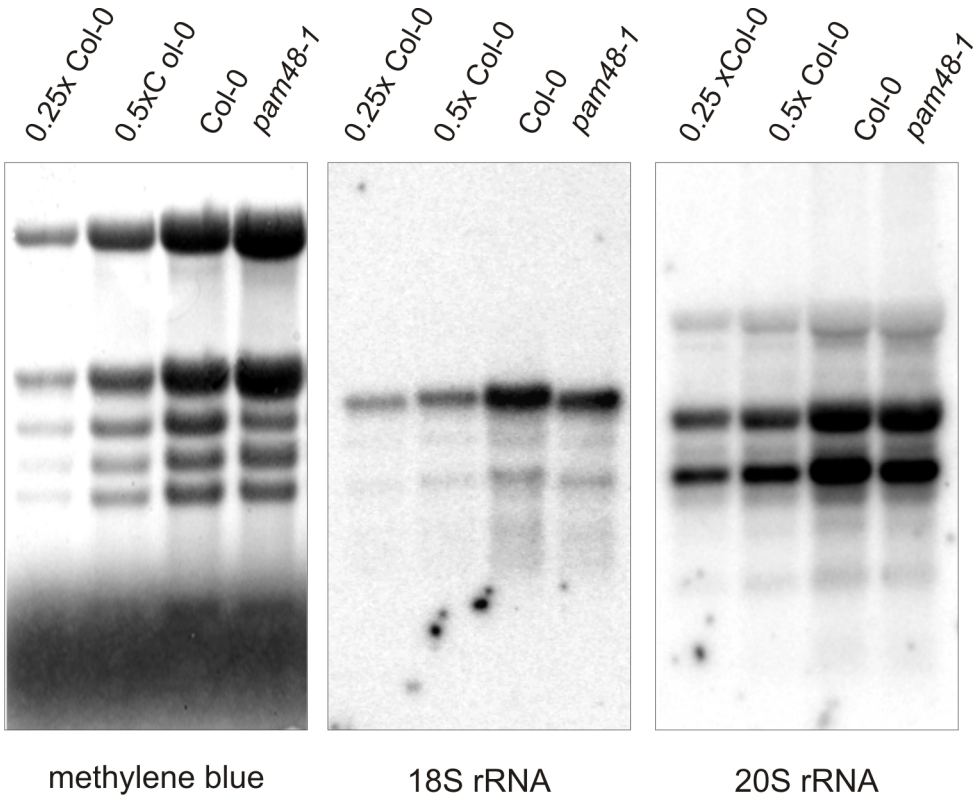

Figure 3.17.4 **-** Northern blot analysis of mitochondrial rRNA transcription and maturation in Col-0 and *pam48-1*. Increasing amount (0.25, 0.5x and 1x) of total RNA extracted from WT and *pam48-1* were loaded on denaturing formaldehyde gels. After blot transfer, the resulting membranes were hybridized with different ^{32}P-labelled DNA probes (indicated below the panels) and transcripts visualized by autoradiography. Methylene blue staining of membranes (first panel) served as a loading reference.

To summarize, even if the exact molecular mechanism is still unclear, PAM48 has an influence – either direct or indirect – on mechanisms that are part of the correct rRNA maturation in the chloroplasts, but not in mitochondria.

4 DISCUSSION

4.1 MTERFs have different roles in the plant cell

Despite the large number of proteins that are part of the MTERF family, their implicit importance and the increasing efforts in the study of these termination factors, to date the role of MTERFs in plants remains largely unclear.

Considering that MTERFs are represented by a handful of members in metazoans and that they are even absent in fungi, why have higher plants multiplied their MTERFs during evolution?

A partial explanation could be the presence of a second organelle in plants that adds complexity to the cell. In addition, flowering plant genomes underwent extensive duplication and rearrangement events during evolution (Van de Peer et al., 2009). Consequently, the large number of MTERFs in higher plants might reflect a maze of different functions.

The role of different MTERFs in plants has been the subject of recent studies and thus their importance in different cellular functions is gradually being unravelled. For example, a mutation in SOLDAT10 is able to partially rescue the *flu* phenotype (Meskauskiene et al., 2010), and BSM is a fundamental factor for plastid gene expression and for overall plant development (Babiychuk et al., 2011; Quesada et al., 2011). Furthermore, PTAC15 is an MTERF found to be one of the proteins associated with the transcriptionally active plastid chromosome (Pfalz et al., 2006).

The present work started when knowledge about MTERFs in plants was scarce. Even though metazoan MTERFs are better known, fundamental notions about their function, especially *in vivo*, are still to be uncovered.

In this work, studies were focused on a MTERF protein in the model plant *A. thaliana*, referred to as PAM48.

4.2 PAM48 is important for correct photosynthetic functions

The *pam48-1* mutant was previously isolated through screening of a collection of T -DNA-mutagenized Arabidopsis lines for plants with alterations in the effective quantum yield of PSII (Varotto et al., 2000). Detailed fluorimetric analysis of WT, *pam48-1* and complemented *pam48-1* lines confirmed the photosynthetic defect and showed a significant decrease in the

efficiency of PSII photochemistry in *pam48-1*, successfully rescued in the *pam48-1* complemented lines (see Table 3.4.1).

The mutant phenotype itself suggests impairment in photosynthesis, since *pam48-1* leaves are chlorotic and smaller in comparison to wild-type plants. Interestingly, the cotyledons appear wild-type-like, but as soon as the first true leaves emerge (i.e. when the plant overcomes the autotrophic phase and starts photosynthesis) the defect appears clearly. Moreover, *pam48-1* plants show a shorter, smaller habitus and a slower development, but they are able to complete their life cycle producing viable seeds (see Figure 3.2.1).

As shown in real-time PCR and semi quantitative RT-PCR (Figure 3.5.1) analyses, the *pam48-1* allele is only knocked down and retains a certain degree of transcription. It is remarkable that even partial depletion of *PAM48* transcript levels is able to cause such a strong phenotype, giving evidence of an important function of PAM48 in the plant.

Blue native – PAGE analysis indicated (see Figure 3.10.1) a general perturbation in thylakoid protein complexes. In *pam48-1* a general depletion in the amount of certain complexes is observed, particularly in PSI monomers, PSII dimers and Cyt b6f/PSII monomers. Interestingly, in *pam48-1* all bands containing LHCII are shifted to a lower molecular weight. This could be due to a defect in pigment-binding, resulting in lighter antenna complexes. However, it remains a hypothesis to be confirmed and the possibility of a solubilisation artefact is still open.

Western blot analysis on singular components of the thylakoid complexes revealed a specific de-regulation of chloroplast-encoded proteins, such as PetB, AtpB, PsbA, PsbB, PsbC, PsaA and PsaB (see Figure 3.12.1). Strikingly, no change in levels of the investigated nuclear-encoded proteins was observed: all the light harvesting complexes subunits were unaffected, and the same was true for the Rieske protein, Psbp and PsbS. Interestingly, Northern blot analysis performed on a variety of photosynthetic gene transcripts showed no difference in transcription levels for *pam48-1* (Figure 3.13.1). These data are in accordance with the microarray analysis, in which no significant fold change in transcription of photosynthetic genes was observed. Notably, transcription of photosynthetic subunits that are affected on a translational level appears normal in the mutant.

Taken together, the results of Western blot and Northern blot analysis imply that *pam48-1* has a defect in translation of proteins for photosynthetic functions, and that this defect is limited to the chloroplast compartment.

All these experiments were performed using the *pam48-1* knock-down line, as - despite the pale and small phenotype - the mutant plants are giving enough material and viable seeds.

When *PAM48* transcript levels are strongly depleted, as in the *pam48-2* mutant (see Figure 3.5.1), the phenotype appears more severe. Indeed, *pam48-2* was not able to grow on soil, but only on media supplemented with sugar, showing albino cotyledons and growth arrest at early stages (Figure 3.2.2). Transmission electron microscopy of *pam48-2* embryos (Figure 3.11.1) revealed a dramatic perturbation of plastid development: the organelles showed thylakoids lacking structure and scarce accumulation of lipid and starch. All together these data - including the depletion in levels of proteins belonging to photosynthetic complexes, the chlorotic phenotype in the *pam48-1* line and the albino leaves in the *pam48-2* line, the low photosynthetic capacity revealed by fluorimetric analysis - indicate a linkage between the mutation in the *At4g38160* gene and correct photosynthetic functions in *A. thaliana*.

4.3 PAM48 is dually targeted to mitochondria and chloroplasts, but it functions mainly in chloroplasts

Recently, localisation of GFP fusion proteins of all MTERF members found in *A. thaliana* has been investigated and PAM48 was found to be targeted exclusively to mitochondria (Babiychuk et al., 2011). However, the photosynthetic phenotype of *pam48-1* and *pam48-2*, the impairment of chloroplast translation in *pam48-1* and the defect in plastid formation in *pam48-2* suggest that PAM48 functions in chloroplasts.

Transformation with a PAM48-GFP fusion construct led to complementation of the *pam48-1* phenotype, with the localisation of PAM48 both in mitochondria and in chloroplasts (Figure 3.8.3). Immunoblot analysis confirmed the targeting in chloroplasts, and in particular in the stroma (Figure 3.8.4).

In the past years the number of reported dual-targeted proteins increased, and to date around 50 cases are known (Carrie et al., 2009a). The study and discovery of dual-targeted proteins is challenging in many aspects. Bioinformatics prediction can be often misleading, as the targeting peptide might be ambiguous, be the product of an alternative transcription initiation (Dinkins et al., 2008), or even be missing (e.g. the RPS16 protein, that was found to be dual targeted in *Medicago truncatula* and *Populus alba* without a cleavable N-terminal targeting signal, Ueda et al. (2008)). Due to the complex and various mechanisms behind dual targeting processes, *in vitro* import approaches are often not applicable (Carrie et al., 2009a). A common approach to investigate dual targeting is the fusion of proteins to GFP, but in a wide study on dual-targeted proteins it was found that the labelling of the two compartments differed considerably depending on the system used (Carrie et al., 2009b). Some reports have described dual targeting in GFP reporter assays as a non-simultaneous process, with

predominant localization to mitochondria observed in one experiment, and to plastids when the experiment was repeated (Beardslee et al., 2002). *In vitro* systems have strong limitation too; because of the lack of an intact cellular system the import of some proteins might be unsuccessful (Pavlov et al., 2007). These difficulties in empirical approaches might result in false-negative results, therefore the number of dual-targeted proteins could be far bigger than expected. This might also represent the reason why the secondary targeting of PAM48 to the chloroplast was in a first attempt not detected, as it happened in the *in vitro* import (Figure 3.8.2).

The reasons for having proteins located in more than one compartment are multiple; for example, dual targeting of proteins does not increase the number of proteins in a cell, but can expand their functions, in that a protein located in more than one location will presumably function with a distinct biochemical process in each location (Carrie et al., 2009a). Moreover, dual targeting could represent a strategy to regulate inter-organelle communication: sending the same proteins to both organelles at the same time ensures that they are capable of carrying out their functions in a co-ordinated manner (Carrie et al., 2009a). Remarkably, dual-targeted proteins often fall in functional categories that are important for general organellar housekeeping processes such as DNA and RNA maintenance functions and translation components (Mackenzie, 2005).

Among the MTERF members in *A. thaliana*, an example of dual-targeting is already known: BSM was firstly found to be a protein uniquely targeted to chloroplast (Babiychuk et al., 2011), but an additional targeting to mitochondria was recently reported (Quesada et al., 2011).

The question that remains open is why PAM48 is sent into two compartments. The data collected in the present work strongly point out a chloroplast function, while the possible role in the mitochondrion is still unclear. In *pam48-1* and *pam48-2* the mitochondrial functions seem not to be affected, as seen in Western blot (see Figure 3.12.2), microarray (Figure 3.14.1) and TEM analyses (see Figure 3.11.1). Moreover, when complementing the *pam48-1* phenotype with a construct targeted exclusively to the chloroplast (see Figure 3.9.1, cTP-PAM48), the plants appear wild-type like, while complementation with a mitochondrion-targeted does not lead to a complete phenotypical rescue (mTP-PAM48, see Figure 3.9.1).

An explanation to the possibly dispensable role of PAM48 in the mitochondrion could be found in a potential redundancy of functions. As already mentioned, 35 MTERF-related proteins are found in *A. thaliana* and most of them are mitochondrion-targeted. One could speculate that out of the 17 mitochondrial MTERFs, one or more could overlap with PAM48 mitochondrial function and at least partially compensate for it in the mutant.

On the contrary, no compensation appears to be possible for those functions concerning the chloroplast, at least on the phenotypical level. Thus, the role of PAM48 is fundamental for the chloroplast and its correct performance.

4.4 PAM48 is binding specific sequences of DNA that are found within the plastidial genome

As demonstrated in the tertiary structure prediction analysis with the I-TASSER software (http://zhanglab.ccmb.med.umich.edu/I-TASSER), PAM48 has a predicted structure compatible with that of the human MTERF1 (Figure 3.15.1). The human MTERF1 structure was resolved through X-ray diffraction analysis, together with a DNA oligomer. In the study, it was shown how hMTERF1 is able to wrap the DNA helix, by exposing its positive amino acidic residues and stabilizing the negative charges of the phosphate groups on the backbone.

In addiction, the MTERFs characterized so far in metazoan revealed binding functions to organellar DNA (Roberti et al., 2009).

In the present work the bacterial one-hybrid screening (Meng and Wolfe, 2006) has been chosen to investigate a possible DNA binding function for PAM48 and its relative targets. The system has many advantages; it is a relatively rapid technique and requires standard laboratory equipment. As a consequence of its relative simplicity, the costs for this technique are contained, making it the method of choice for a rapid but effective protein-DNA interaction screening. Apart from its accessibility, this screening method is preferable to other *in vitro* techniques, such as SELEX, as the interactions occur *in vivo.* Proteins interact with DNA in their native conformation, starting from an mRNA that is processed and translated by a cellular system, with no need to purify and re-fold the protein of interest (Lopato et al., 2006). The disadvantages are the same that are found in other hybrid screening systems: the number of false positives and negatives can often represent an intrinsic problem of this technique.

The outcome of the experiment in the present work was satisfactory: a number of matches with high e-score have been found within the plastidial genome (Table 3.15.1). For instance, one of the targets was found in a region downstream the plastidial *rrn16* gene, coding for 16S rRNA, and other targets were found in regulative regions of genes with ribosome-related functions. These data are of particular interest when compared to the literature, as the human

MTERF1 is able to bind a region downstream the gene coding for the 16S rRNA in the mitochondrial genome (Chomyn et al., 1992).

It was possible to independently confirm the binding of PAM48 to two of the putative targets found in the bacterial one-hybrid screening; the EMSA assays showed a specific interaction between the purified PAM48 protein and the *RRN16* downstream region, corresponding to a spacer within the rRNA exons immediately after the first $tRNA^{Ile}$ intron (Figure 3.17.1). Thus, it is possible to conclude that PAM48 is a nucleic acid-binding protein that interacts with specific regions within the chloroplast chromosome.

4.5 *pam48-1* and *pam48-2* show defect in maturation of 16S rRNA

The maturation of 16S rRNA and other two rRNAs – 5S and 23S – was investigated, in order to find possible effects of the interaction between PAM48 and the *rrn16* downstream region *in planta*.

The Northern blot analysis in Figure 3.17.3 shows that both *pam48-1* and *pam48-2* mutants accumulate 16S rRNA precursor. The relative abundance of the mature and unprocessed rRNA species changes significantly, being the mature form scarcer in both mutated lines. The defect in plastidial rRNA accumulation is so prominent that can be observed on the total RNA staining.

Interestingly, in the *pam48-1* mutant the pattern of maturation of the 5S rRNA seems to be perturbed while the 23S rRNA is correctly spliced and the typical bands pattern is respected in the mutant (Figure 3.17.2).

The genes for chloroplast rRNAs (23S, 16S, 5S, and 4.5S) are located in the large inverted repeat region of land plant chloroplast genomes, where they form part of the *rrn* operon (Palmer, 1985). The *rrn* operon, which includes three tRNA genes ($tRNA^{Val}$, $tRNA^{Ile}$, $tRNA^{Ala}$), is transcribed as a large polycistronic RNA that is processed by endoribonucleases and exoribonucleases to yield the mature rRNA and tRNA species (Bollenbach et al., 2005). The primary precursor is initially processed by excision of the tRNAs and by additional endonucleolytic cleavages to generate 16S and 5S rRNA precursors, and a dicistronic 23S–4.5S processing intermediate. Subsequent endonucleolytic processing of the 23S–4.5S rRNA dicistron to generate monocistronic 23S and 4.5S rRNAs appears to occur on the ribosome and is thought to require prior 3' end maturation of 4.5S rRNA. The 16S, 23S and 5S rRNA precursors generated by endonucleolytic cleavage require further processing to establish mature 5' and 3' ends (Bollenbach, 2005 and Figure 3.17.1).

The molecular components that mediate plastid rRNA processing are poorly understood, but it is known that they include two 3' to 5' exoribonucleases. One is a polynucleotide phosphorylase (PNPase) that is involved in 23S rRNA processing and in the metabolism of tRNAs and mRNAs (Walter et al., 2002; Sauret-Gueto et al., 2006), and the other is a homolog of *E. coli* RNase R (RNR1) that is involved in the maturation of 23S, 16S, and 5S rRNAs (Kishine et al., 2004; Bollenbach et al., 2005).

Other factors that affect chloroplast rRNA maturation are defined by mutants that accumulate rRNA intermediates. In particular, mutants found to accumulate 16S rRNA precursors are: *hcf7,* maize high chlorophyll fluorescence7 (Barkan, 1993), maize *rnc1* (Watkins et al., 2007), *wco,* Arabidopsis white cotyledon (Yamamoto et al., 2000) and *suv1,* suppressor of variegation1 (Yu et al., 2008). In the mutants cited, a defect in the normal 16S rRNA maturation – visible as altered rRNA patterns in ethidum bromide-stained gels and Northern hybridization - is accompanied by normal levels of chloroplast mRNAs, but by decreased rates of chloroplast protein synthesis and by reduced accumulation of chloroplast proteins, as seen in *pam48-1* and *pam48-2* mutants.

Other mutants in factors that affect chloroplast rRNA maturation are Arabidopsis *dal,* which accumulates 16S and 23S precursor rRNAs (Bisanz et al., 2003); and tomato *dcl* (for defective chloroplasts and leaves), in which 4.5S rRNA processing is defective (Bellaoui et al., 2003); 4.5S rRNA processing is also impaired in Arabidopsis mutants with downregulated *DCL* gene expression (Bellaoui and Gruissem, 2004).

Concerning their phenotypes, mutants with defects in the correct maturation of the rrn operon are often showing white cotyledons *(wco)* and white leaves *(hcf7, rnc1);* in some cases are incapable of autotrophic growth *(rnr1*), or they have defects in embryo development and general morphogenesis *(rnr1, dal).* These mutants show poorly developed plastids, lacking structure and membrane organisation *(wco, rnr1, and dal).* The *pam48-2* mutant shares all of these phenotypic features: plants are unable to survive without sugar supply and have white cotyledons and leaves (see Figure 3.2.2), where very little chloroplasts are found (Figure 3.11.2). Furthermore, plastid formation in the embryonic stages is strongly perturbed (Figure 3.11.1).

Mutants with defects in chloroplast rRNA maturation need not defined genes whose products are directly involved in the process; it is not rare that mutants with primary lesions in ribosome assembly or function show altered rRNA maturation (Yu et al., 2008). For example, PPR4 is a pentatricopeptide repeat protein that promotes the correct splicing of a ribosome-related protein (RPS12) precursor (Schmitz-Linneweber et al., 2006). *ppr4* mutants, accumulate

increased levels of pre-16S rRNA, although the direct interaction of PPR4 with ribosomal RNA is unlikely to occur. In a complementary manner, PNPase and RNR1 mutants, which have primary defects in chloroplast rRNA processing, have pleiotropic effects that include reduced rates of chloroplast translation and protein accumulation (Bollenbach et al., 2005; Sauret-Gueto et al., 2006).

As demonstrated by the bacterial one-hybrid screening and its subsequent confirmation through gel mobility shift, PAM48 is a nucleic acid-binding protein, with specific targets that were confirmed *in planta*, corresponding to the rRNA operon in the chloroplast. The exact mechanism by which the lack of binding of PAM48 to its target(s) is influencing the correct splicing of 16S rRNA, leading to an accumulation of its precursors, is still a matter of study. As discussed above, defects in mechanisms that are connected to ribosomal functions are representing a challenge; the effect of this mutations are pleiotropic and hard to reduce to a single event, as they are involving translation, a process that is fundamental for every other cellular function.

The number of proteins known to bind both DNA and RNA is to date limited (Cassiday and Maher, 2002) and the studies conducted so far on metazoan and plant MTERFs showed DNA interactions only. However, in order to either confirm or exclude a possible interaction between PAM48 and RNA, a RIP-ChIp analysis is ongoing in the laboratory of Prof. Schmitz-Linneweber (Humboldt University, Berlin).

4.6 In *pam48-1*, impairment of chloroplast translation does not affect the expression of nuclear-encoded genes for photosynthetic components

In the *pam48-1* mutant, chloroplast-encoded genes show lower translation rates (Figure 3.12.1), and the defect appears to be limited to the chloroplast compartment. Despite the dual targeting of PAM48, levels of protein targeted to or translated in the mitochondrion appear unaffected (Figure 3.12.2). Microarray analysis did not reveal abnormalities in the transcription of organellar genes and mitochondrial rRNAs are - on the contrary of chloroplast – normally transcribed and maturated (Figure 3.17.4). Moreover, TEM analysis of the *pam48-2* mutant showed that the plastid development is strongly perturbed in the embryo, while mitochondria develop normally. Nuclear transcription and cytosolic translation of photosynthetic components are unaltered (Figure 3.13.1 and Figure 3.12.1). This indicates that the mutation in *pam48-1* has no effect on the retrograde signalling pathway involving the expression of the investigated genes, since the lower translational rate in the chloroplast does not correspond to a lower transcriptional rate in the nucleus. This observation was similarly

found in the *wco* mutant (Yamamoto et al., 2000), in which the incomplete splicing of 16S rRNA leads to lower transcription rates in the chloroplast (in a cotyledon-specific manner), but it does not affect nuclear gene expression.

Taking together the cited observations from Pesaresi et al. (2006) and the data presented, it might be concluded that OGE has possibly an influence on nuclear gene expression (NGE) of photosynthetic genes only when the two organelles are concertedly sending their retrograde signal to the nucleus.

Although examples of proposed models including crosstalk between mitochondrion and chloroplast are present in the literature (Leister et al., 2005; Woodson and Chory, 2006 Pfannschmidt, 2010), the study of retrograde signalling in plants has mostly been dedicated to the chloroplast as a single and freestanding unit (with some exceptions: Pesaresi et al., 2006; Giraud et al., 2009). This has plausibly happened for sake of simplicity and because of the uniqueness of the chloroplast to the plant cell. It should be considered though that the plant mitochondrion has unique features in comparison to non-plant mitochondria (e.g.: cyanide-resistant alternative oxidase in the respiratory chain, AOX). In the same way, a remarkable and unique feature of the plant cell is the ability to coordinate three different genomic compartments, namely the nucleus, the chloroplast and the mitochondrion. It is therefore implicit that the signals shared between the two organelles are crucial for the whole cell. For instance, the shift form heterotrophic to autotrophic metabolism in young plants (i.e. from cotyledonary to the first true leaves stage) represents a moment of intense exchange between mitochondria, chloroplasts and nucleus (Pfannschmidt, 2010).

Considering the dual-targeting of PAM48, the protein could represent a good candidate to dissect retrograde signalling, as part of the chloroplast-mitochondrion-nucleus network. The understanding of its role in both organelles appears therefore of great interest. The implementation of the artificial targeting experiments started in the present work, which aimed to the singular targeting of PAM48 to each organelle, might represent a good starting point. Another strategy could be the production of double mutants in mitochondrial MTERFs, to overcome the possible redundancy of PAM48 in the mitochondrion.

4.7 PAM48 role in the plant cell: a first model

All the data discussed in this session are summarized in a model of the putative function of PAM48 in the context of the whole plant cell (Figure 4.7.1).

The *PAM48* gene is transcribed in the nucleus, translated by the cytosolic machinery and subsequently targeted to both chloroplasts and mitochondria, through a mechanism that is not

yet clarified, as the PAM48 protein has no predicted targeting peptide. PAM48 can be seen as part of the anterograde signalling pathway, as one of the proteins coded by the nucleus to take part to organellar functions, such as OGE.

The role of PAM48 in the mitochondrion remains heretofore undiscovered: the lack of any effect on the transcriptional or translational levels of mitochondrial components makes it necessary to explore the possible role of PAM48 in this compartment with further experiments.

On the other hand, the present work shed some light on the function of PAM48 within the chloroplast. PAM48 is able to bind to plastidial DNA, in a specific region that corresponds to the rRNA operon, downstream the *16S rRNA* gene (Figure 4.7.1-1). This binding has most likely an effect on the quality of rRNA maturation (Figure 4.7.1-2), as the *pam48-1* and *pam48-2* mutants accumulate 16SrRNA precursors (Figure 4.7.1-3). The link between the DNA binding activity and the maturation of ribosomal RNA is yet to be understood. Many works in the literature have demonstrated how a defect in ribosome assembly and functioning can be produced by a plethora of defects in cellular mechanisms, which can also be unrelated to ribosomal activity. Experiments on the quality of ribosome assembly, such as polysome association assay, would be useful to clarify the extent of the rRNA splicing defect on translational activity in the *pam48* mutants. Moreover, the investigation of a possible direct interaction of PAM48 with RNA would give insights in a potential involvement of the protein in RNA maturation or processing. The ongoing RNA-ChIp analysis in the laboratory of Prof. Schmitz-Linnenweber (Humboldt University, Berlin) might provide an answer to this question.

A defect in ribosomal function is suggested by the low translation rates in the chloroplast. The effect is limited exclusively to chloroplast-encoded proteins and strongly suggests a linkage between the pre-16S rRNA accumulation, the ribosome quality in the chloroplast and the low efficiency in translation. The hypothesis is that the accumulation of pre-16S rRNA (Figure 4.7.1-3) and the consequent lower amount of mature 16S rRNA leads to a defect in the ribosome assembly and function (Figure 4.7.1-4) and eventually to a decrease in the translational rate of chloroplast-encoded proteins (Figure 4.7.1-5). As a consequence, the drop in translation rates leads to a general defect in photosynthesis, as the components involved are not sufficient to the correct performance of photosynthetic functions (Figure 4.7.1-6). How these changes in translation rates and photosynthesis capacity are involved in retrograde signalling to the nucleus is still a matter of study. A hypothesis would

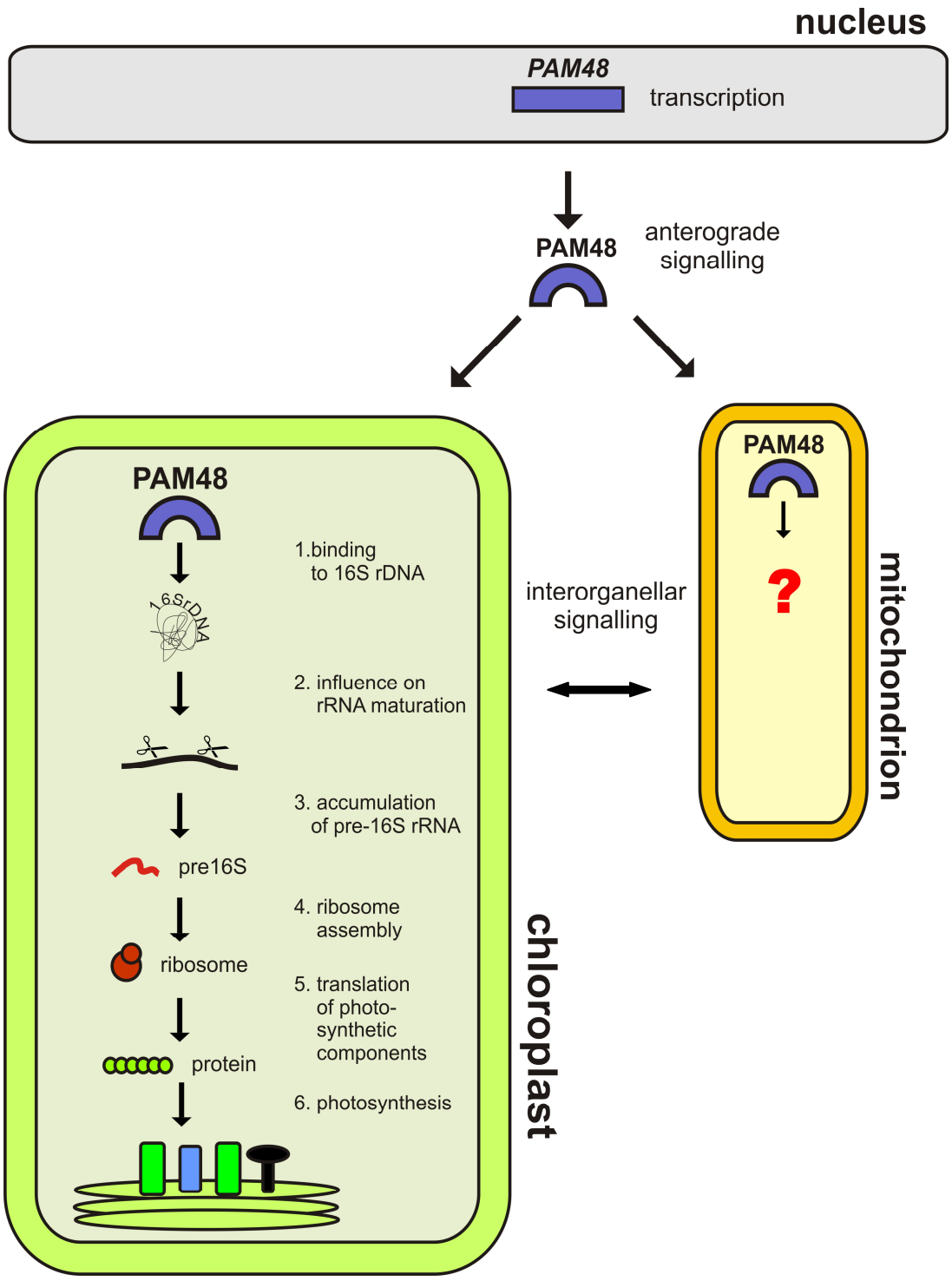

Figure 4.7.1 - Proposed scheme for the role of PAM48 in the plant cell. PAM48 is transcribed in the nucleus and translated by the cytosolic machinery. Subsequently, PAM48 is dually imported into mitochondria – where its function is still unclear- and into chloroplasts. Here, PAM48 is able to bind downstream the 16S rDNA (1) and by a not yet clarified mechanism influence the maturation of rRNA (2). When PAM48 is missing, the chloroplast accumulates 16S rRNA precursor (3) indicating that PAM48 could have a role in its correct maturation. Accumulation of 16S rRNA has an influence on plastidial ribosome assembly and function (4) that results in a decrease of translation rate of photosynthetic components (5). The loss of efficiency in translation results in turn in an overall photosynthetic defect (6).

be that the synergistic action of chloroplast and mitochondrion would be necessary to activate nuclear gene transcription. Therefore, it would be interesting to characterize the effect of the PAM48 mutation in mitochondria.

Furthermore, considering the seedling-lethal phenotype of the *pam48-2* mutant and the strongly perturbed plastids found in its cotyledons, it is possible to conclude that PAM48 has a fundamental function in plastid development and differentiation in the early stages of plant ontogenesis.

In summary, the data presented show that also in plants MTERFs are able to bind nucleic acids and interact with the chloroplast chromosome, influencing the quality of maturation of rRNAs. In the future, deeper studies of the MTERF protein family in plants could contribute to the understanding of yet unknown mechanisms related to organellar gene expression and intra-cellular signalling.

5 REFERENCES

Alonso J. M., Stepanova A. N. (2003). T-DNA mutagenesis in Arabidopsis. *Methods Mol. Biol*. 236, 177-188

Aronsson H., Jarvis P. (2002). A simple method for isolating import-competent *Arabidopsis* chloroplasts. *FEBS Letters* 529: 215-220

Asin-Cayuela J., Helm M., Attardi G. (2004). A monomer-to-trimer transition of the human mitochondrial transcription termination factor (MTERF) is associated with a loss of in vitro activity. *J Biol. Chem.* 279: 15670–15677.

Babiychuk E., Vandepoele K., Wissing J., García-Diaz M., De Rycke R., et al. (2011). Plastid gene expression and plant development require a plastidic protein of the mitochondrial transcription termination factor family. *Proc. Natl. Acad. Sci.* USA 108: 6674–6679.

Barbrook A.C., Howe C.J., Kurniawan D.P., Tarr S.J. (2010) Organization and expression of organellar genomes. *Philos*. *Trans. R. Soc. Lond. B Biol. Sci*.:365:785–797.

Barkan A. (2011). Expression of plastid genes: Organelle-specific elaborations on a prokaryotic scaffold. *Plant Physiol*. 155: 1520–1532.

Barkan A. (1993). Nuclear mutants of maize with defects in chloroplast polysome assembly have altered chloroplast RNA metabolism. *Plant Cell* 5: 389–402.

Bassi R, dal Belin Peruffo A, Barbato R, Ghisi R. Differences in chlorophyll-protein complexes and composition of polypeptides between thylakoids from bundle sheaths and mesophyll cells in maize. *Eur. J. Biochem*. 1985;146:589–595.

Beardslee T.A., Roy-Chowdhury S., Jaiswal P., Buhot L., Lerbs-Mache S., Stern D.B., Allison L.A. (2002). A nucleus-encoded maize protein with sigma factor activity accumulates in mitochondria and chloroplasts. *Plant J*. 31: 199–209.

Bellaoui M., Gruissem W. (2004). Altered expression of the Arabidopsis ortholog of *DCL* affects normal plant development. *Planta* 219: 819–826.

Bellaoui M., Keddie J.S., Gruissem W. (2003). DCL is a plant specific protein required for plastid ribosomal RNA processing and embryo development. *Plant Mol. Biol*. 53: 531–543.

Bisanz C., Begot L., Carol P., Perez P., Bligny M., Pesey H., Gallois J.-L., Lerbs-Mache S., Mache R. (2003). The Arabidopsis nuclear *DAL* gene encodes a chloroplast protein which is required for the maturation of the plastid ribosomal RNAs and is essential for chloroplast differentiation. *Plant Mol*. Biol. 51: 651–663.

Bollenbach T.J., Lange H., Gutierrez R., Erhardt M., Stern D.B., Gagliardi, D. (2005). RNR1, a 39-59 exoribonuclease belonging to the RNR superfamily, catalyzes 3' maturation of chloroplast ribosomal RNAs in Arabidopsis thaliana. *Nucleic Acids Res*. 33: 2751–2763.

Bölter B, Soll J. (2007) Import of plastid precursor proteins into pea chloroplasts. *Methods Mol Biol*. 390: 195–206

Boyes D. C., Zayed A. M., Ascenzi R., McCaskill A. J., Hoffman N. E. (2001). Growth stage-based phenotypic analysis of Arabidopsis: a model for high throughput functional genomics in plants. *Plant Cell* 13: 1499–1510.

Bradbeer J.W., Atkinson Y.A., Borner T., Hagemann, R. (1979). Cytoplasmic synthesis of plastid polypeptide may be controlled by plastid-synthesized RNA. *Nature* 279: 816-817.

Carrie C., Giraud E., Whelan J. (2009a). Protein transport in organelles: Dual Targeting of Proteins to Mitochondria and Chloroplasts. *FEBS Journal* 276:1187-95.

Carrie C., Kühn K., Murcha M.W., Duncan O., Small I.D., O'Toole N., Whelan J. (2009b). Approaches to Defining Dual-Targeted Proteins in Arabidopsis. *Plant J.* 57:1128-39.

Cassiday L.A., Maher L.J. (2009). Having it both ways: transcription factors that bind DNA and RNA. *Nucleic Acids Res*., 30:4118-4126.

Chomyn A., Martinuzzi A., Yoneda M., Daga A., Hurko O. et al. (1992). MELAS mutation in mtDNA binding site for transcription termination factor causes defects in protein synthesis and in respiration but no change in levels of upstream and downstream mature transcripts. *Proc. Natl. Acad. Sci.* USA 89: 4221–4225.

Clough S.J., Bent A.F. (1998). Floral dip: a simplified method for Agrobacterium-mediated transformation of *Arabidopsis thaliana*. *Plant J.* 16:735–743.

Condon, C., Squires C., Squires C.L. (1995). Control of rRNA transcription in *Escherichia coli*. *Microbiol. Rev*. 59:623–645.

Deplancke B., Dupuy D., Vidal M., Walhout A.J. (2004). A gateway-compatible yeast one-hybrid system. *Genome Res*. 14: 2093–2101

Desveaux D., Subramaniam R., Després C., Mess J.-N., Lévsque C., Fobert P.R., Dangl J.L.., Brisson N. (2004). A ‘‘Whirly’’ transcription factor is required for salicylic acid-dependent disease resistance in Arabidopsis. *Dev. Cell*. 6:229–240.

Dinkins R.D., Majee S.M., Nayak N.R., Martin D., Xu Q., Belcastro M.P., Houtz R.L., Beach C.M., Downie A.B. (2008). Changing transcriptional initiation sites and alternative 5'- and 3'-splice site selection of the first intron deploys Arabidopsis protein isoaspartyl methyltransferase2 variants to different subcellular compartments. *Plant J*. 55, 1–13.

Dovzhenko A., Dal Bosco C., Meurer J. and Koop H. U. (2003). Efficient regeneration from cotyledon protoplasts in *Arabidopsis thaliana*. *Protoplasma* 222: 107-111.

Dyall S.D., Brown M.T. and Johnson P.J. (2004). Ancient invasions: from endosymbionts to organelles. *Science* 304: 253–257.

Eberhard S., Drapier D., Wollman F.A. (2002). Searching limiting steps in the expression of chloroplast-encoded proteins: relations between gene copy number, transcription, transcript

abundance and translation rate in the chloroplast of Chlamydomonas reinhardtii. *Plant J.* 31: 149–160.

Fernandez-Silva P., Martinez-Azorin F., Micol V., Attardi G. (1997). The human mitochondrial transcription termination factor (mTERF) is a multizipper protein but binds to DNA as a monomer, with evidence pointing to intramolecular leucine zipper interactions, *EMBO J.* 16 1066–1079.

Fujii S., Small I. (2011). The evolution of RNA editing and pentatricopeptide repeat genes. *New Phytol*. 191(1):37-47.

Giegé P., Sweetlove L.J., Cognat V., Leaver C.J. (2005). Coordination of Nuclear and Mitochondrial Genome Expression during Mitochondrial Biogenesis in Arabidopsis. *Plant Cell* 17:1497-1512.

Giraud E., Van Aken O., Ho L.H.M., Whelan J. (2009). The transcription factor ABI4 is a regulator of mitochondrial retrograde expression of ALTERNATIVE OXIDASE1a. *Plant Physiol.* 150: 1286–1296

Gray M. W., Burger G., Lang B. F. (1999). Mitochondrial Evolution. *Science* 283: 1476–1481.

Hajdukiewicz P.T., Allison L.A., Maliga P. (1997). The two RNA polymerases encoded by the nuclear and the plastid compartments transcribe distinct groups of genes in tobacco plastids. *EMBO J*. 16: 4041–4048.

Hanaoka M., Kanamaru K., Takahashi H., Tanaka K. (2003). Molecular genetic analysis of chloroplast gene promoters dependent on SIG2, a nucleus-encoded sigma factor for the plastid-encoded RNA polymerase, in *Arabidopsis thaliana*. *Nucleic Acids Res*. 31:7090–7098.

Hedtke, B., Börner, T., Weihe, A. (1997). Mitochondrial and chloroplast phage-type RNA polymerases in *Arabidopsis*, *Science* 277: 809–811.

Hellman L.M., Fried M.G. (2007) Electrophoretic mobility shift assay (EMSA) for detecting protein-nucleic acid interactions. *Nat. Protoc*. 2: 1849–1861.

Irizarry R.A., Hobbs B., Collin F., Beazer-Barclay Y.D., Antonellis K.J., Scherf U., Speed T.P. (2003). Exploration, normalization, and summaries of high density oligonucleotide array probe level data. *Biostatistics* 4: 249–264.

Ishizaki Y., Tsunoyama Y., Hatano K., Ando K., Kato K., Shinmyo A., Kobori M., Takeba G., Nakahira Y., Shiina T. (2005). A nuclear encoded sigma factor, Arabidopsis SIG6, recognizes sigma-70 type chloroplast promoters and regulates early chloroplast development in cotyledons. *Plant J* 42:133–144.

Joung, J.K., Ramm, E.I., Pabo, C.O. (2000). A bacterial two-hybrid selection system for studying protein-DNA and protein-protein interactions. *Proc. Natl. Acad. Sci. USA* 97: 7382–7387.

Keeling P.J., Palmer J.D. (2008). Horizontal gene transfer in eukaryotic evolution. *Nat Rev Gene*t. 9: 605–18.

Kishine, M., Takabayashi, A., Munekage, Y., Shikanai, T., Endo, T., Sato, F. (2004). Ribosomal RNA processing and an RNase R family member in chloroplasts of Arabidopsis. *Plant Mol. Biol*. 55: 595–606.

Kleine T., Voigt C. and Leister D. (2009). Plastid signalling to the nucleus: messengers still lost in the mists? *Trends Genet*. 25(4):185-92.

Kruse B., Narasimhan N., Attardi G. (1989). Termination of transcription in human mitochondria: identification and purification of a DNA binding protein factor that promotes termination. *Cell* 58: 391–397.

Leister, D. (2005) Genomics-based dissection of the cross-talk of chloroplasts with the nucleus and mitochondria in Arabidopsis. *Gene* 354: 110–116.

Lerbs-Mache S. (2011). Function of plastid sigma factors in higher plants: regulation of gene expression or just preservation of constitutive transcription? *Plant Mol Biol* 76: 235–249.

Liere K., Börner T. (2007). Transcription and transcriptional regulation in chloroplasts. In R Bock, Cell and Molecular Biology of Plastids. Springer-Verlag, Heidelberg, pp 121–174.

Linder T., Park C.B., Asin-Cayuela J., Pellegrini M., Larsson N.G., Falkenberg M., Samuelsson T., Gustafsson C.M. (2005). A family of putative transcription termination factors shared amongst metazoans and plants. *Curr. Genet*. 48: 265–9.

Lopato S., Bazanova N., Morran S., Milligan A.S., Shirley N., Langridge P. (2006). Isolation of plant transcription factors using a modified yeast one-hybrid system. *Plant Methods*:2:3.

Loschelder H., Schweer J., Link B., Link G. (2006). Dual temporal role of plastid sigma factor 6 in Arabidopsis development. *Plant Physiol.* 142: 642–650.

Mackenzie, S.A. (2005). Plant organellar protein targeting: a traffic plan still under construction. *Trends Cell Biol*. 15: 548–554.

Marienfeld J., Unseld M., Brennicke A. (1999). The mitochondrial genome of Arabidopsis is composed of both native and immigrant information. *Trends Plant Sci*. 4: 495–502.

Martin M., Cho J., Cesare A.J., Griffith J.D., Attardi G. (2005). Termination factor-mediated DNA loop between termination and initiation sites drives mitochondrial rRNA synthesis. *Cell* 123: 1227–1240.

Meng X., Wolfe S.A. (2006). Identifying DNA sequences recognized by a transcription factor using a bacterial one-hybrid system. *Nat. Protoc.* 1:30-45.

Meskauskiene R., Wuersch M., Laloi C., Vidi P.A., Coll N.S., Kessler F., Baruah A., Kim C., Apel K. (2009). A mutation in the Arabidopsis mTERF-related plastid protein SOLDAT10 activates retrograde signaling and suppresses $^1O_2$-induced cell death. *Plant J.* 60: 399–410.

Millar, A.H., Sweetlove, L.J., Giegé, P., and Leaver, C.J. (2001). Analysis of the Arabidopsis mitochondrial proteome. *Plant Physiol.* 127: 1711–1727

Mullet, J. E. & Klein, R. (1987). Transcription and RNA stability are important determinants of higher plant chloroplast RNA levels. *EMBO J.* 6: 1571–1579.

Nagashima A., Hanaoka M., Motohashi R., Seki M., Shinozaki K., Kanamaru K., Takahashi H., Tanaka K. (2004). DNA microarray analysis of plastid gene expression in an Arabidopsis mutant deficient in a plastid transcription factor sigma, SIG2. *Biosci. Biotechnol. Biochem.* 68: 694–704.

Noguchi, K. and Yoshida, K. (2008). Interaction between photosynthesis and respiration in illuminated leaves. *Mitochondrion* 8: 87–99.

Nomura, M. (1999). Regulation of ribosome biosynthesis in *Escherichia coli* and *Saccharomyces cerevisiae*: Diversity and common principles. *J. Bacteriol.* 181: 6857–6864.

Palmer J.D. (1985). Comparative organization of chloroplast genomes. *Annu. Rev. Genet.* 1199: 325–354.

Pavlov P.F., Rudhe C., Bhushan S., Glaser E. (2007). *In vitro* and *in vivo* protein import into plant mitochondria. *Methods Mol. Biol.* 372: 297–314.

Pesaresi P., Masiero S., Eubel H., Braun H.P., Bhushan S., Glaser E., Salamini F., Leister D. (2006). Nuclear photosynthetic gene expression is synergistically modulated by rates of protein synthesis in chloroplasts and mitochondria. *Plant Cell* 18: 970-991.

Pesaresi P., Schneider A., Kleine T., Leister D. (2007). Interorganellar communication. *Curr. Opin. Plant Biol*. 10: 600-606.

Pfaffl M. (2001). A new mathematical model for relative quantification in Real-Time RT-PCR. *Nucleic Acids Research*. 29(9): 2001-2007.

Pfalz J., Liere K., Kandlbinder A., Dietz K-J., Oelmüller R. (2006). pTAC2, -6, and -12 are components of the transcriptionally active chromosome that are required for plastid gene expression. *Plant Cell* 18: 176–197.

Pfannschmidt, T., Nilsson, A., Allen, J. F. (1999). Photosynthetic control of chloroplast gene expression. *Nature* 397: 625–628.

Pfannschmidt T. (2010) Plastidial retrograde signaling—A true “plastid factor” or just metabolite signatures? *Trends Plant Sci.*:15:427–435.

Porra R. J. (2002). The chequered history of the development and use of simultaneous equations for the accurate determination of chlorophylls a and b. *Photosynth. Res.* 73: 149-156.

Prikryl J., Watkins K.P., Friso G., van Wijk K.L., Barkan A. (2008). A member of the Whirly family is a multifunctional RNA- and DNA-binding protein that is essential for chloroplast biogenesis. *Nucleic Acids °Res°*36: 51152–55165.

Puthiyaveetil S., Kavanagh T.A., Cain P., Sullivan J.A., Newell C.A. (2008). The ancestral symbiont sensor kinase CSK links photosynthesis with gene expression in chloroplasts. *Proc. Natl Acad. Sci USA* 105: 10061–10066.

Quesada V., Sarmiento-Manus R., Gonzalez-Bayon R., Hricova A., Perez-Marcos R., Gracia-Martınez E., Medina-Ruiz L., Leyva-Diaz E., Ponce M.R., Micol J.L. (2011). Arabidopsis RUGOSA2 encodes an mTERF family for mitochondrion, chloroplast and leaf development. *Plant J.* 68: 738–753.

Raghavendra, A.S. and Padmasree, K. (2003). Beneficial interactions of mitochondrial metabolism with photosynthetic carbon assimilation. *Trends Plant Sci.* 8: 546–553.

Ramakers et al. (2003). Assumption-free analysis of quantitative real-time PCR data. *Neurosci. Letters* 339: 62-66.

Raven, J. A., and Allen, J. F. (2003). Genomics and chloroplast evolution: what did cyanobacteria do for plants? *Genome Biol*. 4: 209.

Richly, E., Leister, D., (2004). An improved prediction of chloroplast proteins reveals diversities and commonalities in the chloroplast proteomes of Arabidopsis and rice. *Gene* 329: 11 –16.

Roberti M., Bruni F., Loguercio Polosa P., Manzari C., Gadaleta M.N., Cantatore P. (2006). MTERF3, the most conserved member of the mTERF-family, is a modular factor involved in mitochondrial protein synthesis. *Biochim. Biophys. Acta* 1757: 1199–1206.

Roberti, M., Polosa, P.L., Bruni, F., Manzari, C., Deceglie, S., Gadaleta, M.N., and Cantatore, P. (2009). The MTERF family proteins: mitochondrial transcription regulators and beyond. *Biochim. Biophys. Acta*. 1787, 303–311.

Rosso MG, Li Y, Strizhov N, Reiss B, Dekker K, et al. (2003) An Arabidopsis thaliana T-DNA mutagenized population (GABI-Kat) for flanking sequence tag-based reverse genetics. *Plant Mol. Biol.* 53: 247–259.

Sambrook J., Fritsch E. F. and Maniatis T. (1989). Molecular cloning. New York: Cold Spring Harbor Laboratory Press.

Sauret-Gueto, S., Botella-Pavıa, P., Flores-Perez, U., Martìnez-Garcìa, J.F., San Romàn, C., Leòn, P., Boronat, A., Rodrıguez-Concepcion, M. (2006). Plastid cues posttranscriptionally regulate the accumulation of key enzymes of the methylerythritol phosphate pathway in Arabidopsis. *Plant Physiol*. 141: 75–84.

Scarpulla R.C. (2008). Transcriptional paradigms in mammalian mitochondrial biogenesis and function. *Physiol. Rev*. 88: 611–38.

Schaffner W, Weissmann C. (1973). A rapid, sensitive, and specific method for the determination of protein in dilute solution. *Anal. Biochem*. 56: 502–514.

Schmitz-Linneweber C., Small I. (2008). Pentatricopeptide repeat proteins: a socket set for organelle gene expression. *Trends Plant Sci.* 13: 663–670.

Schmitz-Linneweber, C., Williams-Carrier, R.E., Williams-Voelker, P.M., Kroeger, T.S., Vichas, A., and Barkan, A. (2006). A pentatricopeptide repeat protein facilitates the trans-splicing of the maize chloroplast rps12 pre-mRNA. *Plant Cell* 18: 2650–2663.

Schönfeld, C., Wobbe, L., Borgstadt, R., Kienast, A., Nixon, P. J., and Kruse, O. (2004). The nucleus-encoded protein MOC1 is essential for mitochondrial light acclimation in Chlamydomonas reinhardtii. *J. Biol. Chem. 279*, 50366–50374.

Schweer J. (2010). Plant sigma factors come of age: flexible transcription factor network for regulated plastid gene expression. *Endocytobiosis Cell Res.* 20: 1–20.

Shimizu M., Kato H., Ogawa T., Kurachi A., Nakagawa Y., Kobayashi H. (2010). Sigma factor phosphorylation in the photosynthetic control of photosystem stoichiometry. *Proc. Natl Acad. Sci USA* 107: 10760–10764.

Spåhr H., Samuelsson T., Hällberg B.M., Gustafsson C.M. (2010). Structure of mitochondrial transcription termination factor 3 reveals a novel nucleic acid-binding domain. *Biochem. Biophys. Res. Commun*. 397:386–390.

Spurr A.R. (1969). A low viscosity epoxy resin embedding medium for electron microscopy. *J. Ultrastruct. Res.°*26: 31–43.

Strittmatter, G. and Kössel, H. (1984). Cotranscription and processing of 23S, 4.5S and 5S rRNA in chloroplasts from *Zea mays*. *Nucl. Acids Res*. 12: 7633–7647.

Szklarczyk R., Huynen M.A. (2010). Mosaic origin of the mitochondrial proteome. *Proteomics* 10:4012-24.

Taylor, W.C. (1989). Regulatory interactions between nuclear and plastid genes. *Rev. Plant Physiol. Plant Mol. Biol.* 40: 211–233.

Towbin H., Staehelin T. and Gordon J. (1979). Electrophoretic transfer of proteins from polyacrylamide gels to nitrocellulose sheets: procedure and some applications. *Proc. Natl Acad. Sci USA* 76: 4350-4354 .

Ueda M., Nishikawa T., Fujimoto M., Takanashi H., Arimura S.I., Tsutsumi N., Kadowaki K.I. (2008). Substitution of the gene for chloroplast RPS16 was assisted by generation of a dual targeting signal. *Mol. Biol. Evol*. 25: 1566–1575

Unseld, M., Marienfeld, J.R., Brandt, P., Brennicke, A. (1997). The mitochondrial genome of Arabidopsis thaliana contains 57 genes in 366,924 nucleotides. *Nat. Genet*. 15: 57–61.

Van de Peer Y., Fawcett J.A., Proost S., Sterck L., Vandepoele K. (2009). The flowering world: a tale of duplications. *Trends Plant Sci*. 14: 680–688.

Varotto C., Pesaresi P., Meurer J., Oelmuller R., Steiner-Lange S., Salamini F., Leister D. (2000). Disruption of the Arabidopsis photosystem I gene psaE1 affects photosynthesis and impairs growth. *Plant J*. 22, 115–124.

Walter, M., Kilian, J., Kudla, J. (2002). PNPase activity determines the efficiency of mRNA 3'-end processing, the degradation of tRNA and the extent of polyadenylation in chloroplasts. *EMBO J*. 21: 6905–6914.

Watkins, K.P., Kroeger, T.S., Cooke, A.M., Williams-Carrier, R.E., Friso, G., Belcher, S.E., van Wijk, K.J., Barkan, A. (2007). A ribonuclease III domain protein functions in group II intron splicing in maize chloroplasts. *Plant Cell* 19: 2606–2623.

Woodson, J.D. and Chory, J. (2008). Coordination of gene expression between organellar and nuclear genomes. *Nat. Rev. Genet*. 9: 383–395.

Yakubovskaya E., Mejia E., Byrnes J., Hambardjieva E., Garcia-Diaz M. (2010). Helix unwinding and base flipping enable human MTERF1 to terminate mitochondrial transcription. *Cell* 141: 982–993.

Yamamoto, Y.Y., Puente, P., Deng, X.-W. (2000). An Arabidopsis cotyledon-specific albino locus: A possible role in 16S rRNA maturation. *Plant Cell Physiol*. 41: 68–76.

Yoon H.S., Hackett J.D., Ciniglia C., Pinto G., Bhattacharya D. (2004). A molecular timeline for the origin of photosynthetic eukaryotes. *Mol. Biol. Evol*. 21: 809–818.

Yu, F., Liu X., Alsheikh M., Park S., Rodermel S. (2008). Mutations in SUPPRESSOR OF VARIEGATION1, a factor required for normal chloroplast translation, suppress *var2*-mediated leaf variegation in *Arabidopsis*. *Plant Cell* 20: 1786-1804.

Zghidi W., Merendino L., Cottet A., Mache R., Lerbs-Mache S. (2007) Nucleus-encoded plastid sigma factor SIG3 transcribes specifically the psbN gene in plastids. *Nucleic Acids Res*. 35: 455–464.

Acknowledgements

I want to express my gratitude to Prof. Dr. Leister, for the supervision of my project and for the opportunity of working in his group. The experience I made has certainly represented a leap forward for my scientific knowledge, and has given me the chance to live a multicultural experience.

I want to thank Dr. Tatjana Kleine, for her supervision, support and continuous supply of motivation during the project.

Sincere thanks to all the COSI ITN fellows, and in particular to Prof. Markus Teige, for his efforts in the coordination and organization of the network. I had the chance to meet fantastic people among my ESR colleagues, sharing with them an enriching experience, on a professional and personal level. All my thanks to Jenny, Frauke, Daniel, Chhavi, Philipp, Judit, Sascha, Michele and Simon! A special mention for Agostinho, friend and colleague at the LMU, with whom I had scientific and non-scientific discussions

I am thankful to Dr. Iris Finkemeier and her group, for introducing me to the techniques in the study of mitochondria and for providing the antibodies for mitochondrial proteins immunodetection. I want to thank the patient Anne Orwat, for the time she has dedicated to me.

A special thank you goes to my colleagues at LMU and "Mitbewohnerinnen" Anne Koenig and Steffi Otters, for their friendship and all the support and avocado-pesto they gave me, fuel for my scientific research and seed of my integration in Germany.

My work could have not been completed without the help of my lab colleagues, with their precious suggestions and vivid ideas. Alex Hertle and Ute Armbruster helped me in the beginning and throughout my Ph.D., providing constant and valuable advice. Stefania Viola, compatriot and friend, has not only taken part to scientific discussion, but also blessed me with fun and unforgettable parties! For all the time spent together in and out the lab, I want to thank (in alphabetic order): Angie, Ashraf, Elena, Evgenia, Henning, Jafar, Jing Kayo Lukas, Mathias, Michael, Ping, Rhea, Salar, Thomas, Tobi, Wenteng and Yafei and all the people that are or have been part of the group. A special thank to Joana and her moral support.

I want to thank David for being always on my side and all my old friends at home and abroad for their long distance but true friendship, in particular Martina, Martino, and Nicoletta. Thanks to Davide, for supporting and standing me and being often right on many things.

Last, but obviously not least, thanks to Vendramina for making my success possible (and for much more) and to my beloved sister Tatiana.

Curriculum vitae

Personal Data

Name: Arianna Morosetti

Date of birth: 2nd July 1982

Place of birth: Milan, Italy

Citizenship: Italian

Research experience

November 2008 – December 2012

Ludwig-Maximillians-University Munich (Germany)

Department Biology I, Botany

Ph.D. in "Characterization of the pam48 mutant, defective for the MTERF protein PAM48, required for plastid gene expression and development".

Supervisor Prof. Dr. Dario Leister

Education

2006 – 2008

State University of Milan (Italy)

M.Sc. in Plant Biotechnology – Graduated 110 cum laude

Thesis: Regulation of EGG CELL genes in *Arabidopsis thaliana:* a first insight in understanding parthenogenesis – Supervisor: Prof. Dr. Martin Kater, Prof. Dr. Lucia Colombo

2001 – 2007

State University of Milan (Italy)

B.Sc. in Plant Biotechnology – Graduated 102/110

Thesis: Preliminary data on molecular characterisation of Ca. *Phytoplasma mali* associated to Apple Proliferation in apple-orchards of Lombardy

1996-2001

Liceo Classico

A level degree, humanities

Grade: 78/100

Eidesstattliche Erklärung

Hiermit versichere ich, dass ich die vorliegende Arbeit selbständig und nur unter Verwendung der angegebenen Hilfsmittel und Quellen angefertigt habe

Erklärung

Der Autor hat zuvor nicht versucht, anderweitig eine Dissertation einzureichen oder sich einer Doktorprüfung zu unterziehen. Die Dissertation wurde keiner weiteren Prüfungskommission weder in Teilen noch als Ganzes vorgelegt.

München, den ……

Arianna Morosetti

……